Invariants of Legendrian Links

by

Lenhard Lee Ng

A.B. *summa cum laude*, Mathematics and Physics, Harvard University, 1996

Submitted to the Department of Mathematics
in partial fulfillment of the requirements for the degree of

Doctor of Philosophy

at the

MASSACHUSETTS INSTITUTE OF TECHNOLOGY

June 2001

Author .....
Department of Mathematics
2 May 2001

Certified by .....
Tomasz S. Mrowka
Professor of Mathematics
Thesis Supervisor

Accepted by .....
Tomasz S. Mrowka
Chairman, Department Committee on Graduate Students

Invariants of Legendrian Links

by

Lenhard Lee Ng

Submitted to the Department of Mathematics
on 2 May 2001, in partial fulfillment of the
requirements for the degree of
Doctor of Philosophy

Abstract

We introduce new, readily computable invariants of Legendrian knots and links in standard contact three-space, allowing us to answer many previously open questions in contact knot theory. The origin of these invariants is the powerful Chekanov-Eliashberg differential graded algebra, which we reformulate and generalize. We give applications to Legendrian knots and links in three-space and in the solid torus. A related question, the calculation of the maximal Thurston-Bennequin number for a link, is answered for some large classes of links.

Thesis Supervisor: Tomasz S. Mrowka
Title: Professor of Mathematics

Acknowledgments

I am extremely grateful to my advisor, Tom Mrowka, for all of his encouragement and help throughout my graduate years. Besides suggesting my dissertation topic, he asked questions and made suggestions that were invaluable and consistently insightful, and prodded me in directions I would never have found by myself.

During my time at MIT, I have enjoyed the strong support of Isadore Singer, who has acted as a mentor to me. He guided me especially through my first year of graduate school, and has always been eager to help me.

I have learned tremendously from my collaborators. John Etnyre has patiently explained to me a great deal about contact topology, and has answered all of my befuddled questions. Josh Sabloff has been a joy to work with, even from 2700 miles away and through the most gruesome calculations. Besides helping me work through many examples, Lisa Traynor has offered me a large amount of much-appreciated advice, mathematical and otherwise.

My work has benefitted from conversations with a number of people, including Yasha Eliashberg, Dmitry Fuchs, Emmanuel Ferrand, Kirill Michatchev, and Kiran Kedlaya. I would like in particular to thank Nataliya Yufa, whose senior thesis on maximal Thurston-Bennequin numbers provided the basis for Appendix B of this thesis.

I am grateful to those brave enough to read this dissertation and offer suggestions: Lisa Traynor, whose many comments considerably improved this thesis; and my thesis committee, Tom Mrowka, Isadore Singer, and especially Denis Auroux, who caught many mistakes in a preliminary draft.

It is a pleasure to acknowledge several organizations and institutions which facilitated or sponsored my research. I was supported from 1996 to 1999 by an NDSEG Fellowship from the Department of Defense; since then, I have been supported by MIT, and by research assistantships from grants from the Department of Energy and the National Science Foundation. Much of my work resulted from visits to the Contact Geometry program in the fall of 2000, jointly sponsored by the American Institute of Mathematics and Stanford University; I would like to thank both for their hospitality.

I am very fortunate to be surrounded by an exceptional community of mathematics graduate students at MIT, and I am grateful to them all, especially Anda Degeratu, Anthony Henderson, Thom Pietraho, Carmen Young, and (an interloper from Princeton) Manjul Bhargava. A special thank-you goes to Astrid Giugni, whose support helped me through the thesis-writing ordeal.

I am indebted to Julian Stanley, Bud Stuart, Jonathan Wahl, Persi Diaconis, and Joe Gallian, all of whom taught and advised me during my high school and undergraduate years, and helped shape my mathematical career.

Finally, I would like to thank my family, with love: my mother, who invested so much of herself into providing me with all the best opportunities; my brother, who provided distractions from work when they were sorely needed, even when asking me questions from his physics class; and my father, who taught me about motivation, perseverence, and vision. This dissertation is dedicated to them.

Contents

Chapter 1

Introduction

1.1 Legendrian links in standard contact $\mathbb{R}^3$

There has recently been an explosion of interest in contact geometry, largely because of its impact on the geometry and topology of three-manifolds. Contact geometry is also intricately linked with the theory of four-manifolds; see, e.g., [KM] for a link between contact structures and four-dimensional gauge theory.

In studying contact three-manifolds, two special classes of knots and links, Legendrian and transversal, play a critical role. Probably the first application of knots in contact geometry was Bennequin's famous demonstration [B] of the existence of "exotic" contact structures on $\mathbb{R}^3$, using transversal unknots; this work inspired Eliashberg's central tight-versus-overtwisted dichotomy for contact structures on three-manifolds [E2]. Since then, Legendrian knots have been instrumental in distinguishing between homotopic contact structures on manifolds such as homology spheres [LM] and the three-torus [Kan1]. Knots in contact geometry have also produced consequences for general three-manifold topology; for instance, Rudolph [Ru3] has established a relationship between invariants of Legendrian knots and sliceness.

The question underlying contact knot theory is simple: when are two Legendrian or transversal links the same, i.e., isotopic through Legendrian or transversal links? This question, first explicitly stated in [Ar], also appears in Kirby's problem list [Kir]. We restrict our attention to links in $\mathbb{R}^3$ with the standard contact structure, since this provides a local model for any contact manifold. We will further devote our attention solely to Legendrian links, which are better studied and seem to have more structure; the study of Legendrian links may also produce results for transversal links.

An isotopy through Legendrian links is called a *Legendrian isotopy*. There are two "classical" Legendrian-isotopy invariants of Legendrian knots in standard contact $\mathbb{R}^3$, *Thurston-Bennequin number* and *rotation number*. (The story for multi-component links is similar but a bit more complicated.) The first result towards a classification of Legendrian-isotopy classes of knots was Eliashberg and Fraser's demonstration [EF] that the classical invariants completely determine the Legendrian-isotopy class of an unknot. Since then, the classical invariants have also been shown to form a complete set of invariants for torus knots and the figure eight knot [EH].

A breakthrough on the Legendrian isotopy problem occurred in 1997, when Chekanov [Ch] and, independently, Eliashberg and Hofer (unpublished) showed that there are knot types for which the classical invariants do not suffice to characterize Legendrian-isotopy

classes. More specifically, they demonstrated that there are two 5_2 knots, in the familiar terminology of the knot table from [Rol], which have the same classical invariants, but are not Legendrian isotopic.

The tool they used is a new invariant of Legendrian links, which we will call the Chekanov-Eliashberg differential graded algebra (DGA). Eliashberg and Hofer derived this algebra from a relative version of the contact homology introduced in [E4]. The beauty of the DGA is that, unlike general contact homology, there is a simple method for computing it from knot diagrams. Chekanov, motived by the relative contact homology picture, discovered a purely combinatorial formulation of the DGA, and proved its invariance combinatorially, in [Ch]; his work is the starting point for most of this dissertation.

Etnyre, Sabloff, and the author [ENS] have since given a rigorous treatment of the relation between Eliashberg and Hofer's relative contact homology and Chekanov's combinatorial theory. By using ideas from Floer homology concerning coherent orientations, [ENS] also lifts the DGA for a Legendrian knot K from an algebra over $\mathbb{Z}/2$, graded over $\mathbb{Z}/(2r(K))$, to one over $\mathbb{Z}[t,t^{-1}]$, graded over $\mathbb{Z}$.

The Chekanov-Eliashberg DGA, though extraordinarily useful as a tool for distinguishing between Legendrian links, has two drawbacks. The first is that, in practice, it can be difficult to use. Chekanov defines the DGA in terms of the Lagrangian projection of a Legendrian link, but it is not easy to manipulate Lagrangian-projected knots. More importantly, it is hard in general to tell when two DGAs are the same. Until now, the only known technique was to use polynomials defined by Chekanov, which we call the Poincaré-Chekanov polynomials; in essence, these calculate the homology of a finite-dimensional quotient of the DGA. These polynomials, however, are useful only in some cases.

The second drawback of the Chekanov-Eliashberg DGA is that it vanishes for any Legendrian link which is a stabilization. In practice, this renders it useless for any link which does not maximize Thurston-Bennequin number, since stabilization lowers Thurston-Bennequin number by one. It is thus important to know when a link maximizes Thurston-Bennequin number, and to find invariants which do not vanish for stabilized links.

Broadly speaking, the goal of this dissertation is to improve our understanding of Legendrian links in standard contact $\mathbb{R}^3$ by addressing the problems mentioned above. We will reformulate the DGA in the front projection, which is much more often used in practice than the Lagrangian projection, and refine the DGA in the process. Next we introduce new computable invariants from the DGA, most notably the characteristic algebra; these are quite a bit more effective in distinguishing between Legendrian links than previously known invariants. We use our new techniques to answer several open questions about Legendrian links. Finally, we describe invariants which may give interesting information for stabilized links, and we calculate the maximal Thurston-Bennequin number for two large classes of links, two-bridge links and three-stranded pretzel links.

There is obviously much still to be done in this subject. Eliashberg, Givental, and Hofer [EGH] have recently introduced a notion of symplectic field theory which generalizes contact homology; we would like to understand invariants of Legendrian links obtained from symplectic field theory. Also, one important property of Legendrian knots is that we can perform Legendrian (-1)-surgery on them to obtain another tight contact manifold [E3]. Does the new manifold encode the Chekanov-Eliashberg DGA of the knot, and does the DGA give us information about the manifold? Further, more specific open questions are asked throughout this dissertation, but especially in Sections 3.2 and 6.4 and Remark 5.2.7.

Here is an outline of the rest of this dissertation. We supply the necessary technical background in Section 1.2, and review Chekanov's construction of the DGA in Section 1.3.

Chapter 2 defines the DGA (more precisely, the lifting described in [ENS]) for front projections of knots, and discusses an improved version of the DGA for links as well. In Chapter 3, we define the characteristic algebra and demonstrate how it incorporates previously known invariants. Chapter 4 is devoted to applications of the theory from Chapters 2 and 3, specifically to distinguish between several previously indistinguishable Legendrian knots and links. Chapter 5 introduces a new construction, the Legendrian satellite, and uses it to establish some results about Legendrian links on the solid torus; in the future, Legendrian satellites may also produce useful invariants of stabilized links. In Chapter 6, we address a slightly different subject by computing maximal Thurston-Bennequin numbers for two-bridge and pretzel links.

To make this dissertation more self-contained, we include proofs in Appendix A of the main results about the Chekanov-Eliashberg DGA for the front-projection picture, rather than simply referring to the Lagrangian-projection proofs from [Ch] and [ENS]. Appendix B gives a table of maximal Thurston-Bennequin numbers for prime knots with nine or fewer crossings, improving on the table from [Tan].

A note about original content: a fair amount of this dissertation has already appeared in preprints by the author. Chapters 2, 3, and 4 are taken from [Ng3], while the content of Chapter 6 for two-bridge links, as well as Appendix B, is from [Ng2]. Although not explicitly used here, [Ng1] is subsumed into Section 4.1. No material from the coauthored papers [ENS] and [NT] appears in this dissertation, although results from these papers are cited in Chapters 2 and 5, respectively.

1.2 Background material

This section is a clearinghouse for the definitions and results needed for the rest of the dissertation, and also indicates the conventions we will use. We will also suggest a way in which this dissertation connects with the theory of transversal links.

A *contact form* on a smooth three-manifold M is a global 1-form α such that $\alpha \wedge d\alpha \neq 0$ everywhere on M; then $\ker \alpha$ gives a completely nonintegrable distribution on M, which we call a *contact structure*. We may view contact structures as the odd-dimensional analogue of symplectic structures on even-dimensional manifold. A *contactomorphism* between two contact manifolds is a diffeomorphism mapping one contact structure to the other.

As a matter of convention, we will use the word "link" to denote either a knot or a link. Links which are not knots will be called "multi-component links" for clarity where necessary. All multi-component links are assumed to be ordered; that is, there is a specific ordering to the components of the link. If $L_1, \ldots, L_k$ are the ordered components of a link L, we write $L = (L_1, \ldots, L_k)$.

A *Legendrian* (resp. *transversal*) link in a contact three-manifold M is a link on which α vanishes identically (resp. never vanishes). Two Legendrian links are *Legendrian isotopic* if they are isotopic through Legendrian links; we may similarly define transversal isotopy for transversal links. The relative version of a celebrated theorem of Gray [Gr] implies that two links are Legendrian isotopic if and only if there is an ambient contact isotopy of M mapping one to the other.

The *standard contact structure* on $\mathbb{R}^3$ is given by $\alpha = dz - y\,dx$. By Darboux's Theorem, any point in a contact three-manifold has a neighborhood contactomorphic to $\mathbb{R}^3$ with the standard contact structure.

There are two standard methods of representing Legendrian links in standard contact

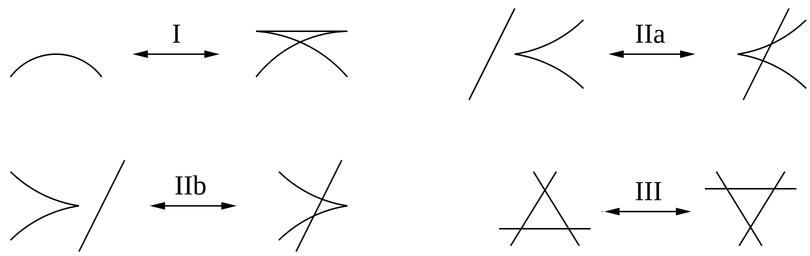

Figure 1-1: The Legendrian Reidemeister moves which relate Legendrian-isotopic fronts. The same moves, reflected about the x (horizontal) axis, are also allowed.

$\mathbb{R}^3$ via projections to $\mathbb{R}^2$: the *Lagrangian projection* to the xy plane, and the *front projection* to the xz plane. We consider each of these projections separately.

Given the Lagrangian projection of a link, we can recover the link by setting $z = \int y\,dx$. This is unique, up to translation in the z direction for each component of the link. The Lagrangian projection of a link gives a *link diagram* in $\mathbb{R}^2$, i.e., an immersion of the appropriate number of copies of S^1 into $\mathbb{R}^2$, along with overcrossing-undercrossing information. Determining conversely whether a link diagram is the Lagrangian projection of a Legendrian link is not easy, although a reasonably useful necessary-and-sufficient condition is given in [Ch]. The signed area $\int y\,dx$ enclosed by a component of the link diagram must be zero; each crossing in the link diagram also implies an inequality on the areas of the regions into which the diagram divides $\mathbb{R}^2$. We will deal only with *generic* link diagrams, for which all crossings are transverse double points.

Define a *front* to be an immersion of some number of copies of S^1 into $\mathbb{R}^2$, with no vertical tangencies, and smooth except for cusp singularities where the front changes direction in x. The front projection of a link is a front, and we can recover the link from its front by setting $y = dz/dx$. It is unnecessary to specify overcrossing-undercrossing information for fronts, since the strand with greater negative slope has smaller y coordinate and hence crosses over the other strand. We will deal only with *generic* fronts, for which all singularities are either cusps or double points.

For practical purposes, fronts are often more useful than Lagrangian projections, because of the difficulty mentioned above in determining when a link diagram represents a Legendrian link. There is a simple condition, in terms of fronts, for two Legendrian links to be Legendrian isotopic: they must be related by a series of the *Legendrian Reidemeister moves* shown in Figure 1-1 [Swi].

The two classical invariants of oriented Legendrian knots under Legendrian isotopy are the Thurston-Bennequin number tb and the rotation number r; these can be easily defined for either projection. For the front projection of an oriented Legendrian knot K, we define

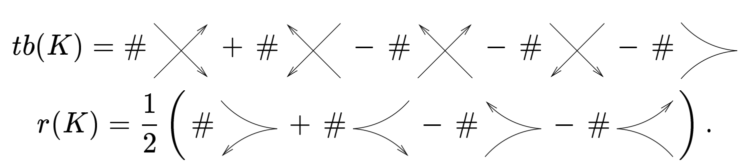

For the Lagrangian projection of K, we define

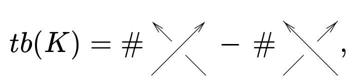

Figure 1-2: Stabilization of a Legendrian link, in the front projection.

and $r(K)$ is the counterclockwise rotation number (in revolutions) of K traversed once in the direction of its orientation.

Remark 1.2.1. Regular isotopy and Lagrangian projection. Recall that a *regular isotopy* of knot diagrams is an isotopy which avoids the usual Reidemeister move I (adding or subtracting a loop). In the Lagrangian projection, a Legendrian isotopy is a special case of a regular isotopy. In this context, tb and r may be more familiar as the classical regular-isotopy invariants, writhe (cf. Figure 6-1) and Whitney degree; see [Kau1].

Note that $tb(K)$ is independent of the orientation of K, while $r(K)$ is negated when we reverse the orientation. It is easy to see that tb and r are preserved by Legendrian isotopy.

For oriented multi-component Legendrian links L, we may also define tb and r as above; in this case, however, tb and r for any subset of the link components also give classical invariants. For instance, for a two-component oriented link $L = (L_1, L_2)$, the full set of classical invariants is given by $\{tb(L), tb(L_1), r(L_1), tb(L_2), r(L_2)\}$. Note that $r(L) = r(L_1) + r(L_2)$, and that $(tb(L) - tb(L_1) - tb(L_2))/2 = \mathrm{lk}(L_1, L_2)$ is the usual linking number of L_1 and L_2.

The operation of *stabilization* on Legendrian links adds a zigzag to a segment of a front, as shown in Figure 1-2. (Both S_+ and S_- will be called stabilizations.) It can be checked that, up to Legendrian isotopy, stabilization is independent of the segment chosen, as long as it is chosen in a fixed link component. Thus, for a Legendrian knot K, $S_+(K)$ and $S_-(K)$ are well-defined up to Legendrian isotopy, and S_+ commutes with S_-. We have

$$tb(S_\pm(L)) = tb(L) - 1$$
$$r(S_\pm(L)) = r(L) \pm 1.$$

In particular, links with maximal Thurston-Bennequin number cannot be stabilizations.

Remark 1.2.2. Transversal knots. If K_1 and K_2 are Legendrian knots of the same topological isotopy class, then they are Legendrian isotopic after applying a suitable number of positive and negative stabilizations to each knot [FT]; a corresponding result also holds for links. We call K_1 and K_2 *stably Legendrian isotopic* if there exists an n such that $(S_+)^n K_1$ and $(S_+)^n K_2$ are Legendrian isotopic.

The concept of stable isotopy is mainly useful because of transversal knots. Any Legendrian knot K can be slightly perturbed in the direction of the positive normal to K within the contact structure, to obtain a transversal knot K^+, and any transversal knot is transversally isotopic to such a K^+. The following result is well-known; see [EFM].

Theorem 1.2.3. *If K_1 and K_2 are oriented Legendrian knots, then the transversal knots K_1^+ and K_2^+ are transversally isotopic if and only if K_1 and K_2 are stably Legendrian isotopic.*

At present, there are no known transversal links which are smoothly isotopic and have the same transversal linking number, but are not transversally isotopic. We hope in the future

to use our techniques for Legendrian links to construct examples of such transversal links; see Remark 5.2.7.

Remark 1.2.4. Legendrian mirrors and inverses. There are other interesting operations besides stabilization that we can perform on Legendrian links. Given a Legendrian link L, let the *Legendrian mirror* $m(L)$ be its image under the contactomorphism $(x, y, z) \mapsto (x, -y, -z)$, and let the *inverse* $-L$ be L with each component's orientation reversed. (In the front projection, $m(L)$ is the reflection of L about the x axis.) We have $tb(m(L)) = tb(-L) = tb(L)$ and $r(m(L)) = r(-L) = -r(L)$.

It is asked in [FT] if $m(L)$ is always Legendrian isotopic to L when $r(L) = 0$; clearly $m(L)$ is always smoothly isotopic to L. Similarly, we can ask if $-L$ is always Legendrian isotopic to L when $r(L) = 0$, for link types L which are *invertible*, i.e., *smoothly* isotopic to their inverses.

In [Ng1], the author answers the question of [FT] by giving an example such that $r(L) = 0$ and $m(L)$ is not Legendrian isotopic to L; this argument is reprised in Section 4.1. A recent result of Etnyre and Honda implies that there are invertible connected sums $K_1 \# K_2$ of Legendrian knots K_1, K_2 with $r(K_1 \# K_2) = 0$ and $-(K_1 \# K_2)$ not Legendrian isotopic to $K_1 \# K_2$. It is not presently known whether there is a Legendrian knot K of invertible, prime topological type, with $r(K) = 0$, which is not Legendrian isotopic to $-K$. We believe, however, that the DGA over $\mathbb{Z}[t, t^{-1}]$, which depends on orientation, should be able to provide examples of such a knot.

1.3 Chekanov's construction of the DGA

In this section, we summarize Chekanov's original construction of the DGA invariant from [Ch], which uses the Lagrangian projection. We will reformulate this construction carefully in the front projection in Chapter 2, which is self-contained; the reader may thus skip to Chapter 2 with no difficulty.

For simplicity, we will confine our discussion to knots. Chekanov defined the DGA of a Legendrian knot K as an algebra over $\mathbb{Z}/2$ graded over $\mathbb{Z}/(2r(K))$; by imposing a coherent set of orientations on the appropriate moduli spaces, J. Etnyre, J. Sabloff, and the author [ENS] subsequently lifted this DGA to an algebra over $\mathbb{Z}[t, t^{-1}]$, where t is an indeterminate, graded over $\mathbb{Z}$. We outline the definition of the original DGA over $\mathbb{Z}/2$, and refer the reader to the two sources above for complete details.

Let K be a Legendrian knot in standard contact $\mathbb{R}^3$, whose Lagrangian projection is a link diagram which we also call K. Label the crossings of K by $a_1, \ldots, a_n$. The DGA for K is the free, noncommutative unital algebra $A = (\mathbb{Z}/2)\langle a_1, \ldots, a_n \rangle$, with grading and differential given below.

To define the grading on A, we temporarily perturb K so that the two intersecting branches at all crossings are orthogonal. For a crossing a_i, consider a path in K beginning at the undercrossing at a_i and following K until we reach the overcrossing at a_i. The

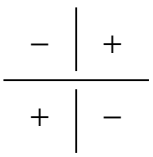

Figure 1-3: Signs associated to the four quadrants at a crossing.

counterclockwise rotation number (in revolutions) of this path is of the form $-(2k+1)/4$ for some integer k; then let $\deg a_i = k$. It is easy to check that, modulo $2r(K)$, this is well-defined. Extending this degree map to all of A (with $\deg 1 = 0$) gives a grading of A over $\mathbb{Z}/(2r(K))$.

We next define the differential on A. At each crossing, label the four quadrants near the crossing by the signs given in Figure 1-3. (Note that these signs are the negation of the signs in [Ch], since we use a differently oriented contact form on $\mathbb{R}^3$.) Define an *admissible immersion* on K to be an immersion f from the disk D^2, with some number of marked points on its boundary, to $\mathbb{R}^2$, satisfying the following conditions:

- $f(\partial D^2)$ lies in K, and $f|_{\partial D^2}$ is smooth away from the marked points;
- f maps marked points to crossings of K;
- f maps a neighborhood of a marked point to exactly one quadrant at a crossing;
- of the signs associated to the resulting quadrants for all marked points, exactly one is a $+$.

The crossing with the $+$ sign is called the *positive corner* of the admissible immersion; the crossings with $-$ signs are called the *negative corners*.

Consider an admissible immersion f with positive corner at a_i. We associate to f the monomial $\alpha(f) = a_{j_1} \cdots a_{j_\ell}$, where $a_{j_1}, \ldots, a_{j_\ell}$ are the negative corners of f, taken in counterclockwise order starting after a_i. (If f has no negative corners, then we set $\alpha(f) = 1$.) Now we define

$$\partial a_i = \sum \alpha(f);$$

here the sum is over all diffeomorphism classes of admissible immersions with positive corner at a_i. We can extend this differential to all of A by setting $\partial(1) = 0$ and imposing the Leibniz rule $\partial(vw) = (\partial v)w + v(\partial w)$.

Remark 1.3.1. Motivation. Admissible immersions are natural objects of study in the relative contact homology theory developed in [E4]. Since the Reeb vector field in standard contact $\mathbb{R}^3$ points in the z direction, Reeb chords in $\mathbb{R}^3$ beginning and ending on K correspond to crossings of the Lagrangian projection of K. In the symplectization $\mathbb{R}^3 \times \mathbb{R}$ of $\mathbb{R}^3$, relative contact homology studies holomorphic curves with boundary on $Y \times \mathbb{R}$ which limit to Reeb chords at $\pm\infty$ in the $\mathbb{R}$ direction, with one Reeb chord at $+\infty$ and some number of Reeb chords at $-\infty$. If we project to $\mathbb{R}^3$, these holomorphic curves become admissible immersions, with the limiting Reeb chords becoming positive and negative corners. See [ENS] for more details.

Example 1.3.2. For the figure eight knot shown in Figure 1-4, with $r = 0$ and $tb = -3$, we can calculate that a_2, a_4, a_5, a_7 have degree 1, a_1, a_3 have degree 0, and a_6 has degree -1. The differential ∂ is given by

$$\begin{aligned} \partial a_1 &= a_6 + a_6a_3 + a_6a_3a_5a_6 & \qquad \partial a_4 &= 1 + a_3 + a_5a_6a_3 \\ \partial a_2 &= 1 + a_1a_3 + a_5a_3a_4 & \qquad \partial a_7 &= 1 + a_3 + a_3a_6a_3a_5 \end{aligned}$$
$$\partial a_3 = \partial a_5 = \partial a_6 = 0.$$

The major properties of the differential are that $\partial^2 = 0$ and ∂ lowers degree by 1; the reader may verify that these properties hold for the example above.

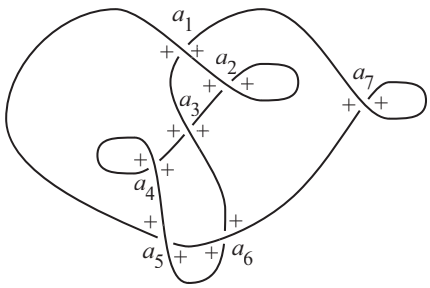

Figure 1-4: The Lagrangian projection of a figure eight knot. Crossings and + quadrants are labelled; − quadrants are omitted to reduce clutter.

Of course, the importance of the DGA stems from the fact that it gives a Legendrian-isotopy invariant. There is a concept of equivalence of DGAs under which two Legendrian-isotopic knots have equivalent DGAs; see Section 2.2. Although it is often not easy to tell when two DGAs are equivalent, Chekanov [Ch] introduced a set of polynomial invariants, derived from the DGA, which are straightforward to compute. He then used these Poincaré-Chekanov polynomials (see Section 3.2 for their definition) to distinguish between two 5_2 knots with identical classical invariants.

Remark 1.3.3. Admissible decompositions. The Chekanov-Eliashberg DGA is not the only known nonclassical invariant of Legendrian isotopy in standard contact $\mathbb{R}^3$. Chekanov and Pushkar [CP] have developed another invariant based on so-called admissible decompositions of fronts, inspired by the work of Eliashberg [E1]. It seems that the admissible-decomposition invariant is closely related to the Poincaré-Chekanov polynomials; see [Fu]. In particular, there is no known example of Legendrian knots which can be distinguished through admissible decompositions but not through the Poincaré-Chekanov polynomials.

Chapter 2

Chekanov-Eliashberg DGA in the front projection

This chapter is devoted to a reformulation of the Chekanov-Eliashberg DGA from the Lagrangian projection to the more useful front projection. In Section 2.1, we introduce resolution, the technique used to translate from front projections to Lagrangian projections. We then define the DGA for the front of a knot in Section 2.2, and discuss a particularly nice and useful case in Section 2.3. In Section 2.4, we review the main results concerning the DGA from [Ch] and [ENS]. Section 2.5 discusses the adjustments that need to be made for multi-component links.

2.1 Resolution of a front

Given a front, we can find a Lagrangian projection which represents the same link through the following construction, which is also considered in [Fer] under the name "morsification."

Definition 2.1.1. The *resolution* of a front is the link diagram obtained by resolving each of the singularities in the front as shown in Figure 2-1.

The usefulness of this construction is shown by the following result, which implies that resolution is a map from front projections to Lagrangian projections which preserves Legendrian isotopy.

Proposition 2.1.2. *The resolution of the front projection of any Legendrian link L is the Lagrangian projection of another link which is Legendrian isotopic to L.*

Note that Proposition 2.1.2 is a bit stronger than the assertion from [Fer] that the regular isotopy type of the resolution is invariant under Legendrian isotopy of the front.

Proof. We will deal only with a Legendrian knot K; the proof for multi-component links is similar. It suffices to distort the front K smoothly to a front K' so that the resolution of K is the Lagrangian projection of the knot corresponding to K'.

Figure 2-1: Resolving a front into the Lagrangian projection of a knot.

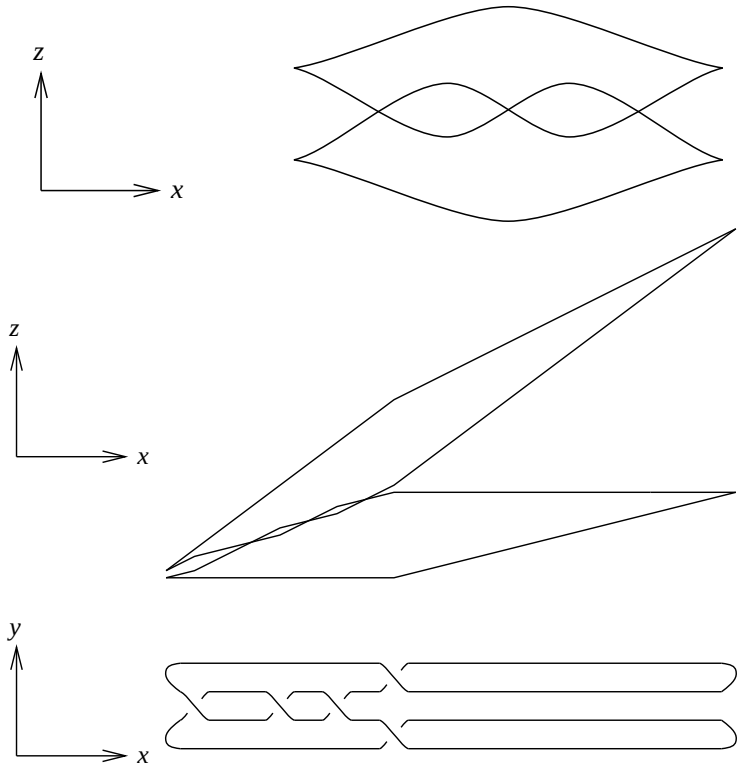

Figure 2-2: A front projection for the left-handed trefoil (top) is distorted (middle) so that the corresponding Lagrangian projection (bottom), given by $y = dz/dx$, with the same x axis as the middle diagram, is the resolution of the original front. The exceptional segments in the middle diagram appear as corners.

We choose K' to have the following properties; see Figure 2-2 for an illustration. Suppose that there are at most k points in K with any given x coordinate. Outside of arbitrarily small "exceptional segments," K' consists of straight line segments. These line segments each have slope equal to some integer between 0 and $k-1$ inclusive; outside of the exceptional segments, for any given x coordinate, the slopes of the line segments at points with that x coordinate are all distinct. The purpose of the exceptional segments is to allow the line segments to change slopes, by interpolating between two slopes. When two line segments exchange slopes via exceptional segments, the line segment with higher z coordinate has higher slope to the left of the exceptional segment, and lower slope to the right.

It is always possible to construct such a distortion K'. Build K' starting from the left; a left cusp is simply two line segments of slope j and $j+1$ for some j, smoothly joined together by appending an exceptional segment to one of the line segments. Whenever two segments need to cross, force them to do so by interchanging their slopes (again, with exceptional segments added to preserve smoothness). To create a right cusp between two segments, interchange their slopes so that they cross, and then append an exceptional segment just before the crossing to preserve smoothness.

We obtain the Lagrangian projection of the knot corresponding to K' by using the relation $y = dz/dx$. This projection consists of horizontal lines (parallel to the x axis), outside of a number of crossings arising from the exceptional segments. These crossings can be naturally identified with the crossings and right cusps of K or K'. In particular, right

cusps in K become the crossings associated to a simple loop. It follows that the Lagrangian projection corresponding to K' is indeed the resolution of K, as desired. □

2.2 The DGA for fronts of knots

Suppose that we are given the front projection Y of an oriented Legendrian knot K. To define the Chekanov-Eliashberg DGA for Y, we simply examine the DGA for the resolution of Y and "translate" this in terms of Y. In the interests of readability, we will concentrate on describing the DGA solely in terms of Y, invoking the resolution only when the translation is not obvious.

The singularities of Y fall into three categories: crossings (nodes), left cusps, and right cusps. Ignore the left cusps, and call the crossings and right cusps *vertices*, with labels $a_1, \ldots, a_n$ (see Figure 2-3); then the vertices of Y are in one-to-one correspondence with the crossings of the resolution of Y.

As an algebra, the Chekanov-Eliashberg DGA of the front Y is defined to be the free, noncommutative algebra with unity $A = \mathbb{Z}[t, t^{-1}]\langle a_1, \ldots, a_n \rangle$ over $\mathbb{Z}[t, t^{-1}]$ generated by $a_1, \ldots, a_n$. We wish to define a grading on A, and a differential ∂ on A which lowers the grading by 1.

We first address the grading of A. For an oriented path γ contained in the diagram Y, define $c(\gamma)$ to be the number of cusps traversed upwards, minus the number of cusps traversed downwards, along γ. Note that this is the opposite convention from the one used to calculate rotation number; if we consider Y itself to be an oriented closed curve, then $r(K) = -c(Y)/2$.

Let the degree of the indeterminate t be $2r(K)$. To grade A, it then suffices to define the degrees of the generators a_i; we follow [ENS].

Definition 2.2.1. Given a vertex a_i, define the *capping path* γ_i, a path in Y beginning and ending at a_i, as follows. If a_i is a crossing, move initially along the segment of higher slope at a_i, in the direction of the orientation of Y; then follow Y, not changing direction at any crossing, until a_i is reached again. If a_i is a right cusp, then γ_i is the empty path, if the orientation of Y traverses a_i upwards, or the entirety of Y in the direction of its orientation, if the orientation of Y traverses a_i downwards.

Definition 2.2.2. If a_i is a crossing, then $\deg a_i = c(\gamma_i)$. If a_i is a right cusp, then $\deg a_i$ is 1 or $1 - 2r(K)$, depending on whether the orientation of Y traverses a_i upwards or downwards, respectively.

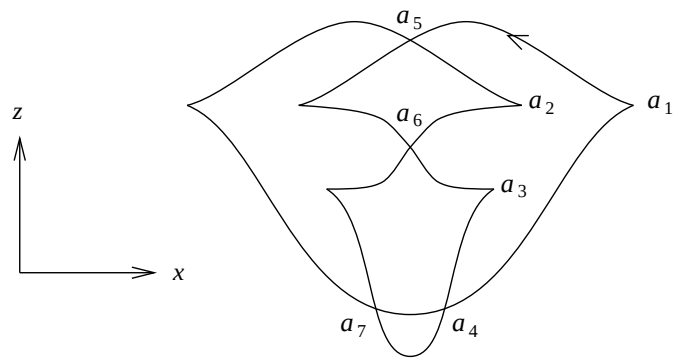

Figure 2-3: The front projection of a figure eight knot, with vertices labelled.

We thus obtain a grading for A over $\mathbb{Z}$. It will be useful to introduce the sign function $\operatorname{sgn} v = (-1)^{\deg v}$ on pure-degree elements of A, including vertices of Y; note that any right cusp has negative sign.

Example 2.2.3. In the figure eight knot shown in Figure 2-3, a_1, a_2, a_3, a_4, a_7 have degree 1, while a_5, a_6 have degree 0. For an illustration of Definition 2.2.2 for a knot of nonzero rotation number, see Remark 4.3.1.

Remark 2.2.4. The Thurston-Bennequin number for K can be written as the difference between the numbers of positive-sign and negative-sign vertices in Y. Since $\deg t = 2r(K)$, we conclude that the graded algebra A incorporates both classical Legendrian-isotopy invariants.

We next wish to define the differential ∂ on A. As in [Ch], we define ∂a_i for a generator a_i by considering a certain class of immersed disks in the diagram Y.

Definition 2.2.5. An *admissible map* on Y is an immersion from the two-disk D^2 to $\mathbb{R}^2$ which maps the boundary of D^2 into the knot projection Y, and which satisfies the following properties: the map is smooth except possibly at vertices and left cusps; the image of the map near any singularity looks locally like one of the diagrams in Figure 2-4, excepting the two forbidden ones; and, in the notation of Figure 2-4, there is precisely one initial vertex.

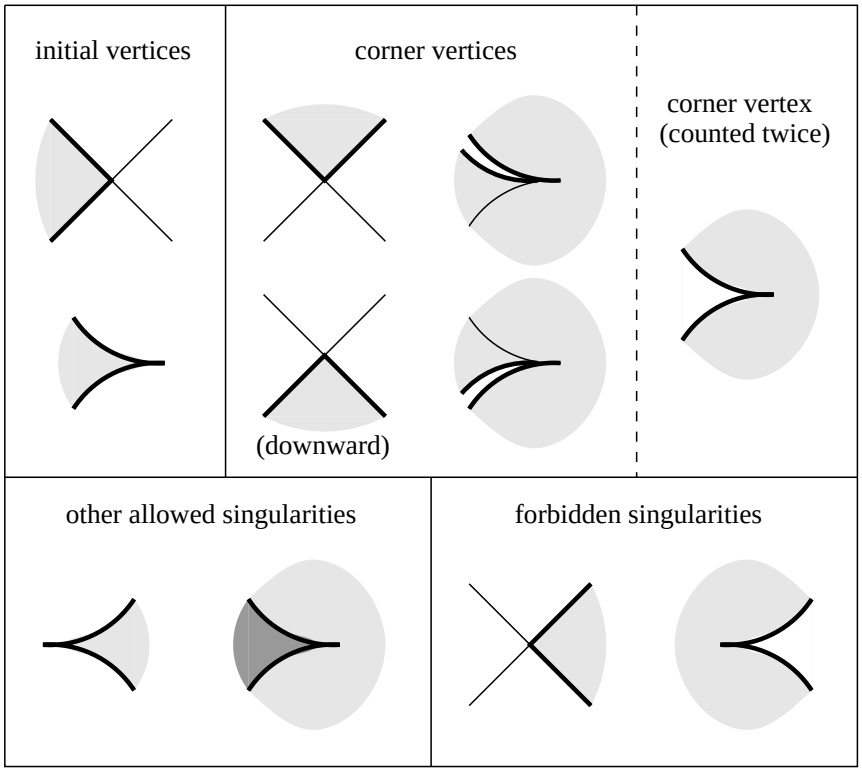

Figure 2-4: Possible singularities in an admissible map, and their classification. The shaded area is the image of the map restricted to a neighborhood of the singularity; the heavy line indicates the image of the boundary of D^2. In two of the diagrams, the heavy line has been shifted off of itself for clarity. The diagram with heavy shading indicates that the image overlaps itself. The last two diagrams are forbidden in an admissible map.

The singularities of an admissible map thus consist of one initial vertex, a number of corner vertices (possibly including some right cusps counted twice), and some other singularities which we will ignore. One type of corner vertex, the "downward" corner vertex as labelled in Figure 2-4, will be important shortly in determining certain signs.

Remark 2.2.6. Forbidden singularities. The possible singularities depicted in Figure 2-4 are all derived by considering the resolution of Y, but it is not immediately obvious why the two forbidden singularities should be disallowed. To justify this, call a point p in the domain of an admissible map, and its image under the map, *locally rightmost* if p attains a local maximum for the x coordinate of its image. (More sloppily, a point in the image of the map is locally rightmost if it locally maximizes x coordinate in the image.) Observe that any locally rightmost point in the image of an admissible map must be the unique initial vertex of the map: this point must be a node or a right cusp, which cannot be a negative corner vertex (cf. Figure 2-4). In particular, there must be a unique locally rightmost point in the image. Of the two forbidden singularities from Figure 2-4, the left one is disallowed because the initial vertex is not rightmost, and the right one because there would be two locally rightmost points.

To each diffeomorphism class of admissible maps on Y, we will now associate a monomial in $\mathbb{Z}[t, t^{-1}]\langle a_1, \ldots, a_n\rangle$. Let f be a representative of a diffeomorphism class, and suppose that f has corner vertices at $a_{j_1}, \ldots, a_{j_\ell}$, counted twice where necessary, in counterclockwise order around the boundary of D^2, starting just after the initial vertex, and ending just before reaching the initial vertex again. Then the monomial associated to f, and by extension to the diffeomorphism class of f, is

$$\alpha(f) = (\operatorname{sgn} f)\, t^{-n(f)} a_{j_1} \cdots a_{j_\ell},$$

where $(\operatorname{sgn} f)$ is the parity ($+1$ for even, -1 for odd) of the number of downward corner vertices of f of even degree, and the winding number $n(f)$ is defined below.

The image $f(\partial D^2)$, oriented counterclockwise, lifts to a collection of oriented paths in the knot K. If a_i is the initial vertex of f, then the lift of $f(\partial D^2)$, along with the lifts of the capping paths $\gamma_i, -\gamma_{j_1}, \ldots, -\gamma_{j_\ell}$, form a closed cycle in K. We then set $n(f)$ to be the winding number of this cycle around K, with respect to the orientation of K.

Definition 2.2.7. Given a generator a_i, we define

$$\partial a_i = \begin{cases} \sum \alpha(f) & \text{if } a_i \text{ is a crossing} \\ 1 + \sum \alpha(f) & \text{if } a_i \text{ is a right cusp oriented upwards} \\ t^{-1} + \sum \alpha(f) & \text{if } a_i \text{ is a right cusp oriented downwards,} \end{cases}$$

where the sum is over all diffeomorphism classes of admissible maps f with initial vertex at a_i. We extend the differential to the algebra A by setting $\partial(\mathbb{Z}[t, t^{-1}]) = 0$ and imposing the signed Leibniz rule $\partial(vw) = (\partial v)w + (\operatorname{sgn} v)v(\partial w)$.

Remark 2.2.8. Consistency of definitions. The power of t in the definition of the monomial $\alpha(f)$ has been taken directly from the definition in [ENS] of ∂ for the resolution of Y. It is easy to check that the signs also correspond to the signs in [ENS], after we replace a_i by $-a_i$ for each a_i which is "right-pointing"; that is, near which the knot is locally oriented from left to right for both strands.

Remark 2.2.9. Unoriented knots. Definition 2.2.7 depends on a choice of orientation of the knot K. For an unoriented knot, we may similarly define the differential without the powers

of t; the DGA is then an algebra over $\mathbb{Z}$ graded over $\mathbb{Z}/(2r(K))$, still a lifting of Chekanov's original DGA over $\mathbb{Z}/2$.

Remark 2.2.10. Stabilizations. If K is a stabilization, then it is easy to see that there is an a_i such that $\partial a_i = 1$ or $\partial a_i = t^{-1}$. In this case, $\partial(a_j - a_i \partial a_j) = 0$ or $\partial(a_j - t a_i \partial a_j) = 0$ for all j, and the DGA collapses modulo tame isomorphisms (see Section 2.4). This was first noted in [Ch, §11.2].

Example 2.2.11. We may compute (somewhat laboriously) that the front in Figure 2-3 satisfies

$$\begin{aligned}
\partial a_1 &= 1 + a_6 - t^2 a_6 a_4 a_6 a_7 - t^2(1 - t a_6 a_5) a_3 a_6 a_7 + t a_6 a_2 (1 - t a_6 - t^2 a_7 a_4 a_6) a_7 \\
\partial a_2 &= 1 - t a_5 a_6 \\
\partial a_3 &= t^{-1} - a_6 - t a_6 a_7 a_4 \\
\partial a_4 &= \partial a_5 = \partial a_6 = \partial a_7 = 0.
\end{aligned}$$

See Figure 2-5 for a depiction of two of the admissible maps counted in ∂a_1.

To illustrate the calculation of the sign and power of t associated to an admissible map, consider the term $t^3 a_6 a_5 a_3 a_6 a_7$ in ∂a_1 above. The sign of this term is $(-\operatorname{sgn} a_5)(-\operatorname{sgn} a_6) = +1$; see Example 2.2.3. To calculate the power of t, we count, with orientation, the number of times the cycle corresponding to this map passes through a_1. The boundary of the

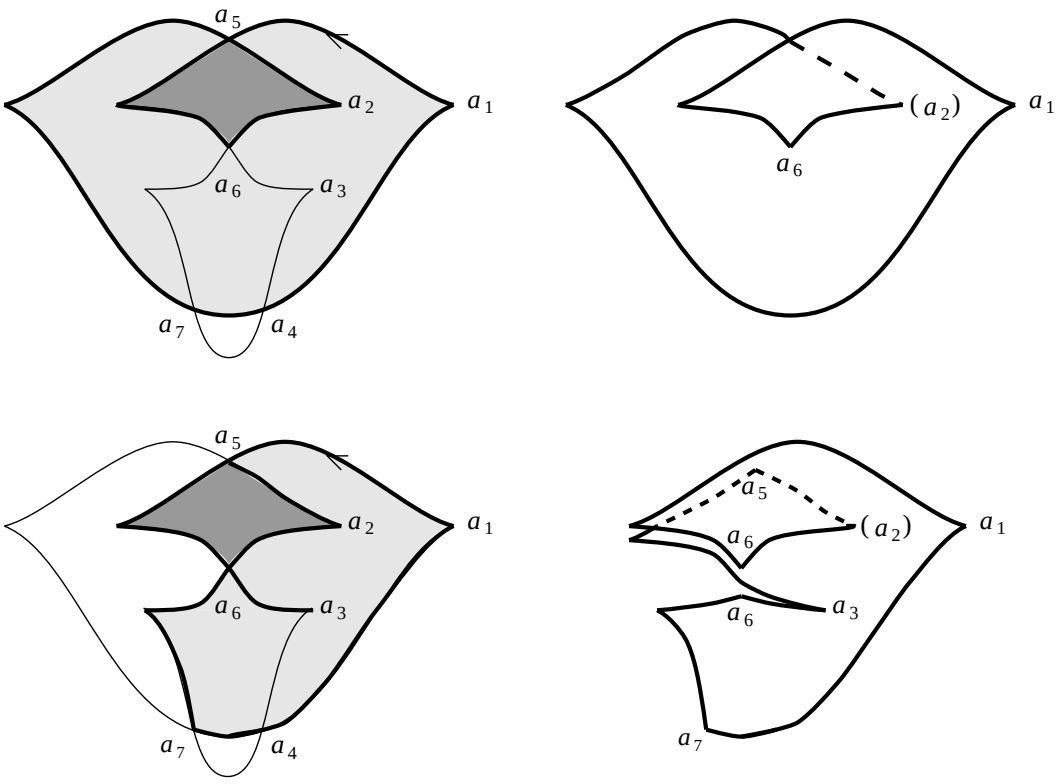

Figure 2-5: The admissible maps corresponding to the terms a_6 (top) and $t^3 a_6 a_5 a_3 a_6 a_7$ (bottom) in ∂a_1 for the front from Figure 2-3. The heavy lines indicate the image of the boundary of D^2; the heavy shading indicates where the images overlap themselves. For clarity, the images of the maps are redrawn to the right.

immersed disk passes through a_1, contributing 1; γ_1 trivially does not pass through a_1, contributing 0; and $-\gamma_3, -\gamma_6, -\gamma_7$ pass through a_1, while $-\gamma_5$ does not, contributing a total of -4. It follows that the power of t is $t^{-(1+0-4)} = t^3$.

2.3 Simple fronts

Since the behavior of an admissible map near a right cusp can be complicated, our formulation of the differential algebra may seem no easier to compute than Chekanov's. There is, however, one class of fronts for which the differential is particularly easy to compute.

Definition 2.3.1. A front is *simple* if it is smoothly isotopic to a front all of whose right cusps have the same x coordinate.

Any front can be Legendrian-isotoped to a simple front: "push" all of the right cusps to the right until they share the same x coordinate. (In the terminology of Figure 1-1, a series of IIb moves can turn any front into a simple front.)

For a simple front, the boundary of any admissible map must begin at a node or right cusp (the initial vertex), travel leftwards to a left cusp, and then travel rightwards again to the initial vertex. Outside of the initial vertex and the left cusp, the boundary can only have very specific corner vertices: each corner vertex must be a crossing, and, in a neighborhood of each of these nodes, the image of the map must only occupy one of the four regions surrounding the crossing. In particular, the map is an embedding, not just an immersion.

Example 2.3.2. It is easy to calculate the differential for the simple-front version of the figure eight knot given in Figure 2-6:

$$\begin{aligned}
\partial a_1 &= 1 + a_6 + ta_{10}a_5 & \partial a_4 &= t^{-1} + a_8a_7 - a_9a_6 - ta_9a_{10}a_5 \\
\partial a_2 &= 1 - ta_9a_{10} & \partial a_5 &= a_7 + a_{11} + ta_{11}a_8a_7 \\
\partial a_3 &= t^{-1} - a_{10} - ta_{10}a_{11}a_8 & \partial a_6 &= -ta_{10}a_7 - ta_{10}a_{11} - t^2a_{10}a_{11}a_8a_7
\end{aligned}$$
$$\partial a_7 = \partial a_8 = \partial a_9 = \partial a_{10} = \partial a_{11} = 0.$$

For the signs, note that a_1, a_2, a_3, a_4, and a_8 have degree 1, a_7 and a_{11} have degree -1, and the other vertices have degree 0; for the powers of t, note that γ_3, γ_4, γ_5, γ_6, γ_7, γ_{10}, and γ_{11} pass through a_1, while the other capping paths do not.

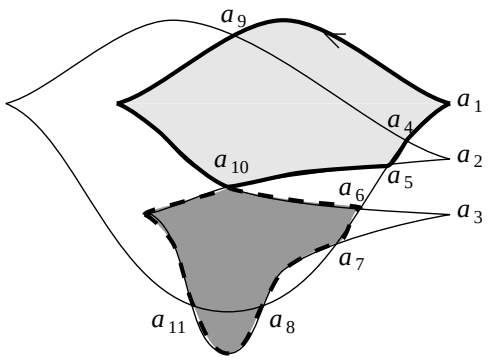

Figure 2-6: A simple-front version of the front from Figure 2-3, with two admissible maps drawn. The top shaded region corresponds to the term $ta_{10}a_5$ in ∂a_1; the bottom shaded region corresponds to the term $-ta_{10}a_7$ in ∂a_6.

2.4 Properties of the DGA

In this section, we summarize the properties of the Chekanov-Eliashberg DGA. These results were originally proven over $\mathbb{Z}/2$ in [Ch], and then extended over $\mathbb{Z}[t,t^{-1}]$ in [ENS]. Proofs are provided, in the front-projection setup, in Appendix A; see also [ENS] for Lagrangian-projection proofs.

Proposition 2.4.1 ([Ch],[ENS]). *For the DGA associated to a Legendrian knot, ∂ lowers degree by* 1.

Proposition 2.4.2 ([Ch],[ENS]). *For the DGA associated to a Legendrian knot, $\partial^2 = 0$.*

To state that the DGA is invariant under Legendrian isotopy, we need to recall several definitions from [Ch] or [ENS].

An (algebra) automorphism of a graded free algebra $\mathbb{Z}[t,t^{-1}]\langle a_1,\dots,a_n\rangle$ is *elementary* if it preserves grading and sends some a_i to $a_i + v$, where v does not involve a_i, and fixes the other generators $a_j, j \neq i$. A *tame automorphism* of $\mathbb{Z}[t,t^{-1}]\langle a_1,\dots,a_n\rangle$ is any composition of elementary automorphisms; a *tame isomorphism* between two free algebras $\mathbb{Z}[t,t^{-1}]\langle a_1,\dots,a_n\rangle$ and $\mathbb{Z}[t,t^{-1}]\langle b_1,\dots,b_n\rangle$ is a grading-preserving composition of a tame automorphism and the map sending a_i to b_i for all i. Two DGAs are then *tamely isomorphic* if there is a tame isomorphism between them which maps the differential on one to the differential on the other.

Let E be a DGA with generators e_1 and e_2, such that $\partial e_1 = \pm e_2$, $\partial e_2 = 0$, both e_1 and e_2 have pure degree, and $\deg e_1 = \deg e_2 + 1$. Then an *algebraic stabilization*[1] of a DGA $(A = \mathbb{Z}[t,t^{-1}]\langle a_1,\dots,a_n\rangle, \partial)$ is a graded coproduct

$$(S(A),\partial) = (A,\partial) \amalg (E,\partial) = (\mathbb{Z}[t,t^{-1}]\langle a_1,\dots,a_n,e_1,e_2\rangle,\partial),$$

with differential and grading induced from A and E. Finally, two DGAs are *equivalent* if they are tamely isomorphic after some (possibly different) number of (possibly different) algebraic stabilizations of each.

We can now state the main invariance result.

Theorem 2.4.3 ([Ch],[ENS]). *Fronts corresponding to Legendrian-isotopic knots have equivalent DGAs.*

Corollary 2.4.4 ([Ch],[ENS]). *The graded homology of the DGA associated to a Legendrian knot is invariant under Legendrian isotopy.*

2.5 The DGA for fronts of links

In this section, we describe the modifications of the definition of the Chekanov-Eliashberg DGA necessary for Legendrian links in standard contact $\mathbb{R}^3$. Here the DGA has an infinite family of gradings, as opposed to one, and is defined over a ring more complicated than $\mathbb{Z}[t,t^{-1}]$. The DGA for links also includes some information not found for knots.

Let L be an oriented Legendrian link, with components $L_1,\dots,L_k$; in this section, for ease of notation, we will also use $L, L_1,\dots,L_k$ to denote the corresponding fronts.

[1] This is not related to the stabilizations of Figure 1-2.

Chekanov's original definition [Ch] of the DGA for L gives an algebra over $\mathbb{Z}/2$ graded over $\mathbb{Z}/(2r(L))$, where $r(L) = \gcd(r(L_1), \dots, r(L_k))$; we will extend this to an algebra over $\mathbb{Z}[t_1, t_1^{-1}, \dots, t_k, t_k^{-1}]$ graded over $\mathbb{Z}$, and our set of gradings will be more refined than Chekanov's. We will also discuss an additional structure on the DGA discovered by K. Michatchev [Mi].

As in Section 2.2, let $a_1, \dots, a_n$ be the vertices (crossings and right cusps) of L. We associate to L the algebra

$$A = \mathbb{Z}[t_1, t_1^{-1}, \dots, t_k, t_k^{-1}]\langle a_1, \dots, a_n \rangle,$$

with differential and grading to be defined below.

For each crossing a_i, let $N_u(a_i)$ and $N_l(a_i)$ denote neighborhoods of a_i on the two strands intersecting at a_i, so that the slope of $N_l(a_i)$ is greater than the slope of $N_u(a_i)$; then $N_u(a_i)$ is *lower* than $N_l(a_i)$ in y coordinate, since the y axis points into the page. If a_i is a right cusp, define $N_u(a_i) = N_l(a_i)$ to be a neighborhood of a_i in L. For any vertex a_i, we may then define two numbers $u(a_i)$ and $l(a_i)$, the indices of the link components containing $N_u(a_i)$ and $N_l(a_i)$, respectively.

For each $j = 1, \dots, k$, fix a base point p_j on L_j, away from the singularities of L, so that L_j is oriented from left to right in a neighborhood of p_j. To a crossing a_i, we associate two capping paths γ_i^u and γ_i^l: γ_i^u is the path beginning at $p_{u(a_i)}$ and following $L_{u(a_i)}$ in the direction of its orientation until a_i is reached through $N_u(a_i)$; γ_i^l is the analogous path in $L_{l(a_i)}$ beginning at $p_{l(a_i)}$ and ending at a_i through $N_l(a_i)$. (If $u(a_i) = l(a_i)$, then one of γ_i^u and γ_i^l will contain the other.) Note that, by this definition, when a_i is a right cusp, γ_i^u and γ_i^l are both the path beginning at $p_{u(a_i)} = p_{l(a_i)}$ and ending at a_i.

Definition 2.5.1. For $(\rho_1, \dots, \rho_{k-1}) \in \mathbb{Z}^{k-1}$, we may define a $\mathbb{Z}$ grading on A by

$$\deg a_i = \begin{cases} 1 & \text{if } a_i \text{ is a right cusp} \\ c(\gamma_i^u) - c(\gamma_i^l) + 2\rho_{u(a_i)} - 2\rho_{l(a_i)} & \text{if } a_i \text{ is a crossing,} \end{cases}$$

where we set $\rho_k = 0$. We will only consider gradings on A obtained in this way.

The set of gradings on A is then indexed by $\mathbb{Z}^{k-1}$. Our motivation for including precisely this set of gradings is given by the following easily proven observation.

Lemma 2.5.2. *The collection of possible gradings on A is independent of the choices of the points p_j.*

Remark 2.5.3. Signs. We may define the sign function on vertices, as usual, by $\operatorname{sgn} a_i = (-1)^{\deg a_i}$. This is well-defined and independent of the choice of grading: $\operatorname{sgn} a_i = -1$ if a_i is a right cusp; $\operatorname{sgn} a_i = 1$ if a_i is a crossing with both strands pointed in the same direction (either both to the left or both to the right); and $\operatorname{sgn} a_i = -1$ if a_i is a crossing with strands pointed in opposite directions. Note that $tb(L) = \sum_{i=1}^n \operatorname{sgn} a_i$.

Remark 2.5.4. If a_i is contained in component L_j, the degree of a_i may differ from how we defined it in Definition 2.2.2 with L_j a knot by itself. It is easy to calculate that the difference between the two degrees will always be either 0 or $2r(L_j)$.

The differential of a generator a_i is still given by Definition 2.2.7, but we must now redefine $\alpha(f)$ for an admissible map f. Suppose that f has initial vertex a_i and corner vertices $a_{i_1}, \dots, a_{i_m}$. Then the lift of $f(\partial D^2)$ to L, together with the lifts of γ_i^u, $-\gamma_i^l$,

$-\gamma^u_{i_1}, \dots, -\gamma^u_{i_m}, \gamma^l_{i_1}, \dots, \gamma^l_{i_m}$, form a closed cycle in L. Let the winding number of this cycle around component L_j be $n_j(f)$. Also, define $\operatorname{sgn} f$, as before, to be the parity of the number of downward corner vertices of f with positive sign.

We now set

$$\alpha(f) = (\operatorname{sgn} f)\, t_1^{-n_1(f)} \cdots t_k^{-n_k(f)} a_{i_1} \cdots a_{i_m}.$$

The differential ∂ can then be defined on A essentially as in Definition 2.2.7, except that we now have $\partial(\mathbb{Z}[t_1, t_1^{-1}, \dots, t_k, t_k^{-1}]) = 0$, and

$$\partial a_i = \begin{cases} \sum \alpha(f) & \text{if } a_i \text{ is a crossing} \\ 1 + \sum \alpha(f) & \text{if } a_i \text{ is a right cusp.} \end{cases}$$

Note that the signed Leibniz rule does not depend on the choice of base points p_j, since, by Remark 2.5.3, the signs $(\operatorname{sgn} a_i)$ are independent of this choice. Also, because of a different choice of capping paths, we always add 1 to a right cusp, rather than adding either 1 or t^{-1}, as in Definition 2.2.7.

Remark 2.5.5. There is a simple way to calculate $n_j(f)$: it is the signed number of times $f(\partial D^2)$ crosses p_j. Indeed, the winding number of the appropriate cycle around L_j is the signed number of times that it crosses a point on L_j just to the left of p_j. No capping path γ^u_i or γ^l_i, however, crosses this point. Hence $n_j(f)$ counts the number of times $f(\partial D^2)$ crosses a point just to the left of p_j; we could just as well consider p_j instead of this point.

We next examine the effect of changing the base points p_j on the differential ∂. Consider another set of base points $\tilde{p}_j$, giving rise to capping paths $\tilde{\gamma}^u_i, \tilde{\gamma}^l_i$, and let ξ_j be the oriented path in L_j from p'_j to p_j. Then

$$\tilde{\gamma}^u_i - \gamma^u_i = \begin{cases} \xi_{u(a_i)}, & N_u(a_i) \subset \xi_{u(a_i)} \\ \xi_{u(a_i)} - L_{u(a_i)}, & N_u(a_i) \not\subset \xi_{u(a_i)}, \end{cases}$$

and similarly for $\tilde{\gamma}^l_i - \gamma^l_i$. We conclude the following result.

Lemma 2.5.6. *The differential on A, calculated with base points $\tilde{p}_j$, is related to the differential calculated with p_j, by intertwining with the following automorphism on A:*

$$a_i \mapsto \begin{cases} a_i, & N_u(a_i) \subset \xi_{u(a_i)} \text{ and } N_l(a_i) \subset \xi_{l(a_i)} \\ t^{-1}_{l(a_i)} a_i, & N_u(a_i) \subset \xi_{u(a_i)} \text{ and } N_l(a_i) \not\subset \xi_{l(a_i)} \\ t_{u(a_i)} a_i, & N_u(a_i) \not\subset \xi_{u(a_i)} \text{ and } N_l(a_i) \subset \xi_{l(a_i)} \\ t_{u(a_i)} t^{-1}_{l(a_i)} a_i, & N_u(a_i) \not\subset \xi_{u(a_i)} \text{ and } N_l(a_i) \not\subset \xi_{l(a_i)}. \end{cases}$$

Example 2.5.7. Consider the link L in Figure 2-7, with base points as shown. To give a grading to the DGA on L, choose $(\rho_1, \rho_2) \in \mathbb{Z}^2$. We calculate the degree of a_4 as an example: $u(a_4) = 2$, $l(a_4) = 1$, $c(\gamma^u_4) = 0$, and $c(\gamma^l_4) = -1$, and so $\deg a_4 = 1 + 2\rho_2 - 2\rho_1$. The full list of degrees is as follows:

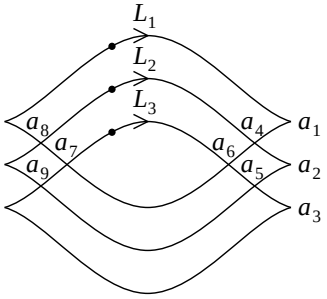

Figure 2-7: An oriented link L with components L_1, L_2, and L_3, with corresponding base points p_1, p_2, and p_3 marked but not labelled.

$$\begin{array}{lll} \deg a_1 = 1 & \deg a_4 = 1 + 2\rho_2 - 2\rho_1 & \deg a_7 = -1 + 2\rho_1 \\ \deg a_2 = 1 & \deg a_5 = 1 - 2\rho_2 & \deg a_8 = -1 + 2\rho_1 - 2\rho_2 \\ \deg a_3 = 1 & \deg a_6 = 1 - 2\rho_1 & \deg a_9 = -1 + 2\rho_2. \end{array}$$

The differential ∂ is then given by

$$\begin{array}{lll} \partial a_1 = 1 + t_1 + t_1 t_2^{-1} a_8 a_4 + t_1 t_3^{-1} a_7 a_6 & \partial a_4 = t_2 t_3^{-1} a_9 a_6 & \partial a_7 = a_8 a_9 \\ \partial a_2 = 1 + t_2 + t_2 t_3^{-1} a_9 a_5 + a_4 a_8 & \partial a_5 = a_6 a_8 & \partial a_8 = 0 \\ \partial a_3 = 1 + t_3 + a_5 a_9 + a_6 a_7 & \partial a_6 = 0 & \partial a_9 = 0. \end{array}$$

We can now state several properties of the link DGA, the analogues of the results for knots in Section 2.4.

Proposition 2.5.8. *If (A, ∂) is a DGA associated to the link L, then $\partial^2 = 0$, and ∂ lowers degree by 1 for any of the gradings of A.*

The main invariance result requires a slight tweaking of the definitions. Define elementary and tame automorphisms as in Section 2.4; now, however, let a tame isomorphism between algebras generated by $a_1, \ldots, a_n$ and $b_1, \ldots, b_n$ be a grading-preserving composition of a tame automorphism and a map sending a_i to $\left(\prod_{m=1}^{k} t_m^{\nu_{k,m}}\right) b_i$, for any set of integers $\{\nu_{k,m}\}$. (This definition is motivated by Lemma 2.5.6.) Define algebraic stabilization and equivalence as before.

Proposition 2.5.9. *If L and L' are Legendrian-isotopic oriented links, then for any grading of the DGA for L, there is a grading of the DGA for L' so that the two DGAs are equivalent.*

The proofs of Propositions 2.5.8 and 2.5.9 will be omitted here, as they are simply variants on the proofs of Propositions 2.4.1 and 2.4.2 and Theorem 2.4.3, given in Appendix A; see also [Ch].

Remark 2.5.10. Allowed gradings. Our set of gradings for A is more restrictive than the set of "admissible gradings" postulated in [Ch]. To see this, we first translate our criteria for gradings to the Lagrangian-projection picture, and then compare with Chekanov's original criteria.

Consider a Legendrian link L with components $L_1, \ldots, L_k$. By perturbing L slightly, we may assume that the crossings of $\pi_{xy}(L)$ are orthogonal, where π_{xy} is the projection map $(x, y, z) \mapsto (x, y)$; as usual, label these crossings $a_1, \ldots, a_n$. Choose neighborhoods $N_u(a_i)$ and $N_l(a_i)$ in L of the two points mapping to a_i under π_{xy}, so that $N_u(a_i)$ lies above $N_l(a_i)$ in z coordinate, and let $u(a_i)$ and $l(a_i)$ be the indices of the link components on which these neighborhoods lie.

For each j, choose a point p_j on L_j, and let θ_j be an angle, measured counterclockwise, from the positive x axis to the oriented tangent to L_j at p_j; note that θ_j is only well-defined up to multiples of 2π. Let $r_u(a_i)$ be the counterclockwise rotation number (the number of revolutions made) for the path in $\pi(L_{u(a_i)})$ beginning at $p_{u(a_i)}$ and following the orientation of $L_{u(a_i)}$ until a_i is reached via $N_u(a_i)$; similarly define $r_l(a_i)$. Then the gradings for the DGA of L are given by choosing $(\rho_1, \ldots, \rho_{k-1}) \in \mathbb{Z}^{k-1}$ and setting

$$\deg a_i = 2(r_l(a_i) - r_u(a_i)) + (\theta_{l(a_i)} - \theta_{u(a_i)})/\pi + 2\rho_{u(a_i)} - 2\rho_{l(a_i)} - 1/2.$$

By comparison, the allowed degrees in [Ch] are given by

$$\deg a_i = 2(r_l(a_i) - r_u(a_i)) + (\theta_{l(a_i)} - \theta_{u(a_i)})/\pi + \rho_{u(a_i)} - \rho_{l(a_i)} - 1/2.$$

The difference arises from the fact that Chekanov never uses the orientations of the link components; this forces $\theta_{l(a_i)}$ and $\theta_{r(a_i)}$ to be well-defined only up to integer multiples of π, rather than 2π.

We now discuss an additional structure on the DGA for a link L, inspired by [Mi]. More precisely, we will describe a variant of the relative homotopy splitting from [Mi]; our variant will split something which is essentially a submodule of the DGA into k^2 pieces which are invariant under Legendrian isotopy.

Definition 2.5.11. For $j_1 \neq j_2$ between 1 and k, inclusive, define $\Gamma_{j_1 j_2}$ to be the module over $\mathbb{Z}[t_1, t_1^{-1}, \ldots, t_k, t_k^{-1}]$ generated by words of the form $a_{i_1} \cdots a_{i_m}$, with $u(a_{i_1}) = j_1$, $l(a_{i_m}) = j_2$, and $u(a_{i_{p+1}}) = l(a_{i_p})$ for $1 \leq p \leq m-1$. If $j_1 = j_2 = j$, then let $\Gamma_{j_1 j_2}$ be the module generated by such words, along with an indeterminate e_j. Finally, let $\Gamma = \oplus \Gamma_{j_1 j_2}$.

The indeterminates e_j will replace the 1 terms in the definition of ∂; see below. Note that $a_i \in \Gamma_{u(a_i) l(a_i)}$.

Although Γ itself is not an algebra, we have the usual multiplication map $\Gamma_{j_1 j_2} \times \Gamma_{j_2 j_3} \to \Gamma_{j_1 j_3}$, given on generators by concatenation, once we stipulate that the e_j's act as the identity.

Our introduction of Γ is motivated by the fact that ∂a_i is essentially in $\Gamma_{u(a_i) l(a_i)}$ for all i. Define $\partial' a_i$ as follows: if $u(a_i) \neq l(a_i)$, then $\partial' a_i = \partial a_i$; if $u(a_i) = l(a_i)$, then $\partial' a_i$ is ∂a_i, except that we replace any 1 or 2 term in ∂a_i by $e_{u(a_i)}$ or $2e_{u(a_i)}$. (It is easy to see that these are the only possible terms in ∂a_i which involve only the t_j's and no a_m's.)

Lemma 2.5.12. *$\partial' a_i \in \Gamma_{u(a_i) l(a_i)}$ for all i.*

Proof. For a term in ∂a_i of the form $a_{i_1} \ldots a_{i_k}$, where we exclude powers of t_j's, we wish to prove that $u(a_{i_1}) = u(a_i)$, $l(a_{i_k}) = l(a_i)$, and $u(a_{i_{p+1}}) = l(a_{i_p})$ for all p. Consider the boundary of the map which gives the term $a_{i_1} \ldots a_{i_k}$. By definition, the portion of this boundary connecting a_{i_p} to $a_{i_{p+1}}$ belongs to link component $l(a_{i_p})$ on one hand, and $u(a_{i_{p+1}})$ on the other. We similarly find that $u(a_{i_1}) = u(a_i)$ and $l(a_{i_k}) = l(a_i)$. $\square$

Definition 2.5.13. The *differential link module* of L is (Γ, ∂'), where we have defined $\partial' a_i$ above, and we extend ∂' to Γ by applying the signed Leibniz rule and setting $\partial' e_j = 0$ for all j. A grading for Γ is one inherited from the DGA of L, with $\deg e_j = 0$ for all j.

We may define (grading-preserving) elementary and tame automorphisms and tame isomorphisms for differential link modules as for DGAs, with the additional stipulation that all maps must preserve the link module structure by preserving $\Gamma_{j_1 j_2}$ for all j_1, j_2. Similarly, we may define an algebraic stabilization of a differential link module, with the additional stipulation that the two added generators both belong to the same $\Gamma_{j_1 j_2}$. As usual, we then define two differential link modules to be equivalent if they are tamely isomorphic after some number of algebraic stabilizations. We omit the proof of the following result, which again is simply a variant on the proofs given in Appendix A.

Proposition 2.5.14. *If L and L' are Legendrian-isotopic oriented links, then for any grading of the differential link module for L, there is a grading of the differential link module for L' so that the two are equivalent.*

In this dissertation, we will not use the full strength of the differential link module. We will, however, apply first-order Poincaré-Chekanov polynomials derived from the differential link module; we now describe these polynomials, first mentioned in [Mi]. For the definition of augmentations for knots, and background on Poincaré-Chekanov polynomials, please refer to Section 3.2.

Assume that $r(L_1) = \cdots = r(L_k) = 0$, and let Γ be the differential link module for L, with some fixed grading. We consider the DGAs for L and $L_1, \ldots, L_k$ over $\mathbb{Z}/2$; that is, set $t_j = 1$ for all j, and reduce modulo 2.

Definition 2.5.15. Suppose that, when considered alone as a knot, the DGA for each of $L_1, \ldots, L_k$ has an augmentation $\varepsilon_1, \ldots, \varepsilon_k$. Extend these augmentations to all vertices a_i of L by setting

$$\varepsilon(a_i) = \begin{cases} \varepsilon_{u(a_i)}(a_i) & \text{if } u(a_i) = l(a_i) \\ 0 & \text{otherwise.} \end{cases}$$

We define an *augmentation* of L to be any function ε obtained in this way.

An augmentation ε, as usual, gives rise to a first-order Poincaré-Chekanov polynomial $P^{\varepsilon,1}(\lambda)$; we may say, a bit imprecisely, that this polynomial splits into k^2 polynomials $P^{\varepsilon,1}_{j_1 j_2}(\lambda)$, corresponding to the pieces in $\Gamma_{j_1 j_2}$.

The polynomials $P^{\varepsilon,1}_{jj}(\lambda)$ are precisely the polynomials $P^{\varepsilon_j,1}(\lambda)$ for each individual link component L_j. For practical purposes, we can define $P^{\varepsilon,1}_{j_1 j_2}(\lambda)$ for $j_1 \neq j_2$ as follows. For $a_i \in \Gamma_{j_1 j_2}$, define $\partial^{(1)}_\varepsilon a_i$ to be the image of ∂a_i under the following operation: discard all terms in ∂a_i containing more than one a_m with $u(a_m) \neq l(a_m)$, and replace each a_m in ∂a_i by $\varepsilon(a_m)$ whenever $u(a_m) = l(a_m)$. If we write $V_{j_1 j_2}$ as the vector space over $\mathbb{Z}/2$ generated by $\{a_i \in \Gamma_{j_1 j_2}\}$, then $\partial^{(1)}_\varepsilon$ preserves $V_{j_1 j_2}$ and $\left(\partial^{(1)}_\varepsilon\right)^2 = 0$. We may then set $P^{\varepsilon,1}_{j_1 j_2}(\lambda)$ to be the Poincaré polynomial of $\partial^{(1)}_\varepsilon$ on $V_{j_1 j_2}$, i.e., the polynomial in λ whose λ^i coefficient is the dimension of the i-th graded piece of $(\ker \partial^{(1)}_\varepsilon)/(\operatorname{im} \partial^{(1)}_\varepsilon)$.

We may also define higher-order Poincaré-Chekanov polynomials $P^{\varepsilon,n}_{j_1 j_2}(\lambda)$ by examining the action of ∂' on $\Gamma_{j_1 j_2}$, but we will not need these here.

The following result, which follows directly from Proposition 2.5.14 and Chekanov's corresponding result from [Ch], will be used extensively in Chapter 4.

Theorem 2.5.16. *Suppose that L and L' are Legendrian-isotopic oriented links. Then, for any given grading and augmentation of the DGA for L, there is a grading and augmentation of the DGA for L' so that the first-order Poincaré-Chekanov polynomials $P^{\varepsilon,1}_{j_1 j_2}$ for L and L' are equal for all j_1, j_2.*

Remark 2.5.17. While $P^{\varepsilon,1}_{jj}(-1) = tb(L_j)$ as usual, we also have $P^{\varepsilon,1}_{j_1 j_2}(-1) = \mathrm{lk}(L_{j_1}, L_{j_2})$, the linking number of L_{j_1} and L_{j_2}, for $j_1 \neq j_2$. Also, we have $\sum_{j_1,j_2} P^{\varepsilon,1}_{j_1 j_2}(-1) = tb(L)$. We conclude that the first-order Poincaré-Chekanov polynomials incorporate the classical invariants for oriented links (see Section 1.2.

Example 2.5.18. For the link from Example 2.5.7, an augmentation is any map with $\varepsilon(a_i) = 0$ for $i \geq 4$. Then $\partial^{(1)}_\varepsilon$ is identically zero, and the first-order Poincaré-Chekanov polynomials simply measure the degrees of the a_i. More precisely, for a choice of grading $(\rho_1, \rho_2) \in \mathbb{Z}^2$, we have

$$\begin{array}{lll} P^{\varepsilon,1}_{11}(\lambda) = \lambda & P^{\varepsilon,1}_{21}(\lambda) = \lambda^{1+2\rho_2-2\rho_1} & P^{\varepsilon,1}_{31}(\lambda) = \lambda^{1-2\rho_1} \\ P^{\varepsilon,1}_{12}(\lambda) = \lambda^{-1+2\rho_1-2\rho_2} & P^{\varepsilon,1}_{22}(\lambda) = \lambda & P^{\varepsilon,1}_{32}(\lambda) = \lambda^{1-2\rho_2} \\ P^{\varepsilon,1}_{13}(\lambda) = \lambda^{-1+2\rho_1} & P^{\varepsilon,1}_{23}(\lambda) = \lambda^{-1+2\rho_2} & P^{\varepsilon,1}_{33}(\lambda) = \lambda. \end{array}$$

Remark 2.5.19. Unoriented links. For *unoriented* links, we simply expand the set of allowed gradings $(\rho_1, \ldots, \rho_{k-1})$ to allow half-integers, as in [Ch]. Indeed, a grading of half-integers $(\rho_1, \ldots, \rho_{k-1})$ corresponds to changing the original orientation of L by either reversing the orientation of $\{L_j : 2\rho_j \text{ odd}\}$, or reversing the orientations of L_k and $\{L_j : 2\rho_j \text{ even}\}$. We may deduce this by examining how the capping paths and degrees change when we change the orientation (and hence base point) of one link component L_j.

Chapter 3

The characteristic algebra

We would like to use the Chekanov-Eliashberg DGA to distinguish between Legendrian isotopy classes of knots. Unfortunately, it is often hard to tell when two DGAs are equivalent. In particular, the homology of a DGA is generally infinite-dimensional and difficult to grasp; this prevents us from applying Corollary 2.4.4 directly.

Until now, the only known "computable" Legendrian invariants—that is, nonclassical invariants which can be used in practice to distinguish between Legendrian isotopy classes of knots—were the first-order Poincaré-Chekanov polynomial and its higher-order analogues. However, the Poincaré-Chekanov polynomial is not defined for all Legendrian knots, nor is it necessarily uniquely defined; in addition, as we shall see, there are many nonisotopic knots with the same polynomial. The higher-order polynomials, on the other hand, are difficult to compute, and have not yet been successfully used to distinguish Legendrian knots.

In Section 3.1, we introduce the characteristic algebra, a Legendrian invariant derived from the DGA, which is nontrivial for most, if not all, Legendrian knots with maximal Thurston-Bennequin number. The characteristic algebra encodes the information from at least the first- and second-order Poincaré-Chekanov polynomials, as we explain in Section 3.2. We will demonstrate the efficacy of our invariant, through examples, in Chapter 4.

Although the results of this chapter hold for links as well, we will confine our attention to knots for simplicity, except in Remark 3.1.5.

3.1 Definition of the characteristic algebra

The definition of our new invariant is quite simple.

Definition 3.1.1. Let (A, ∂) be a DGA over $\mathbb{Z}[t, t^{-1}]$, where $A = \mathbb{Z}[t, t^{-1}]\langle a_1, \dots, a_n \rangle$, and let I denote the (two-sided) ideal in A generated by $\{\partial a_i \mid 1 \leq i \leq n\}$. The *characteristic algebra* $\mathcal{C}(A, \partial)$ is defined to be the algebra A/I, with grading induced from the grading on A.

Definition 3.1.2. Two characteristic algebras A_1/I_1 and A_2/I_2 are *tamely isomorphic* if we can add some number of generators to A_1 and the same generators to I_1, and similarly for A_2 and I_2, so that there is a tame isomorphism between A_1 and A_2 sending I_1 to I_2.

In particular, tamely isomorphic characteristic algebras are isomorphic as algebras. Strictly speaking, Definition 3.1.2 only makes sense if we interpret the characteristic algebra as a pair (A, I) rather than as A/I, but we will be sloppy with our notation. Recall that we defined tame isomorphism between free algebras in Section 2.4.

A stabilization of (A, ∂), as defined in Section 2.4, adds two generators e_1, e_2 to A and one generator e_2 to I; thus A/I changes by adding one generator e_1 and no relations.

Definition 3.1.3. Two characteristic algebras A_1/I_1 and A_2/I_2 are *equivalent* if they are tamely isomorphic, after adding a (possibly different) finite number of generators (but no additional relations) to each.

Theorem 3.1.4. *Legendrian-isotopic knots have equivalent characteristic algebras.*

Proof. Let (A, ∂) be a DGA with $A = \mathbb{Z}[t, t^{-1}]\langle a_1, \dots, a_n \rangle$. Consider an elementary automorphism of A sending a_j to $a_j + v$, where v does not involve a_j; since $\partial(a_j + v)$ is in I, it is easy to see that this automorphism descends to a map on characteristic algebras. We conclude that tamely isomorphic DGAs have tamely isomorphic characteristic algebras. On the other hand, equivalence of characteristic algebras is defined precisely to be preserved under stabilization of DGAs. □

Remark 3.1.5. Characteristic module for links. In the case of a link, we may also define the *characteristic module* arising from the differential link module (Γ, ∂') introduced in Section 2.5. This is the module over $\mathbb{Z}[t_1, t_1^{-1}, \dots, t_k, t_k^{-1}]$ generated by Γ, modulo the relations

$$v_1(\partial' a_i)v_2 = 0 \,:\, v_1 \in \Gamma_{j_1 j_2}, a_i \in \Gamma_{j_2 j_3}, v_2 \in \Gamma_{j_3 j_4} \text{ for some } j_1, j_2, j_3, j_4.$$

Define equivalence of characteristic modules similarly to equivalence of characteristic algebras, except that replacing a generator a_i by $t_{u(a_i)}^{\pm 1} a_i$ or $t_{l(a_i)}^{\pm 1} a_i$ is allowed. Then Legendrian-isotopic links have equivalent characteristic modules. An approach along these lines is used in [Mi] to distinguish between particular links.

3.2 Relation to the Poincaré-Chekanov polynomial invariants

In this section, we work over $\mathbb{Z}/2$ rather than over $\mathbb{Z}[t, t^{-1}]$; simply set $t = 1$ and reduce modulo 2. Thus we consider the DGA (A, ∂) of a Legendrian knot K over $\mathbb{Z}/2$, graded over $\mathbb{Z}/(2r(K))$; let $\mathcal{C} = A/I$ be its characteristic algebra.

We first review the definition of the Poincaré-Chekanov polynomials. The following term is taken from [EFM].

Definition 3.2.1. Let (A, ∂) be a DGA over $\mathbb{Z}/2$. An algebra map $\varepsilon : A \to \mathbb{Z}/2$ is an *augmentation* if $\varepsilon(1) = 1$, $\varepsilon \circ \partial = 0$, and ε vanishes for any element in A of nonzero degree.

Given an augmentation ε of (A, ∂), write $A_\varepsilon = \ker \varepsilon$; then ∂ maps $(A_\varepsilon)^n$ into itself for all n, and thus ∂ descends to a map $\partial^{(n)} : A_\varepsilon/A_\varepsilon^{n+1} \to A_\varepsilon/A_\varepsilon^{n+1}$. We can break $A_\varepsilon/A_\varepsilon^{n+1}$ into graded pieces $\sum_{i \in \mathbb{Z}/(2r(K))} C_i^{(n)}$, where $C_i^{(n)}$ denotes the piece of degree i. Write $\alpha_i^{(n)} = \dim_{\mathbb{Z}/2} \ker(\partial^{(n)} : C_i^{(n)} \to C_{i-1}^{(n)})$ and $\beta_i^{(n)} = \dim_{\mathbb{Z}/2} \operatorname{im}(\partial^{(n)} : C_{i+1}^{(n)} \to C_i^{(n)})$, so that $\alpha_i^{(n)} - \beta_i^{(n)}$ is the dimension of the i-th graded piece of the homology of $\partial^{(n)}$.

Definition 3.2.2. The *Poincaré-Chekanov polynomial of order n* associated to an augmentation ε of (A, ∂) is $P_{\varepsilon,n}(\lambda) = \sum_{i \in \mathbb{Z}/(2r(K))} \left(\alpha_i^{(n)} - \beta_i^{(n)}\right) \lambda^i$.

Note that augmentations of a DGA do not always exist.

The main result of this section states that we can recover some Poincaré-Chekanov polynomials from the characteristic algebra. To do this, we need one additional bit of information, besides the characteristic algebra.

Definition 3.2.3. Let γ_i be the number of generators of degree i of a DGA (A, ∂) graded over $\mathbb{Z}/(2r(K))$. Then the *degree distribution* $\gamma : \mathbb{Z}/(2r(K)) \to \mathbb{Z}_{\geq 0}$ of A is the map $i \mapsto \gamma_i$.

Clearly, the degree distribution can be immediately computed from a diagram of K by calculating the degrees of the vertices of K.

We are now ready for the main result of this section. Note that the following proposition uses the *isomorphism* class, not the equivalence class, of the characteristic algebra.

Proposition 3.2.4. *The set of first- and second-order Poincaré-Chekanov polynomials for all possible augmentations of a DGA (A, ∂) is determined by the isomorphism class of the characteristic algebra $\mathcal{C}$ and the degree distribution of A.*

Before we can prove Proposition 3.2.4, we need to establish a few ancillary results. Our starting point is the observation that there is a one-to-one correspondence between augmentations and maximal ideals $\langle a_1 + c_1, \dots, a_n + c_n \rangle \subset A$ containing I and satisfying $c_i = 0$ if $\deg a_i \neq 0$.

Fix an augmentation ε. We first assume for convenience that $\varepsilon = 0$; then $I \subset M$, where M is the maximal ideal $\langle a_1, \dots, a_n \rangle$. For each i, write

$$\partial a_i = \partial_1 a_i + \partial_2 a_i + \partial_3 a_i,$$

where $\partial_1 a_i$ is linear in the a_j, $\partial_2 a_i$ is quadratic in the a_j, and $\partial_3 a_i$ contains terms of third or higher order. The following lemma writes ∂_1 in a standard form.

Lemma 3.2.5. *After a tame automorphism, we can relabel the a_i as $a_1, \dots, a_k, b_1, \dots, b_k$, $c_1, \dots, c_{n-2k}$ for some k, so that $\partial_1 a_i = b_i$ and $\partial_1 b_i = \partial_1 c_i = 0$ for all i.*

Proof. For clarity, we first relabel the a_i as $\tilde{a}_i$. We may assume that the $\tilde{a}_i$ are ordered so that $\partial \tilde{a}_i$ contains only terms involving $\tilde{a}_j$, $j < i$; see [Ch]. Let i_1 be the smallest number so that $\partial_1 \tilde{a}_{i_1} \neq 0$. We can write $\partial_1 \tilde{a}_{i_1} = \tilde{a}_{j_1} + v_1$, where $j_1 < i_1$ and the expression v_1 does not involve $\tilde{a}_{j_1}$. After applying the elementary isomorphism $\tilde{a}_{j_1} \mapsto \tilde{a}_{j_1} + v_1$, we may assume that $v_1 = 0$ and $\partial_1 \tilde{a}_{i_1} = \tilde{a}_{j_1}$.

For any $\tilde{a}_i$ such that $\partial_1 \tilde{a}_i$ involves $\tilde{a}_{j_1}$, replace $\tilde{a}_i$ by $\tilde{a}_i + \tilde{a}_{i_1}$. Then $\partial_1 \tilde{a}_i$ does not involve $\tilde{a}_{j_1}$ unless $i = i_1$; in addition, no $\partial_1 \tilde{a}_i$ can involve $\tilde{a}_{i_1}$, since then $\partial_1^2 \tilde{a}_i$ would involve $\tilde{a}_{j_1}$. Set $a_1 = \tilde{a}_{i_1}$ and $b_1 = \tilde{a}_{i_1}$; then $\partial_1 a_1 = b_1$ and $\partial_1 \tilde{a}_i$ does not involve a_1 or b_1 for any other i.

Repeat this process with the next smallest $\tilde{a}_{i_2}$ with $\partial_1 \tilde{a}_{i_2} \neq 0$, and so forth. At the conclusion of this inductive process, we obtain $a_1, \dots, a_k, b_1, \dots, b_k$ with $\partial_1 a_i = b_i$ (and $\partial_1 b_i = 0$), and the remaining $\tilde{a}_i$ satisfy $\partial_1 \tilde{a}_i = 0$; relabel these remaining generators with c's. □

Now assume that we have relabelled the generators of A in accordance with Lemma 3.2.5.

Lemma 3.2.6. *$\beta_\ell^{(1)}$ is the number of b_j of degree ℓ, while $\beta_\ell^{(2)} - \beta_\ell^{(1)}$ is the dimension of the degree ℓ subspace of the vector space generated by*

$$\{\partial_2 b_i, \partial_2 c_i, a_i b_j + b_i a_j, b_i b_j, b_i c_j, c_i b_j\},$$

where i, j range over all possible indices.

Proof. The statement for $\beta_\ell^{(1)}$ is obvious. To calculate $\beta_\ell^{(2)} - \beta_\ell^{(1)}$, note that the image of $\partial^{(2)}$ in A/A^3 is generated by $\partial a_i = b_i + \partial_2 a_i$, $\partial b_i = \partial_2 b_i$, $\partial c_i = \partial_2 c_i$, $\partial(a_i a_j) = a_i b_j + b_i a_j$, $\partial(a_i b_j) = b_i b_j$, $\partial(b_i a_j) = b_i b_j$, $\partial(a_i c_j) = b_i c_j$, and $\partial(c_i a_j) = c_i b_j$. □

We wish to write $\beta_\ell^{(n)}$ in terms of $\mathcal{C}$, but we first pass through an intermediate step. Let $N^{(n)}$ be the image of I in M/M^{n+1}, and let $\delta_\ell^{(n)}$ be the dimension of the degree ℓ part of $N^{(n)}$. Lemma 3.2.8 below relates $\beta_\ell^{(n)}$ to $\delta_\ell^{(n)}$ for $n = 1, 2$.

Lemma 3.2.7. *$\delta_\ell^{(1)}$ is the number of b_i of degree ℓ, while $\delta_\ell^{(2)} - \delta_\ell^{(1)}$ is the dimension of the degree ℓ subspace of the vector space generated by*

$$\{\partial_2 b_i, \partial_2 c_i, a_i b_j, b_i a_j, b_i b_j, b_i c_j, c_i b_j\},$$

where i, j range over all possible indices.

Proof. This follows immediately from the fact that I is generated by $\{\partial a_i, \partial b_i, \partial c_i\}$. □

Lemma 3.2.8. *$\beta_\ell^{(1)} = \delta_\ell^{(1)}$ and $\beta_\ell^{(2)} = \delta_\ell^{(2)} - \sum_{\ell'} \delta_{\ell'} \delta_{\ell - \ell' - 1}$.*

Proof. We use Lemmas 3.2.6 and 3.2.7. The first equality is obvious. For the second equality, we claim that, for fixed i and j, $a_i b_j$ only appears in conjunction with $b_i a_j$ in the expressions $\partial_2 b_m$ and $\partial_2 c_m$, for arbitrary m. It then follows that $\delta_\ell^{(2)} - \beta_\ell^{(2)}$ is the number of $a_i b_j$ of degree ℓ, which is $\sum_{\ell'} \delta_{\ell'} \delta_{\ell - \ell' - 1}$.

To prove the claim, suppose that $\partial_2 b_m$ contains a term $a_i b_j$. Since $\partial_2^2 b_m = 0$ and $\partial_2(a_i b_j) = b_i b_j$, there must be another term in $\partial_2 b_m$ which, when we apply ∂_2, gives $b_i b_j$; but this term can only be $b_i a_j$. The same argument obviously holds for $\partial_2 c_m$. □

Now let ε be any augmentation, and let $M_\varepsilon = \langle a_1 + \varepsilon(a_1), \ldots, a_n + \varepsilon(a_n) \rangle$ be the corresponding maximal ideal in A. If we define $N^{(n)}$ and $\delta_\ell^{(n)}$ as above, except with M replaced by M_ε, then Lemma 3.2.8 still holds. We are now ready to prove Proposition 3.2.4.

Proof of Proposition 3.2.4. Note that

$$(M_\varepsilon / M_\varepsilon^{n+1}) / N^{(n)} \cong (M_\varepsilon / I) / (M_\varepsilon / I)^{n+1};$$

the characteristic algebra $\mathcal{C} = A/I$ and the choice of augmentation ε determine the right hand side. On the other hand, the dimension of the degree ℓ part of $M_\varepsilon / M_\varepsilon^{n+1}$ is γ_ℓ if $n = 1$, and $\gamma_\ell + \sum_{\ell'} \gamma_{\ell'} \gamma_{\ell - \ell'}$ if $n = 2$. It follows that we can calculate $\{\delta_\ell^{(1)}\}$ and $\{\delta_\ell^{(2)}\}$ from $\mathcal{C}$, ε, and γ.

Fix $n = 1, 2$. By Lemma 3.2.8, we can then calculate $\{\beta_\ell^{(n)}\}$ and hence the Poincaré-Chekanov polynomial

$$P_{\varepsilon,n}(\lambda) = \sum_\ell \left((\alpha_\ell^{(n)} + \beta_{\ell-1}^{(n)}) - \beta_\ell^{(n)} - \beta_{\ell-1}^{(n)} \right) \lambda^\ell.$$

Letting ε vary over all possible augmentations yields the proposition. □

Remark 3.2.9. Another set of invariants, similar to the Poincaré-Chekanov polynomials, are obtained by ignoring the grading of the DGA, and considering ungraded augmentations. In this case, the invariants are a set of integers, rather than polynomials, in each order. A

proof similar to the one above shows that the first- and second-order ungraded invariants are determined by the characteristic algebra.

Remark 3.2.10. The situation for higher-order Poincaré-Chekanov polynomials seems more difficult; we tentatively make the following conjecture.

Conjecture 3.2.11. *The isomorphism class of $\mathcal{C}$ and the degree distribution of A determine the Poincaré-Chekanov polynomials in all orders.*

Remark 3.2.12. In practice, we apply Proposition 3.2.4 as follows. Given two DGAs, stabilize each with the appropriate number and degrees of stabilizations so that the two resulting DGAs have the same degree distribution. If these new DGAs have isomorphic characteristic algebras, then they have the same first- and second-order Poincaré-Chekanov polynomials (if augmentations exist). If not, then we can often see that their characteristic algebras are not equivalent, and so the original DGAs are not equivalent. Thus calculating characteristic algebras often obviates the need to calculate first- and second-order Poincaré-Chekanov polynomials.

Remark 3.2.13. Abelianized characteristic algebras. Note that the first-order Poincaré-Chekanov polynomials depends only on the abelianization of (A, ∂). If the procedure described in Remark 3.2.12 yields two characteristic algebras whose abelianizations are isomorphic, then the original DGAs have the same first-order Poincaré-Chekanov polynomials.

On a related note, empirical evidence leads us to propose the following conjecture, which would yield a new topological knot invariant.

Conjecture 3.2.14. *For a Legendrian knot K with maximal Thurston-Bennequin number, the equivalence class of the abelianized characteristic algebra of K, considered without grading and over $\mathbb{Z}$, depends only on the topological class of K.*

Here the abelianization is unsigned: $vw = wv$ for all v, w.

Remark 3.2.15. Scheme interpretation. We can view the abelianization of $\mathcal{C}$ in terms of algebraic geometry. If $\mathcal{C} = (\mathbb{Z}/2)\langle a_1, \ldots, a_n\rangle \,/\, I$, then the abelianization of $\mathcal{C}$ gives rise to a scheme X in $\mathbb{A}^n$, affine n-space over $\mathbb{Z}/2$. Theorem 3.1.4 immediately implies the following result.

Corollary 3.2.16. *The scheme X is a Legendrian-isotopy invariant, up to changes of coordinates and additions of extra coordinates (i.e., we can replace $X \subset \mathbb{A}^n$ by $X \times \mathbb{A} \subset \mathbb{A}^{n+1}$).*

There is a conjecture about first-order Poincaré-Chekanov polynomials, suggested by Chekanov, which has a nice interpretation in our scheme picture.

Conjecture 3.2.17 ([Ch]). *The first-order Poincaré-Chekanov polynomial is independent of the augmentation ε.*

Augmentations are simply the $(\mathbb{Z}/2)$-rational points in X, graded in the sense that all coordinates corresponding to a_j of nonzero degree are zero. It is not hard to see that the first-order Poincaré-Chekanov polynomial at a $(\mathbb{Z}/2)$-rational point p in X is precisely the "graded" codimension in $\mathbb{A}^n$ of T_pX, the tangent space to X at p. The following conjecture, which we have verified in many examples, would imply Conjecture 3.2.17.

Conjecture 3.2.18. *The scheme X is irreducible and smooth at each $(\mathbb{Z}/2)$-rational point.*

Chapter 4

Applications

In this chapter, we give several illustrations of the constructions and results from Chapters 2 and 3, especially Theorems 2.5.16 and 3.1.4. The first four examples, all knots, both illustrate the computation of the characteristic algebra described in Section 3.1, and demonstrate its usefulness in distinguishing between Legendrian knots. The last three, all multi-component links, apply the techniques of Section 2.5 to conclude some results about Legendrian links.

Instead of using the full DGA over $\mathbb{Z}[t, t^{-1}]$ or $\mathbb{Z}[t_1, t_1^{-1}, \ldots, t_k, t_k^{-1}]$, we will work over $\mathbb{Z}/2$ by setting $t = 1$ and reducing modulo 2. We hope soon to have applications of the full algebra.

4.1 Example 1: 6_2

Our first example revisits the argument of [Ng1], which showed that there exist knots not Legendrian isotopic to their Legendrian mirrors. Let K be the unoriented Legendrian knot given in Figure 4-1, which is of knot type 6_2, with $r = 0$ and $tb = -7$. Here we will use the characteristic algebra to give a proof which is essentially identical to the one in [Ng1], but slightly cleaner.

With vertices labelled as in Figure 4-1, the differential on the DGA (A, ∂) for K is given by $A = \mathbb{Z}\langle a_1, \ldots, a_9, b_1, b_2 \rangle$ and

$$\begin{aligned} \partial a_1 &= 1 + a_8 a_3 b_1 & \qquad \partial a_4 &= a_6 a_8 \\ \partial a_2 &= 1 + b_1(1 + a_5 a_8 + a_9 a_4) & \qquad \partial a_5 &= a_9 a_6 \\ \partial b_2 &= a_9 + (1 + a_5 a_8 + a_9 a_4) a_3 & \qquad \partial a_7 &= 1 + a_8 a_9 \end{aligned}$$
$$\partial a_3 = \partial a_6 = \partial a_8 = \partial a_9 = \partial b_1 = 0.$$

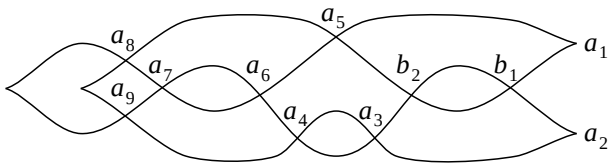

Figure 4-1: Front projection for the Legendrian knot K, of type 6_2, with vertices labelled. The use of a_i and b_i to label the vertices is not related to the a_i and b_i from Lemma 3.2.5; we use a and b to denote vertices of odd and even degree, respectively.

The ideal I is generated by the above expressions. More precisely, $I = \langle f_1, f_2, f_3, f_4, f_5, f_6 \rangle$, where

$$\begin{aligned} f_1 &= 1 + a_8 a_3 b_1 & f_4 &= a_6 a_8 \\ f_2 &= 1 + b_1(1 + a_5 a_8 + a_9 a_4) & f_5 &= a_9 a_6 \\ f_3 &= a_9 + (1 + a_5 a_8 + a_9 a_4) a_3 & f_6 &= 1 + a_8 a_9. \end{aligned}$$

The characteristic algebra of K is then given by $\mathcal{C} = A/I$.

The grading on A and $\mathcal{C}$ is given as follows: a_1, a_2, a_4, a_7, and a_8 have degree 1; b_1, b_2 have degree 0; and a_3, a_5, a_6, a_9 have degree -1.

Note that the characteristic algebra for the Legendrian mirror of K is the same as $\mathcal{C} = A/I$, but with each term in I reversed.

Lemma 4.1.1. *We have*

$$\begin{aligned} \mathcal{C} \cong (\mathbb{Z}/2)\langle a_1, \ldots, a_5, a_7, a_8, b_1, b_2 \rangle \,/ \\ \langle 1 + a_8 a_3 b_1, 1 + b_1 a_8 a_3, 1 + a_8^2 a_3^2, 1 + a_8 a_3 + a_5 a_8 + a_8 a_3^2 a_4 \rangle. \end{aligned}$$

Proof. We perform a series of computations in $\mathcal{C} = A/I$:

$$a_6 = a_6 + (1 + a_8 a_9) a_6 = a_8 (a_9 a_6) = 0;$$

$$1 + a_5 a_8 + a_9 a_4 = a_8 a_3 b_1 (1 + a_5 a_8 + a_9 a_4) = a_8 a_3;$$

$$a_9 = (1 + a_5 a_8 + a_9 a_4) a_3 = a_8 a_3^2.$$

Substituting for a_6 and a_9 in the relations f_i yields the relations in the statement of the lemma. Conversely, given the relations in the statement of the lemma, and setting $a_6 = 0$ and $a_9 = a_8 a_3^2$, we can recover the relations f_i. □

Decompose $\mathcal{C}$ into graded pieces $\mathcal{C} = \oplus_i \mathcal{C}_i$, where $\mathcal{C}_i$ is the piece of degree i.

Lemma 4.1.2. *There do not exist $v \in \mathcal{C}_{-1}, w \in \mathcal{C}_1$ such that $vw = 1 \in \mathcal{C}$.*

Proof. Suppose otherwise, and consider the algebra $\mathcal{C}'$ obtained from $\mathcal{C}$ by setting $b_1 = 1, a_1 = a_2 = a_4 = a_5 = a_7 = 0$. There is an obvious projection from $\mathcal{C}$ to $\mathcal{C}'$ which is an algebra map; under this projection, v, w map to $v' \in \mathcal{C}'_{-1}, w' \in \mathcal{C}'_1$, with $v'w' = 1$ in $\mathcal{C}'$. But it is easy to see that $\mathcal{C}' = (\mathbb{Z}/2)\langle a_3, a_8 \rangle \,/\, \langle 1 + a_8 a_3 \rangle$, with $a_3 \in \mathcal{C}'_{-1}$ and $a_8 \in \mathcal{C}'_1$, and it follows that there do not exist such v', w'. □

Proposition 4.1.3. *K is not Legendrian isotopic to its Legendrian mirror.*

Proof. Let $\tilde{\mathcal{C}}$ be the characteristic algebra of the Legendrian mirror of K. Since the relations in $\tilde{\mathcal{C}}$ are precisely the relations in $\mathcal{C}$ reversed, Lemma 4.1.2 implies that there do not exist $v \in \tilde{\mathcal{C}}_1, w \in \tilde{\mathcal{C}}_{-1}$ such that $vw = 1$. On the other hand, there certainly do exist $v \in \mathcal{C}_1, w \in \mathcal{C}_{-1}$ such that $vw = 1$; for instance, take $v = a_8$ and $w = -a_3 b_1$. Hence $\mathcal{C}$ and $\tilde{\mathcal{C}}$ are not isomorphic. This argument still holds if some number of generators is added to $\mathcal{C}$ and $\tilde{\mathcal{C}}$, and so $\mathcal{C}$ and $\tilde{\mathcal{C}}$ are not equivalent. The result follows from Theorem 3.1.4. □

Remark 4.1.4. More generally, the characteristic algebra technique seems to be an effective way to distinguish between some knots and their Legendrian mirrors; see Remark 4.2.5 for another example. Note that Poincaré-Chekanov polynomials of any order can never tell

between a knot and its mirror, since, as noted above, the differential for a mirror is the differential for the knot, with each monomial reversed.

4.2 Example 2: 7_4

Our second example shows that the characteristic algebra is effective even when Poincaré-Chekanov polynomials do not exist. In addition, Examples 2, 3, and 4 are the first examples, known to the author, in which the DGA grading is not needed to distinguish between knots.

Consider the Legendrian knots K_1, K_2 shown in Figure 4-2; both are of smooth type 7_4, with $r = 0$ and $tb = 1$. We will show that K_1 and K_2 are not Legendrian isotopic. We present this example before the 6_3 and 7_2 examples of Sections 4.3 and 4.4 because the algebra is a bit simpler in this case.

The differential on the DGA for K_1 is given by

$$\begin{aligned} \partial a_1 &= 1 + b_4 b_7 b_1 & \partial a_5 &= 1 + b_7 b_6 \\ \partial a_2 &= 1 + b_1 b_7 b_4 & \partial a_6 &= 1 + b_6 b_7 \\ \partial a_3 &= b_7(1 + b_4 b_3) & \partial b_2 &= a_3 b_4 b_7 + b_7 b_4 a_4 \\ \partial a_4 &= (1 + b_3 b_4) b_7 & \partial b_5 &= b_7 a_6 - a_5 b_7; \end{aligned}$$

the differential for K_2 is given by

$$\begin{aligned} \partial a_1 &= 1 + (1 + b_4 b_5 + b_4 b_7 + b_6 b_7 + b_4 b_5 b_6 b_7 + b_4 a_5 a_6 b_7) b_1 \\ \partial a_2 &= 1 + b_1 b_7 b_4 \\ \partial a_3 &= b_7(1 + b_4 b_3) \\ \partial a_4 &= b_3 + b_5 + b_7 + b_3 b_4 b_5 + b_3 b_4 b_7 + b_3 b_6 b_7 + b_5 b_6 b_7 + b_3 b_4 b_5 b_6 b_7 + a_5 a_6 b_7 + b_3 b_4 a_5 a_6 a_7 \\ \partial a_6 &= 1 + b_7 b_6 \end{aligned}$$

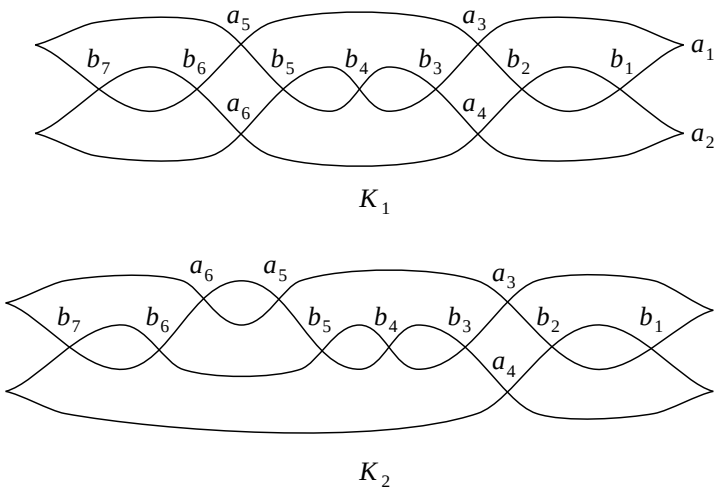

Figure 4-2: The fronts for the Legendrian knots K_1 and K_2, of type 7_4, with vertices labelled.

$$\partial b_2 = b_7 b_4 a_4 + a_6 b_7 + a_3(1 + b_4 b_5 + b_4 b_7 + b_6 b_7 + b_4 b_5 b_6 b_7 + b_4 a_5 a_6 b_7)$$
$$\partial b_5 = a_5 b_7.$$

Denote the characteristic algebras of K_1 and K_2 by $\mathcal{C}_1 = A/I_1$ and $\mathcal{C}_2 = A/I_2$, respectively; here $A = (\mathbb{Z}/2)\langle a_1, \ldots, a_6, b_1, \ldots, b_7\rangle$, and I_1 and I_2 are generated by the respective expressions above.

Lemma 4.2.1. *We have*

$$\mathcal{C}_1 \cong (\mathbb{Z}/2)\langle a_1, a_2, a_3, a_5, b_1, b_2, b_4, b_5, b_7\rangle \,/\, \langle 1 + b_1 b_4 b_7, b_1 b_4 + b_4 b_1, b_1 b_7 + b_7 b_1, b_4 b_7 + b_7 b_4\rangle.$$

Proof. In $\mathcal{C}_1$, we compute that

$$b_1 b_4 b_7 = b_1 b_4 b_7 b_1 b_7 b_4 = b_1 b_7 b_4 = 1$$
$$b_3 = b_1 b_7 b_4 b_3 = b_1 b_7 b_6 b_7 b_4 b_3 = b_1 b_7 b_6 b_7 = b_1 b_7$$
$$b_6 = b_1 b_4 b_7 b_6 = b_1 b_4$$
$$a_4 = b_1 b_7 b_4 a_4 = b_1 a_3 b_4 b_7$$
$$a_6 = b_1 b_4 b_7 a_6 = b_1 b_4 a_5 b_7;$$

substituting for a_4, a_6, b_3, b_6 in the relations for $\mathcal{C}_1$ gives the result. □

Lemma 4.2.2. *There is no expression in $\mathcal{C}_1$ which is invertible from one side but not from the other.*

Proof. It is clear that the only expressions in $\mathcal{C}_1$ which are invertible from either side are products of some number of b_1, b_4, and b_7, with inverses of the same form. Since b_1, b_4, b_7 all commute, the lemma follows. □

Lemma 4.2.3. *In $\mathcal{C}_2$, b_7 is invertible from the right but not from the left.*

Proof. Since $b_7 b_6 = 1$, b_7 is certainly invertible from the right. Now consider adding to $\mathcal{C}_2$ the relations $b_1 = 1$, $b_3 = b_7$, $b_4 = b_6$, $b_2 = b_5 = 0$, and $a_i = 0$ for all i. A straightforward computation reveals that the resulting algebra is isomorphic to $(\mathbb{Z}/2)\langle b_6, b_7\rangle \,/\, \langle 1 + b_7 b_6\rangle$, in which b_7 is not invertible from the left. We conclude that b_7 is not invertible from the left in $\mathcal{C}_2$ either, as desired. □

Proposition 4.2.4. *The Legendrian knots K_1 and K_2 are not Legendrian isotopic.*

Proof. From Lemmas 4.2.2 and 4.2.3, $\mathcal{C}_1$ and $\mathcal{C}_2$ are not equivalent. □

Remark 4.2.5. Although $\mathcal{C}_1$ and $\mathcal{C}_2$ are not equivalent, one may compute that their abelianizations are isomorphic. It is also easy to check that K_1 and K_2 have no augmentations, and hence no Poincaré-Chekanov polynomials.

The computation from the proof of Lemma 4.2.3 also demonstrates that K_2 is not Legendrian isotopic to its Legendrian mirror; we may use the same argument as in Section 4.1, along with the fact that b_6 and b_7 have degrees 2 and -2, respectively, in $\mathcal{C}_2$. By contrast, we see from inspection that K_1 is the same as its Legendrian mirror.

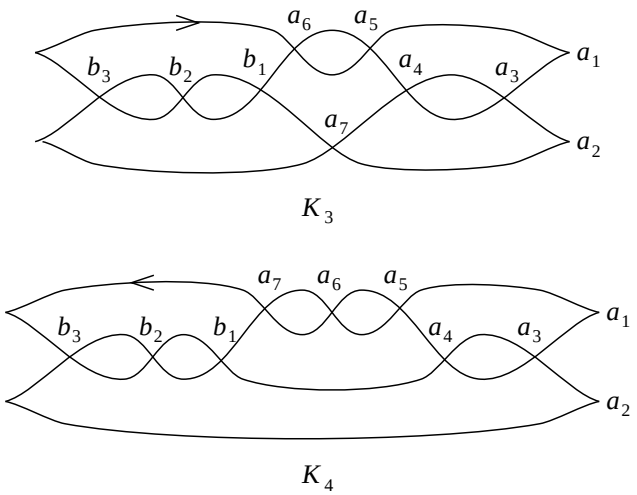

Figure 4-3: The oriented Legendrian knots K_3 and K_4, of type 6_3.

4.3 Example 3: 6_3

This section provides another example of the efficacy of the characteristic algebra when Poincaré-Chekanov polynomials do not exist. It is also the first example, known to the author, of two Legendrian knots with nonzero rotation number which have the same classical invariants but are not Legendrian isotopic. The knots are K_3, K_4 shown in Figure 4-3; both are of smooth type 6_3, with $r = 1$ and $tb = -4$.

We will omit some details in both this section and Section 4.4, since the arguments in both sections are very similar to the argument from Section 4.2.

Remark 4.3.1. We will not need these for the computation, but for both K_1 and K_2, b_2 has degree 0, b_1, b_3 have degree -2, and a_i has degree -1 for all i.

Over $\mathbb{Z}/2$, the differential on the DGA for K_3 is given by

$$\begin{aligned}
\partial a_1 &= 1 + ((1 + b_3b_2)a_7 + a_6(1 + b_2b_3))a_3 \\
\partial a_2 &= 1 + a_3a_5(1 + b_3b_2) \\
\partial a_4 &= 1 + b_2b_3 + a_5((1 + b_3b_2)a_7 + a_6(1 + b_2b_3)) \\
\partial a_6 &= b_1 + b_3 + b_3b_2b_1 \\
\partial a_7 &= b_1 + b_3 + b_1b_2b_3;
\end{aligned}$$

the differential for K_4 is given by

$$\begin{aligned}
\partial a_1 &= 1 + a_6(1 + b_3b_2)a_3 \\
\partial a_2 &= 1 + (1 + a_3a_4)(b_1 + b_3 + b_1b_2b_3) + a_3(a_5 + a_7 + a_5a_6a_7)(1 + b_2b_3) \\
\partial a_4 &= (1 + a_5a_6)(1 + b_3b_2) \\
\partial a_7 &= b_1 + b_3 + b_3b_2b_1.
\end{aligned}$$

Denote the characteristic algebras of K_3 and K_4 by $\mathcal{C}_3$ and $\mathcal{C}_4$, respectively.

Lemma 4.3.2. *We have*

$$\mathcal{C}_3 \cong (\mathbb{Z}/2)\langle a_1, a_2, a_3, a_4, a_6, b_2, b_3\rangle \,/ \\ \langle 1 + a_3(1 + b_2b_3)a_3(1 + b_3b_2), 1 + (1 + b_3b_2)a_3(1 + b_2b_3)a_3\rangle.$$

Proof. In $\mathcal{C}_3$, we compute that

$$(1 + b_1b_2)(1 + b_3b_2) = 1 + (b_1 + b_3 + b_1b_2b_3)b_2 = 1$$
$$(1 + b_3b_2)(1 + b_1b_2) = 1 + b_2(b_1 + b_3 + b_3b_2b_1) = 1$$
$$b_1 = a_3a_5(1 + b_3b_2)b_1 = a_3a_5b_3$$
$$a_5 = a_5((1 + b_3b_2)a_7 + a_6(1 + b_2b_3))a_3 = (1 + b_2b_3)a_3$$
$$a_5(1 + b_3b_2) = ((1 + b_3b_2)a_7 + a_6(1 + b_2b_3))a_3a_5(1 + b_3b_2) = (1 + b_3b_2)a_7 + a_6(1 + b_2b_3)$$
$$a_7 = (1 + b_1b_2)(1 + b_3b_2)a_7 = (1 + b_1b_2)(a_5(1 + b_3b_2) + a_6(1 + b_2b_3));$$

substituting for a_5, a_7, b_1 in the relations for $\mathcal{C}_3$ gives the result. □

Lemma 4.3.3. *There is no expression in $\mathcal{C}_3$ which is invertible from one side but not from the other.*

Proof. It follows from the representation for $\mathcal{C}_3$ given by Lemma 4.3.2 that the expressions a_3, $1+b_2b_3$, and $1+b_3b_2$ are all invertible (from both sides). The only invertible expressions in $\mathcal{C}_3$ which are invertible from either side are derived from these, and are hence invertible from both sides. □

Lemma 4.3.4. *In $\mathcal{C}_4$, a_3 is invertible from the left but not from the right.*

Proof. Since $a_6(1+b_3b_2)a_3 = 1$, a_3 is invertible from the left. Now consider adding to $\mathcal{C}_4$ the relations $a_5 = (b_3+1)a_3$, $a_6 = (b_3+1)a_3$, $b_1 = 1+a_3(b_3+1)a_3$, $b_2 = 1$, $a_1 = a_2 = a_4 = a_7 = 0$. The resulting algebra is isomorphic to $(\mathbb{Z}/2)\langle a_3, b_3\rangle \,/\, \langle 1 + ((b_3 + 1)a_3)^2\rangle$, in which a_3 is not invertible from the right. □

Proposition 4.3.5. *The Legendrian knots K_3 and K_4 are not Legendrian isotopic.*

Remark 4.3.6. The abelianizations of $\mathcal{C}_3$ and $\mathcal{C}_4$ are isomorphic. Neither K_3 nor K_4 has a Poincaré-Chekanov polynomial; it can also be shown that K_3 and K_4 are each isotopic to their Legendrian mirrors (with, of course, the reverse orientations).

4.4 Example 4: 7_2

Our next example applies the characteristic algebra to a case where the first-order Poincaré-Chekanov polynomials exist but fail to distinguish between two knots. Let K_5 and K_6 be the unoriented Legendrian knots shown in Figure 4-4; both are of smooth type 7_2, with $r = 0$ and $tb = 1$.

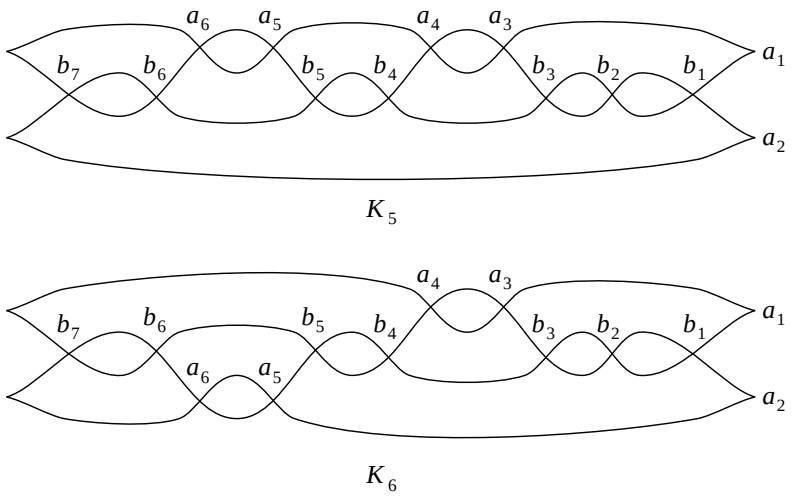

Figure 4-4: The Legendrian knots K_5 and K_6, of type 7_2.

The differential on the DGA for K_5 is given by

$$\begin{aligned}
\partial a_1 &= 1 + ((1 + b_7 b_6)b_5 + b_7(1 + a_6 a_5))(1 + b_2 b_1) \\
\partial a_2 &= 1 + ((b_1 + b_3 + b_1 b_2 b_3)b_4 + (1 + b_1 b_2)(1 + a_3 a_4))b_7 + (1 + b_1 b_2)a_3 b_7 a_6 \\
\partial a_4 &= (1 + b_7 b_6)(1 + b_5 b_4) + b_7(1 + a_6 a_5)b_4 \\
\partial a_6 &= 1 + b_6 b_7 \\
\partial b_3 &= a_3(1 + b_7 b_6)b_5 + a_3 b_7(1 + a_6 a_5) \\
\partial b_5 &= b_7 a_5;
\end{aligned}$$

the differential for K_6 is given by

$$\begin{aligned}
\partial a_1 &= 1 + b_7(1 + b_2 b_1) \\
\partial a_2 &= 1 + ((b_1 + b_3 + b_1 b_2 b_3)(1 + b_4 b_5) + (1 + b_1 b_2)(1 + a_3 a_4)b_5)(1 + b_6 b_7) \\
&\quad + (((b_1 + b_3 + b_1 b_2 b_3)b_4 + (1 + b_1 b_2)(1 + a_3 a_4))\,(1 + a_5 a_6) + (1 + b_1 b_2)a_3 a_6)\,b_7 \\
\partial a_4 &= b_7 b_4 \\
\partial a_6 &= 1 + b_7 b_6 \\
\partial b_3 &= a_3 b_7 \\
\partial b_5 &= a_5 b_7.
\end{aligned}$$

Denote the characteristic algebras of K_5 and K_6 by $\mathcal{C}_5$ and $\mathcal{C}_6$, respectively.

Lemma 4.4.1. *We have*

$$\mathcal{C}_5 \cong (\mathbb{Z}/2)\langle a_1, a_2, a_4, a_6, b_1, b_2, b_3, b_5, b_7 \rangle \,/\, \langle 1 + (1 + b_2 b_1)b_7,\, 1 + b_7(1 + b_2 b_1),\, b_2 b_1 + b_1 b_2 \rangle.$$

Proof. In $\mathcal{C}_5$, we compute that

$$a_5 = (1 + b_6 b_7) a_5 = 0$$
$$a_3 = a_3(b_5 + b_7 + b_7 b_6 b_5)(1 + b_2 b_1) = 0$$
$$b_4 = b_4 + (1 + b_6 b_7) b_4 = b_6((1 + b_7 b_6)(1 + b_5 b_4) + b_7 b_4) = 0$$
$$b_6 = (1 + b_1 b_2) b_7 b_6 = 1 + b_1 b_2;$$

substituting for a_3, a_5, b_4, b_6 in the relations for $\mathcal{C}_5$ gives the result. □

Lemma 4.4.2. *There is no expression in $\mathcal{C}_5$ which is invertible from one side but not from the other.*

Lemma 4.4.3. *In $\mathcal{C}_6$, b_7 is invertible from the right but not from the left.*

Proof. Since $b_7 b_6 = 1$, b_7 is invertible from the right. Now consider adding to $\mathcal{C}_6$ the relations $b_1 = 1$, $b_2 = b_6 + 1$, $b_3 = b_4 = b_5 = 0$, and $a_i = 0$ for all i. The resulting algebra is isomorphic to to $(\mathbb{Z}/2)\langle b_6, b_7 \rangle \,/\, \langle 1 + b_7 b_6 \rangle$, in which b_7 is not invertible from the left. □

Proposition 4.4.4. *The Legendrian knots K_5 and K_6 are not Legendrian isotopic.*

Remark 4.4.5. K_5 and K_6 have the same abelianized characteristic algebras, as usual, and the same degree distributions; hence, by Proposition 3.2.4, they have the same first-order Poincaré-Chekanov polynomial, which we can calculate to be $\lambda + 2$.

4.5 Example 5: triple of the unknot

In this section, we rederive a result of [Mi] by using the link grading from Section 2.5. Our proof is different from the ones in [Mi].

Definition 4.5.1 ([Mi]). Given a Legendrian knot K, let the *n-copy* of K be the link consisting of K, along with $n-1$ copies of K slightly perturbed in the transversal direction. In the front projection, the n-copy is simply n copies of the front of K, differing from each other by small shifts in the z direction. We will call the 2-copy and 3-copy the *double* and *triple*, respectively.

Let $L = (L_1, L_2, L_3)$ be the unoriented triple of the usual "flying-saucer" unknot; this is the unoriented version of the link shown in Figure 2-7.

Proposition 4.5.2 ([Mi]). *The unoriented links (L_1, L_2, L_3) and (L_2, L_1, L_3) are not Legendrian isotopic.*

Proof. In Example 2.5.18, we have already calculated the first-order Poincaré-Chekanov polynomials for (L_1, L_2, L_3), once we allow the grading (ρ_1, ρ_2) to range in $(\frac{1}{2}\mathbb{Z})^2$, as stipulated by Remark 2.5.19. The polynomials for the link (L_2, L_1, L_3) and grading $(\sigma_1, \sigma_2) \in (\frac{1}{2}\mathbb{Z})^2$ are identical, except with the indices 1 and 2 reversed:

$$P_{11}^{\varepsilon,1}(\lambda) = \lambda \qquad P_{21}^{\varepsilon,1}(\lambda) = \lambda^{-1+2\sigma_1-2\sigma_2} \qquad P_{31}^{\varepsilon,1}(\lambda) = \lambda^{1-2\sigma_2}$$
$$P_{12}^{\varepsilon,1}(\lambda) = \lambda^{1+2\sigma_2-2\sigma_1} \qquad P_{22}^{\varepsilon,1}(\lambda) = \lambda \qquad P_{32}^{\varepsilon,1}(\lambda) = \lambda^{1-2\sigma_1}$$
$$P_{13}^{\varepsilon,1}(\lambda) = \lambda^{-1+2\sigma_2} \qquad P_{23}^{\varepsilon,1}(\lambda) = \lambda^{-1+2\sigma_1} \qquad P_{33}^{\varepsilon,1}(\lambda) = \lambda.$$

It is easy to compute that there is no choice of $\rho_1, \rho_2, \sigma_1, \sigma_2$ for which these polynomials coincide with the polynomials for (L_1, L_2, L_3) given in Example 2.5.18. The result now follows from Theorem 2.5.16. □

4.6 Example 6: double of the figure eight knot

In [Mi], it is asked whether there is an unoriented Legendrian knot whose double is not Legendrian isotopic to the double with components exchanged. We will give an example of such a knot in this section.

Let $L = (L_1, L_2)$ be the unoriented double of the figure eight knot, shown in Figure 4-5. To calculate gradings, we temporarily give L an orientation and base points as marked. We have labelled the vertices of L so that $a_i \in \Gamma_{11}$ for $1 \leq i \leq 7$, $a_i \in \Gamma_{22}$ for $8 \leq i \leq 14$, $a_i \in \Gamma_{12}$ for $15 \leq i \leq 21$, and $a_i \in \Gamma_{21}$ for $22 \leq i \leq 28$.

Proposition 4.6.1. *The unoriented links (L_1, L_2) and (L_2, L_1) are not Legendrian isotopic.*

Proof. As usual, we work modulo 2 and ignore powers of t_1 and t_2. An easy calculation on the DGAs for L_1 and L_2 shows that any augmentation ε of the DGA for L, as defined in Section 2.5, must satisfy $\varepsilon(a_6) = \varepsilon(a_7) = \varepsilon(a_{13}) = \varepsilon(a_{14}) = 1$ and $\varepsilon(a_4) = \varepsilon(a_5) = \varepsilon(a_{11}) =$

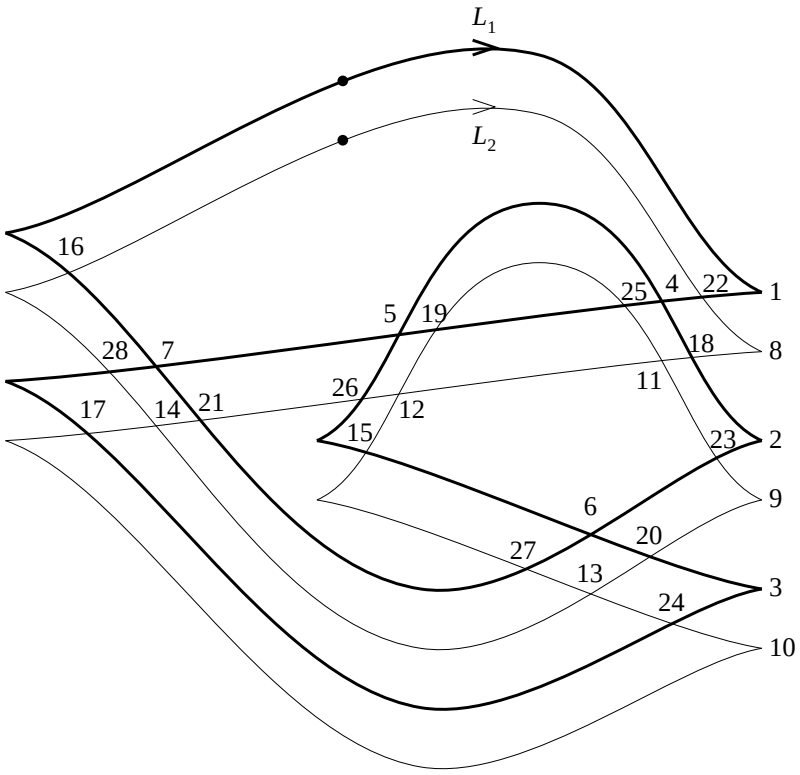

Figure 4-5: The link L, with vertices labelled (the a's are suppressed). To calculate gradings, orientations and base points are given.

$\varepsilon(a_{12}) = 0$. With that in mind, we find that

$$\begin{aligned} \partial_\varepsilon^{(1)} a_{19} &= a_{15} + a_{16} & \qquad \partial_\varepsilon^{(1)} a_{22} &= a_{28} \\ \partial_\varepsilon^{(1)} a_{21} &= a_{16} + a_{17} & \partial_\varepsilon^{(1)} a_{23} &= a_{27} \\ & & \partial_\varepsilon^{(1)} a_{24} &= a_{27} + a_{28}, \end{aligned}$$

and $\partial_\varepsilon^{(1)} a_i = 0$ for all other $a_i \in \Gamma_{12}$ or $a_i \in \Gamma_{21}$.

Given the orientations and base points from Figure 4-5, we calculate the degrees in Γ_{12} and Γ_{21} to be

$$\deg a_i = \begin{cases} 1 + 2\rho_1 & \text{for } a_{18}, \\ 2\rho_1 & \text{for } a_{19}, a_{21}, \\ -1 + 2\rho_1 & \text{for } a_{15}, a_{16}, a_{17}, a_{20}, \\ 1 - 2\rho_1 & \text{for } a_{22}, a_{23}, a_{24}, a_{25}, \\ -2\rho_1 & \text{for } a_{27}, a_{28}, \\ -1 - 2\rho_1 & \text{for } a_{26}. \end{cases}$$

It follows that $P_{12}^{\varepsilon,1}(\lambda) = \lambda^{1+2\rho_1} + 2\lambda^{-1+2\rho_1}$ and $P_{21}^{\varepsilon,1}(\lambda) = 2\lambda^{1+2\rho_1} + \lambda^{-1+2\rho_1}$. We disregard the orientations of L_1 and L_2 by allowing any $\rho_1 \in \frac{1}{2}\mathbb{Z}$.

For the link (L_2, L_1) and a choice of grading $\sigma_1 \in \frac{1}{2}\mathbb{Z}$, we have the same Poincaré-Chekanov polynomials, except with indices 1 and 2 switched; hence, for (L_2, L_1), $P_{12}^{\varepsilon,1}(\lambda) = 2\lambda^{1+2\sigma_1} + \lambda^{-1+2\sigma_1}$. It is clear that this is never equal to $P_{12}^{\varepsilon,1}(\lambda)$ for (L_1, L_2) for any choice of ρ_1, σ_1. The result follows. □

4.7 Example 7: Whitehead link

In this section, we give an example where orientation is important. Consider the Legendrian form of the Whitehead link shown in Figure 4-6, with oriented components L_1 and L_2, and let $-L_j$ denote L_j with reversed orientation, as usual. By playing with the diagrams, one can show that (L_1, L_2), $(L_2, -L_1)$, $(-L_1, -L_2)$, and $(-L_2, L_1)$ are Legendrian isotopic, as are $(-L_1, L_2)$, $(-L_2, -L_1)$, $(L_1, -L_2)$, and $(-L_2, -L_1)$. It is also the case that these two families are smoothly isotopic to each other. We will show, however, that they are not Legendrian isotopic.

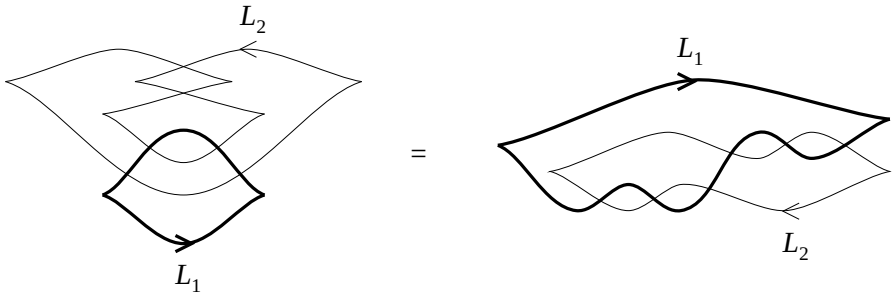

Figure 4-6: The oriented Whitehead link. On the left, a form which is recognizably the Whitehead link; on the right, the Legendrian-isotopic form which we will use.

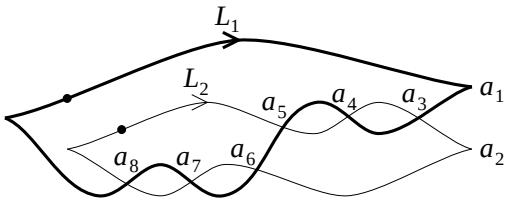

Figure 4-7: The oriented link (L_1, L_2), with vertices labelled and base points as shown.

Proposition 4.7.1. *The oriented links (L_1, L_2) and $(-L_1, L_2)$ are not Legendrian isotopic.*

Proof. Refer to Figure 4-7 for vertices and base points. Any map ε with $\varepsilon(a_i) = 0$ for $i \geq 3$ is an augmentation. The only a_i with $a_i \in \Gamma_{12}$ are a_4 and a_7, both of which satisfy $\partial a_i = 0$; their degrees are $\deg a_4 = -1 + 2\rho_1$ and $\deg a_7 = 2\rho_1$ for some $\rho_1 \in \mathbb{Z}$, and so $P_{12}^{\varepsilon,1}(\lambda) = \lambda^{2\rho_1} + \lambda^{-1+2\rho_1}$.

On the other hand, if we reverse the orientation of L_1 (and choose a new base point p_1 on the lower half of L_1), then we find $\deg a_4 = 2\sigma_1$ and $\deg a_7 = 1 + 2\sigma_1$ for some $\sigma_1 \in \mathbb{Z}$, and so $P_{12}^{\varepsilon,1}(\lambda) = \lambda^{1+2\sigma_1} + \lambda^{2\sigma_1}$. It follows that, regardless of the choice of ρ_1, σ_1, the polynomial $P_{12}^{\varepsilon,1}(\lambda)$ will be different for (L_1, L_2) and $(-L_1, L_2)$. □

Examples 6 and 7 will be applied to knots on the solid torus in Chapter 5.

Chapter 5

Legendrian satellites

In the smooth category, there is a satellite construction which glues a link in the solid torus $S^1 \times \mathbb{R}^2$ into a tubular neighborhood of a knot in $\mathbb{R}^3$ to produce a link in $\mathbb{R}^3$. The motivation for this chapter is that there is a Legendrian form of this construction which is invariant under Legendrian isotopy. We can then deduce results about Legendrian solid-torus links from results about Legendrian $\mathbb{R}^3$ links, and vice versa. In addition, we hope in the future to use Legendrian satellites to give nontrivial, nonclassical invariants of stabilized Legendrian links in $\mathbb{R}^3$.

We define the construction in Section 5.1, and show how it immediately implies facts about solid-torus links, including some that could not be shown using any previously known techniques. In Section 5.2, we show that the DGAs of some simple Legendrian satellites of stabilized knots, unfortunately, do not contain any useful information; the key step is Lemma 5.2.4, which is proven in Section 5.3. The computation performed in Section 5.3 may be of interest as the first involved computation known to this author which works directly on the DGA, rather than manipulating easier invariants such as the Poincaré-Chekanov polynomials or the characteristic algebra.

5.1 Construction

The solid torus $S^1 \times \mathbb{R}^2$ inherits a contact structure from $\mathbb{R}^3$. View $S^1 \times \mathbb{R}^2$ as $\mathbb{R}^3$ modulo the relation $(x, y, z) \sim (x+1, y, z)$; then the standard contact structure $\alpha = dz - y\,dx$ on $\mathbb{R}^3$ descends to the solid torus. As in $\mathbb{R}^3$, Legendrian links in the solid torus may be represented by their front projections to the xz plane, with the understanding that the x direction is now periodic. If we view $S^1 \times \mathbb{R}^2$ as $[0,1] \times \mathbb{R}^2$ with $\{0\} \times \mathbb{R}^2$ identified with $\{1\} \times \mathbb{R}^2$, then we can draw the front projection of a solid-torus Legendrian link as a front in $[0,1] \times \mathbb{R}$ with the two boundary components identified. We depict the boundary components by dashed lines; see Figure 5-1 for an illustration. For a Legendrian link $\tilde{L}$ in the solid torus, let the *endpoints* of $\tilde{L}$ be $\tilde{L} \cap (\{0\} \times \mathbb{R}^2)$, that is, the points where the front for $\tilde{L}$ intersects the dashed lines.

Remark 5.1.1. Invariants of solid-torus links. There are three classical invariants of links on the solid torus: the Thurston-Bennequin number tb and rotation number r can be calculated from the front of a solid-torus link exactly as in $\mathbb{R}^3$; and the winding number w is the number of times the link winds around the S^1 direction of $S^1 \times \mathbb{R}^2$. Clearly the tb, r, and w associated to any subset of the components of a solid-torus link also give invariants of the link.

In [NT], L. Traynor and the author show that the Chekanov-Eliashberg DGA can be defined for links on the solid torus, thus yielding a nonclassical invariant. For certain links with two components, [Tr] has also defined a nonclassical generating-function invariant. We will give examples in this section of solid-torus knots which are not Legendrian isotopic, but which cannot be distinguished using any of these invariants.

We now introduce the Legendrian satellite construction. Let L be an oriented Legendrian link in $\mathbb{R}^3$ with one distinguished component L_1, and let $\tilde{L}$ be an oriented Legendrian link in $S^1 \times \mathbb{R}^2$. We give two definitions of the Legendrian satellite $S(L, \tilde{L}) \subset \mathbb{R}^3$, one abstract, one concrete.

A tubular neighborhood of L_1 is a solid torus; the characteristic foliation on the boundary of this torus wraps around the torus $tb(L_1)$ times. By cutting the tubular neighborhood at a cross-sectional disk, untwisting it $tb(L_1)$ times, and regluing, we obtain a solid torus contactomorphic to $S^1 \times \mathbb{R}^2$ with the standard contact structure. Thus we can embed $\tilde{L} \subset S^1 \times \mathbb{R}^2$ as a Legendrian link in a tubular neighborhood of L_1. Replacing the component L_1 in L by this new link gives $S(L, \tilde{L})$.

We can redefine $S(L, \tilde{L})$ in terms of the fronts for L and $\tilde{L}$; see Figure 5-1 for a pictorial description. Suppose that $\tilde{L}$ has n endpoints. By cutting along the dotted lines (i.e., the

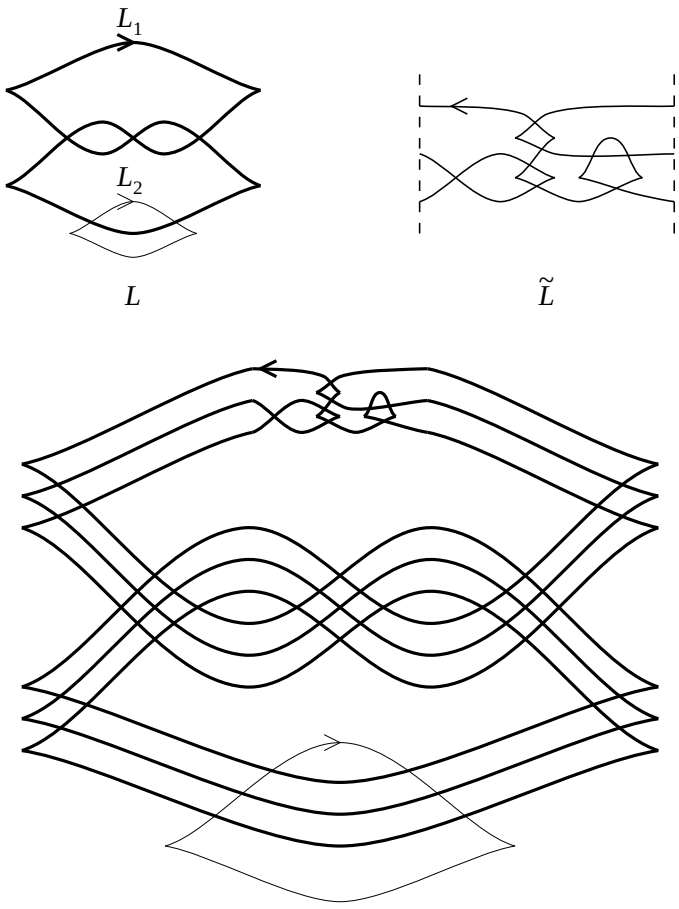

Figure 5-1: Gluing a solid-torus link $\tilde{L}$ into an $\mathbb{R}^3$ link L, to form the satellite link $S(L, \tilde{L})$.

endpoints of $\tilde{L}$), we can embed $\tilde{L}$ as a Legendrian tangle in $\mathbb{R}^3$ with $2n$ ends. Replace the front of the first component L_1 of L by the n-copy of L_1 (see Definition 4.5.1). Now choose a small segment of L_1 which is oriented from left to right; excise the corresponding n pieces of the n-copy of L_1, and replace them by the front for $\tilde{L}$, cut along its endpoints.

Definition 5.1.2. The resulting link $S(L, \tilde{L}) \subset \mathbb{R}^3$ is the *Legendrian satellite* of $L \subset \mathbb{R}^3$ and $\tilde{L} \subset S^1 \times \mathbb{R}^2$. We give $S(L, \tilde{L})$ the orientation derived from the orientations on $\tilde{L}$ (for the glued n-copy of L_1) and on L (for the components of L besides L_1).

The Legendrian satellite construction is motivated by the special case of Whitehead doubles (see Section 5.2), which were introduced by Eliashberg and subsequently used by Fuchs [Fu].

Remark 5.1.3. Classical invariants of Legendrian satellites. Before we show that $S(L, \tilde{L})$ is well-defined up to Legendrian isotopy, we note that the classical invariants of $S(L, \tilde{L})$ are easily computable from those of L and $\tilde{L}$. Indeed, a straightforward computation with front diagrams yields

$$tb(S(L, \tilde{L})) = (w(\tilde{L}))^2\, tb(L) + tb(\tilde{L})$$
$$r(S(L, \tilde{L})) = w(\tilde{L}) r(L) + r(\tilde{L})$$

when L is a knot, with a similar but slightly more complicated formula when L is a multi-component link.

Lemma 5.1.4. *$S(L, \tilde{L})$ is well-defined up to Legendrian isotopy.*

Proof. We need to show that, up to Legendrian isotopy, $S(L, \tilde{L})$ is independent of the piece of the n-copy of L_1 which we excise and replace by $\tilde{L}$, as long as this piece is oriented left to right. The singularities of $\tilde{L}$ consist of crossings, left cusps, and right cusps; we imagine pushing these singularities one by one from one section of the n-copy of L_1 to another.

We can clearly push these singularities through any piece of $S(L, \tilde{L})$ which crosses a neighborhood of $\tilde{L}$ transversely; see the top diagram in Figure 5-2. Figure 5-3 shows that we can also push singularities through a right cusp in L_1, and clearly this argument extends to left cusps as well. We conclude that we can push all of $\tilde{L}$ through a cusp, resulting in the left-to-right mirror reflection of $\tilde{L}$; see the bottom diagrams in Figure 5-2. The lemma follows. □

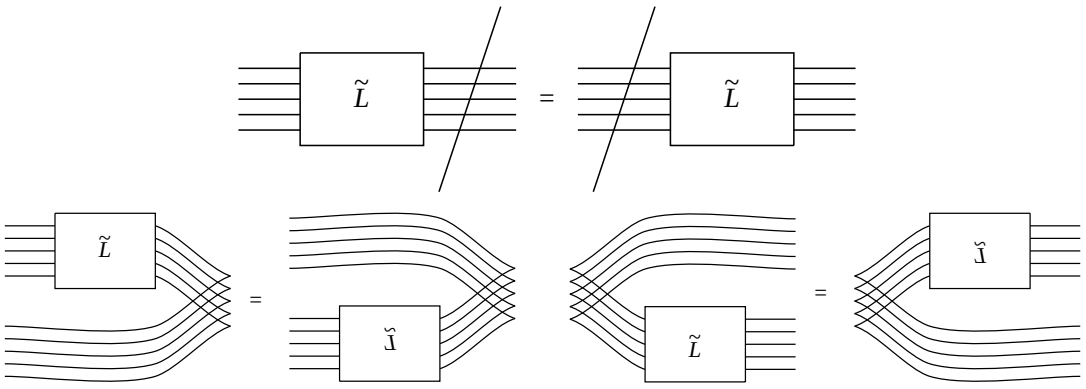

Figure 5-2: Pushing $\tilde{L}$ through singularities in L: a crossing, a right cusp, and a left cusp.

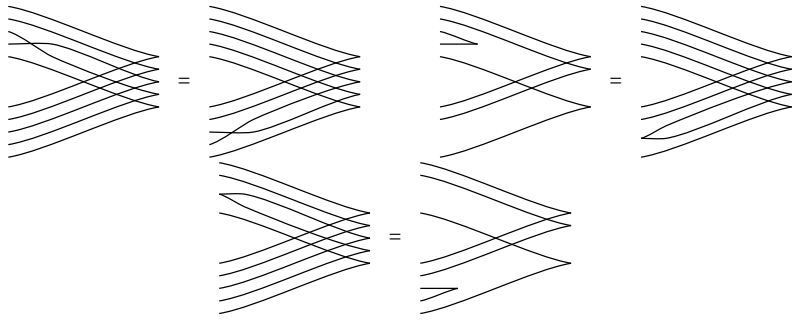

Figure 5-3: Pushing singularities in $\tilde{L}$ through a right cusp.

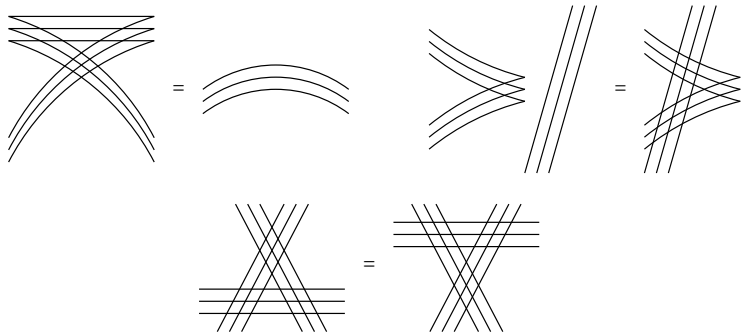

Figure 5-4: Legendrian Reidemeister moves on n-copies; in this illustration, $n = 3$.

Theorem 5.1.5. *$S(L, \tilde{L})$ is a well-defined operation on Legendrian isotopy classes; that is, if we change $L, \tilde{L}$ by Legendrian isotopies, then $S(L, \tilde{L})$ changes by a Legendrian isotopy as well.*

Proof. We first consider Legendrian-isotopy changes of $\tilde{L}$. These fall into two categories: isotopies where the endpoints of $\tilde{L}$ remain fixed, and horizontal translations of $\tilde{L}$ (i.e., moving the dashed lines). The first category clearly preserves the Legendrian isotopy class of $S(L, \tilde{L})$. The second category consists of pushing singularities in $\tilde{L}$ through the dashed lines. But Figure 5-3 shows that we can push individual singularities from one side of $\tilde{L}$ to the other, by moving the singularity all the way around the n-copy of L_1. Hence Legendrian-isotopy changes of $\tilde{L}$ do not change $S(L, \tilde{L})$.

Next consider Legendrian-isotopy changes of L. It suffices to show that $S(L, \tilde{L})$ does not change under Legendrian Reidemeister moves on L. Consider such a move, and push $\tilde{L}$ away from a neighborhood of the move. Then the fact that the Legendrian-isotopy class of $S(L, \tilde{L})$ does not change follows from Figure 5-4. □

Remark 5.1.6. Both the proof of Theorem 5.1.5 and Corollary 5.1.7 below have been known for some time. It is also possible, and probably more natural, to establish Theorem 5.1.5 using the global, non-front definition of Legendrian satellites; we chose to present the front proof because of its concreteness.

Corollary 5.1.7. *Legendrian-isotopic knots in $\mathbb{R}^3$ have Legendrian-isotopic n-copies.*

Proof. The n-copy of a knot K is simply $S(K, \tilde{L}^{(n)})$, where $\tilde{L}^{(n)}$ is the union of n unlinked loops which wind once around $S^1 \times \mathbb{R}^2$; see Figure 5-5 for an illustration of $\tilde{L}^{(2)}$. The result follows from Theorem 5.1.5. □

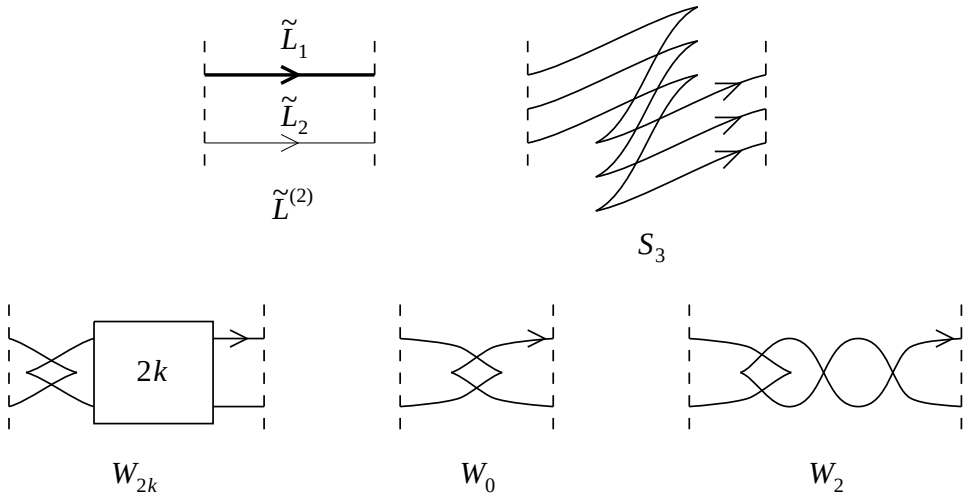

Figure 5-5: The solid-torus links $\tilde{L}^{(2)}$ and S_3 (with obvious generalization to a family of links S_n), and the solid-torus Whitehead knots W_{2k}, $k \geq 0$, with W_0 and W_2 shown as examples. The box indicates $2k$ half-twists.

Corollary 5.1.8 ([Mi]). *Suppose that K is a stabilization of a Legendrian knot. The n-copy of K is Legendrian isotopic to the n-copy with components cyclically permuted. More precisely, if $L_1, \ldots, L_n$ are the components of the n-copy of K, with L_i slightly higher than L_{i+1} in z coordinate, then $(L_1, L_2, \ldots, L_n)$ is Legendrian isotopic to $(L_{1+k}, L_{2+k}, \ldots, L_{n+k})$ for any k, where indices are taken modulo n.*

Proof. Suppose, without loss of generality, that $K = S_+(K')$ for a Legendrian knot K'. Then the n-copy of K is the Legendrian satellite $S(K', S_n)$, where S_n is the solid-torus "n-copy stabilization link" depicted in Figure 5-5. It is easy to see that S_n is Legendrian isotopic to itself with components cyclically permuted; now apply Theorem 5.1.5. □

We now present some applications of Theorem 5.1.5 to knots and links on the solid torus. Consider the link $\tilde{L}^{(2)}$ shown in Figure 5-5. The following result, established in [Tr] using generating functions, is also proven in [NT] using the DGA for solid-torus links. The proof we give is yet another one.

Proposition 5.1.9. *Write $\tilde{L}^{(2)} = (\tilde{L}_1, \tilde{L}_2)$. Then $(\tilde{L}_1, \tilde{L}_2)$ is not Legendrian isotopic to $(\tilde{L}_2, \tilde{L}_1)$.*

Proof. In Section 4.6, we showed that the double of the figure eight knot is not Legendrian isotopic to the double with components swapped; see Proposition 4.6.1. The result now follows from Theorem 5.1.5. □

Now consider the Whitehead knots W_{2k} shown in Figure 5-5. Each W_{2k} has $r = w = 0$ and is thus topologically isotopic to its inverse. By contrast, we can now show the following result.

Proposition 5.1.10. *W_{2k} is not Legendrian isotopic to its inverse.*

Proof. As usual, write $-W_{2k}$ for the inverse of W_{2k}, and let L be the double of the usual "flying-saucer" unknot in $\mathbb{R}^3$. For $k = 1$, it is easy to check that $S(L, W_2)$ is precisely the oriented Whitehead link from Section 4.7, and that $S(L, -W_2)$ is the same link with one

component reversed. Proposition 4.7.1 and Theorem 5.1.5 then imply that W_2 and $-W_2$ are not Legendrian isotopic.

A calculation similar to the one in the proof of Proposition 4.7.1, omitted here, shows that $S(L, W_{2k})$ and $S(L, -W_{2k})$ are not Legendrian isotopic for arbitrary $k \geq 0$. The result follows. □

The solid-torus DGA from [NT] fails to distinguish between W_{2k} and its inverse. Proposition 5.1.10 is thus a result about solid-torus knots whose only presently-known proof uses the Legendrian satellite construction.

5.2 Doubles

As we observed in Remark 2.2.10, the Chekanov-Eliashberg DGA invariant vanishes for links which are stabilizations. The Legendrian satellite construction, however, seems to yield nontrivial nonclassical invariants of *all* Legendrian links; see Remark 5.2.7 below. On the other hand, the main result of this section shows that some of the simplest Legendrian satellites of stabilizations do not contain any new information.

Definition 5.2.1. The *Legendrian Whitehead double* of a Legendrian knot K in $\mathbb{R}^3$ is $S(K, W_0)$, where W_0 is the knot shown in Figure 5-5. More generally, if $\tilde{L}$ has two endpoints, then we call $S(K, \tilde{L})$ a *satellite double* of K.

As mentioned in Section 5.1, the Legendrian Whitehead double was originally defined by Eliashberg, with further study by Fuchs [Fu], who uses the notation $\Gamma_{\text{dbl}}(0,0)$ for our $S(K, W_0)$.

Remark 5.2.2. Legendrian satellites and maximal tb. By Remark 5.1.3, the Legendrian Whitehead double of any Legendrian knot has Thurston-Bennequin number 1. As noted by J. Sabloff and the author, it is easy to show that the Legendrian Whitehead double maximizes tb in its topological class. This follows from the fact that $g(S(K, W_0)) = 1$, along with Bennequin's inequality $tb(K) \leq 2g(K) - 1$ [B], where $g(K)$ is the (three-ball) genus of K. A similar argument shows that the usual double of any Legendrian knot maximizes tb.

It is not true, however, that all satellite doubles maximize tb, even when $\tilde{L}$ maximizes tb. In particular, if $\tilde{L}$ has a half-twist  next to its endpoints, and K is a stabilization, then $S(K, \tilde{L})$ will also be a stabilization.

Proposition 5.2.3. *If K_1 and K_2 are stabilized Legendrian knots in the same topological class with the same tb and r, then the DGAs of the Legendrian Whitehead doubles of K_1 and K_2 are equivalent.*

The key to proving Proposition 5.2.3 is the following result, whose proof we delay until Section 5.3.

Lemma 5.2.4. *For any Legendrian knot K which is a stabilization, the DGAs of $S(K, W_0)$ and of $S(S_+S_-(K), W_0)$ are equivalent.*

Proof of Proposition 5.2.3. By a result of [FT], any two Legendrian knots which are topologically identical and have the same tb and r are Legendrian isotopic after some number of applications of the double stabilization operator S_+S_-. That is, there exists an $n \geq 0$ such that $(S_+S_-)^n K_1$ and $(S_+S_-)^n K_2$ are Legendrian isotopic. The proposition now follows directly from Lemma 5.2.4. □

Remark 5.2.5. It can in fact be shown that the DGA of the Legendrian Whitehead double of a stabilized knot depends only on the tb and r of the knot, and not on its topological class. In particular, we can recover the result of [Fu] that the DGA of a Legendrian Whitehead double always possesses an augmentation.

A slightly modified version of the proof of Lemma 5.2.4, omitted here for simplicity, establishes the following more general result.

Proposition 5.2.6. *If K_1 and K_2 are stabilized Legendrian knots in the same topological class with the same tb and r, and $\tilde{L}$ is any Legendrian link in $S^1 \times \mathbb{R}^2$ with two endpoints and winding number zero, then the DGAs of $S(K_1, \tilde{L})$ and $S(K_2, \tilde{L})$ are equivalent.*

We believe that Proposition 5.2.6 actually holds for *any* satellite doubles of stabilized knots K_1 and K_2 with the same tb and r, regardless of the winding number of $\tilde{L}$. However, the analogue of Lemma 5.2.4 is false if $\tilde{L}$ has winding number ± 2, since $S(K, \tilde{L})$ and $S(S_+S_-(K), \tilde{L})$ have different tb; see Remark 5.1.3. Nevertheless, the argument of the proof of Lemma 5.2.4 shows that the characteristic algebra, at least, can never distinguish between satellite doubles of stabilized knots.

Remark 5.2.7. Invariants of stabilized Legendrian knots. As mentioned earlier, it remains a very interesting open problem to find nonclassical invariants of stabilized Legendrian knots. There are currently no methods to prove that two stabilized knots with the same topological type, tb, and r are not Legendrian isotopic. Such methods would likely yield nonclassical invariants of some transversal knots as well; see Remark 1.2.2.

We are hopeful that satellites more complicated than doubles will encode interesting information for stabilized knots. In particular, it seems that the n-copy of any Legendrian link maximizes Thurston-Bennequin number when $n \geq 2$, and thus probably has a nontrivial DGA. By Corollary 5.1.7, the DGAs of Legendrian satellites of a Legendrian link, including the n-copy, are Legendrian-isotopy invariants, which likely contain interesting nonclassical information in general. The problem we face when dealing with complicated satellites, however, is extracting useful information from the characteristic algebra.

There is another approach to finding invariants of stabilized knots, which is probably more natural than investigating satellites. Eliashberg, Givental, and Hofer [EGH] have recently developed symplectic field theory, which generalizes contact homology; Section 2.8 of [EGH] describes how this method yields invariants of Legendrian links, which would likely not vanish for stabilized knots. Unfortunately, no explicit combinatorial description, à la Chekanov, is presently known for the symplectic field theory associated to Legendrian links.

5.3 Proof of Lemma 5.2.4

We may assume without loss of generality that $K = S_+(K')$ for some Legendrian K'. By using, if necessary, Legendrian Reidemeister moves I (more precisely, the mirror of I) and IIb from Figure 1-1, we may further assume that the rightmost cusp in K' is oriented downwards. If we shift the zigzag in $K = S_+(K')$ next to the rightmost cusp in K', then K and $S(K, W_0)$ look like the diagrams in Figure 5-6 near the rightmost cusp.

The corresponding parts of $S_+S_-(K)$ and $S(S_+S_-(K), W_0)$ are also shown in Figure 5-6, and $S(K, W_0)$ and $S(S_+S_-(K), W_0)$ are identical outside the regions depicted. It is easy to check that the degrees of all vertices not depicted are equal for the two Legendrian Whitehead doubles, and that the degrees of the vertices depicted are 1 for

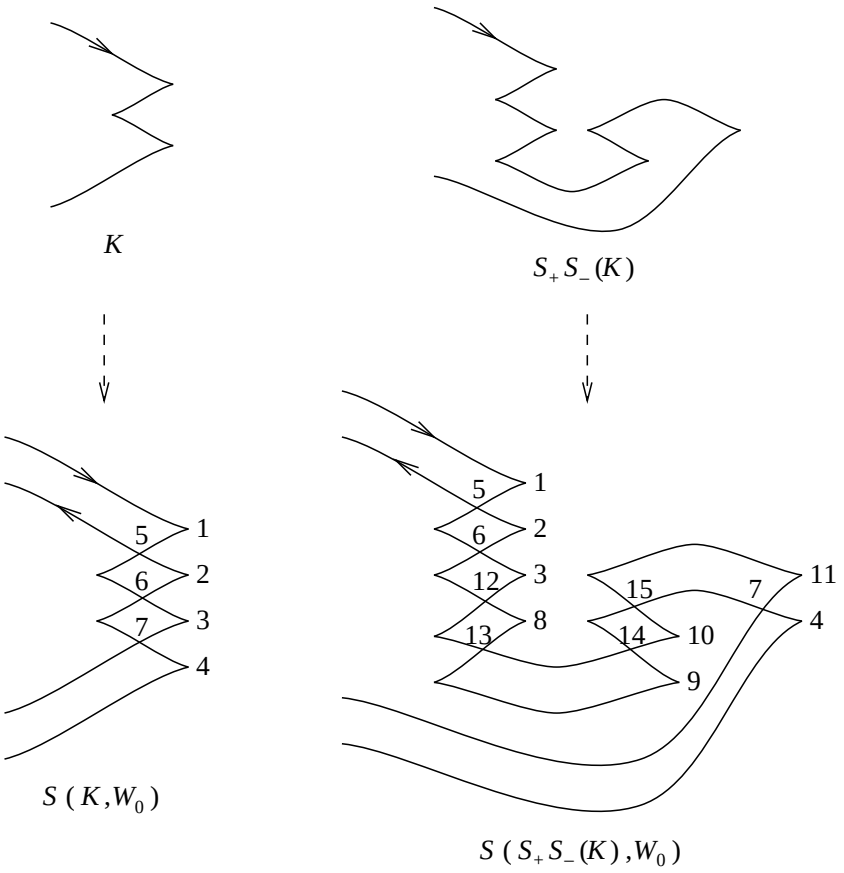

Figure 5-6: Whitehead doubles of stabilizations. In the lower diagrams, vertex a_i is labelled by i.

$a_1, a_2, a_3, a_4, a_8, a_9, a_{10}, a_{11}$ and 0 for $a_5, a_6, a_7, a_{12}, a_{13}, a_{14}, a_{15}$, in either diagram. Since the regions drawn are the rightmost parts of each double, the DGA for $S(S_+S_-(K), W_0)$ is simply obtained from the DGA for $S(K, W_0)$ by making the following replacements:

$$\left\{ \begin{array}{c} \partial a_2 = 1 - ta_5a_6 \\ \partial a_3 = t^{-1} - a_6a_7 \\ \partial a_5 = \partial a_6 = \partial a_7 = 0 \end{array} \right\} \quad \longrightarrow \quad \left\{ \begin{array}{c} \partial a_2 = 1 - ta_5a_6 \\ \partial a_3 = t^{-1} - a_6a_{12} \\ \partial a_8 = 1 - ta_{12}a_{13} \\ \partial a_9 = t^{-1} - a_{14}a_{13} \\ \partial a_{10} = 1 - ta_{15}a_{14} \\ \partial a_{11} = t^{-1} - a_{15}a_7 \\ \partial a_5 = \partial a_6 = \partial a_7 = 0 \\ \partial a_{12} = \partial a_{13} = \partial a_{14} = \partial a_{15} = 0 \end{array} \right\}.$$

We further note that none of the vertices depicted in Figure 5-6, besides a_1, a_4, a_5, a_7, appears anywhere in the DGAs except in the equations above; a_5, a_7 appear additionally in $\partial a_1, \partial a_4$, respectively.

Our goal is to apply elementary automorphisms and algebraic stabilizations to the DGA for $S(S_+S_-(K), W_0)$, until we obtain the DGA for $S(K, W_0)$. Start with the DGA for $S(S_+S_-(K), W_0)$; we begin by rewriting $\partial a_3, \partial a_8, \partial a_9, \partial a_{10}, \partial a_{11}$ in a more manageable

form.

We first wish to rewrite ∂a_3 as $\partial a_3 = t^{-1} - a_6 a_7$. (Intuitively, this follows from the fact that $a_5 = a_7$ in the characteristic algebra or in the homology of the DGA.) We define the words $\alpha_1, \alpha_2, \alpha_3$ in the DGA as follows, and then compute $\partial\alpha_1, \partial\alpha_2, \partial\alpha_3$:

$$\begin{array}{lll} \alpha_1 = ta_{15}a_9 - a_{10}a_{13} & & \partial\alpha_1 = a_{15} - a_{13} \\ \alpha_2 = ta_{11} - \alpha_1 a_7 & \Longrightarrow & \partial\alpha_2 = 1 - ta_{13}a_7 \\ \alpha_3 = a_8 a_7 - a_{12}\alpha_2 & & \partial\alpha_3 = a_7 - a_{12}. \end{array}$$

Then if we apply the elementary automorphism $a_3 \mapsto a_3 + a_6\alpha_3$, we obtain $\partial a_3 = t^{-1} - a_6 a_7$.

In a similar fashion, we can successively replace $\partial a_{11}, \partial a_{10}, \partial a_9, \partial a_8$ as follows: $\partial a_{11} = t^{-1} - a_{15}a_5$; $\partial a_{10} = 1 - ta_6 a_{14}$; $\partial a_9 = t^{-1} - a_5 a_{13}$; $\partial a_8 = 1 - ta_{12}a_6$.

For convenience, we now define

$$\tilde{a}_2 = (1 - ta_6 a_5)a_3 + a_6 a_2 a_7 \qquad \Longrightarrow \qquad \partial\tilde{a}_2 = t^{-1} - a_6 a_5.$$

By applying the elementary automorphisms $a_{11} \mapsto a_{11} + \tilde{a}_2$ and $a_{15} \mapsto a_{15} + a_6$, we obtain $\partial a_{11} = -a_{15}a_5$. Similarly, we may write $\partial a_{10} = -ta_6 a_{14}$, $\partial a_9 = -a_5 a_{13}$, $\partial a_8 = -ta_{12}a_6$.

At this point, the DGA has the following form:

$$\begin{array}{lllllll} \partial a_2 &=& 1 - ta_5 a_6 & & \partial a_9 &=& -a_5 a_{13} \\ \partial a_3 &=& t^{-1} - a_6 a_7 & & \partial a_{10} &=& -ta_6 a_{14} \\ \partial a_8 &=& -ta_{12}a_6 & & \partial a_{11} &=& -a_{15}a_5 \\ \multicolumn{7}{l}{\partial a_5 = \partial a_6 = \partial a_7 = \partial a_{12} = \partial a_{13} = \partial a_{14} = \partial a_{15} = 0.} \end{array}$$

We next eliminate $a_8, a_{11}, a_{12}, a_{15}$ through algebraic stabilization and destabilization. Introduce e_1 and e_2 of degree 0 and -1, respectively, with $\partial e_1 = e_2$ (and $\partial e_2 = 0$). Let Φ_1 be the composition of the following elementary automorphisms in succession:

$$a_{12} \mapsto a_{12} - e_1 a_5; \qquad a_8 \mapsto a_8 - e_1 a_2; \qquad e_1 \mapsto e_1 + ta_{12}a_6 - e_2 a_2.$$

Under Φ_1, the DGA changes as follows:

$$\left\{\begin{array}{c} \partial a_8 = -ta_{12}a_6 \\ \partial e_1 = e_2 \\ \partial a_{12} = 0 \\ \partial e_2 = 0 \end{array}\right\} \quad \xrightarrow{\Phi_1} \quad \left\{\begin{array}{c} \partial a_8 = e_1 \\ \partial e_1 = 0 \\ \partial a_{12} = e_2 a_5 \\ \partial e_2 = 0 \end{array}\right\}.$$

We may then drop a_8 and e_1; these simply correspond to an algebraic stabilization.

Let Φ_2 be the composition of the following maps:

$$a_{15} \mapsto a_{15} - ta_{12}a_6; \;\; a_{11} \mapsto a_{11} - ta_{12}\tilde{a}_2; \;\; a_{12} \mapsto a_{12} + a_{15}a_5 - te_2 a_5 \tilde{a}_2; \;\; a_{15} \mapsto a_{15} + e_2 a_2.$$

Under Φ_2, the DGA now changes as follows:

$$\left\{\begin{array}{c} \partial a_{11} = a_{15}a_5 \\ \partial a_{12} = e_2 a_5 \\ \partial a_{15} = 0 \\ \partial e_2 = 0 \end{array}\right\} \quad \xrightarrow{\Phi_2} \quad \left\{\begin{array}{c} \partial a_{11} = a_{12} \\ \partial a_{12} = 0 \\ \partial a_{15} = e_2 \\ \partial e_2 = 0 \end{array}\right\}.$$

We can now drop $a_{11}, a_{12}, a_{15}, e_2$; these correspond to two algebraic stabilizations.

Hence, up to algebraic stabilizations, we have eliminated $a_8, a_{11}, a_{12}, a_{15}$. An entirely similar process allows us to eliminate $a_9, a_{10}, a_{13}, a_{14}$. The resulting DGA is precisely the DGA of $S(K, W_0)$, as desired. □

Remark 5.3.1. The only part of this proof which uses the structure of W_0 is the calculation of the degrees of the vertices in Figure 5-6. To prove the more general case given in Proposition 5.2.6, we have to take more care vis-à-vis degrees, but the idea is the same. The proof also extends to knots which are not satellite doubles, but whose rightmost parts look like the bottom diagrams in Figure 5-6.

Chapter 6

Maximal Thurston-Bennequin number for two-bridge and pretzel links

This chapter addresses a problem which is closely related to, but slightly different from, the questions of Legendrian isotopy which are the main concern of this dissertation. We study the maximal Thurston-Bennequin number for two classes of links, the two-bridge links and the three-stranded pretzel links. Using a bound provided by the Kauffman polynomial, we are able to calculate maximal tb for most of these links. We conclude with a section which relates the maximal tb problem to the rest of this dissertation.

6.1 Introduction and results

In this chapter, we will use the word "link" to denote either a knot or an oriented link; the Thurston-Bennequin number, of course, is not well defined for unoriented multi-component links. Since the results below are primarily interesting for knots, we will denote links by K.

For a fixed topological link type K, the set of possible Thurston-Bennequin numbers of Legendrian links in $\mathbb{R}^3$ isotopic to K is bounded above; it is then natural to try to compute the maximum $\overline{tb}(K)$ of tb over all such links. Note that we distinguish between a link and its mirror; $\overline{tb}$ is often different for the two. In some sense, tb is the Legendrian equivalent of the genus of a smooth knot, which is also bounded in one direction; the genus, however, seems to be more difficult to compute in general.

Bennequin [B] proved the first upper bound on $\overline{tb}(K)$, in terms of the (three-ball) genus of K. Since then, other upper bounds have been found in terms of the slice (or four-ball) genus [Ru2], the HOMFLY polynomial [FT], and the Kauffman polynomial. The strongest upper bound, in general, seems to be the Kauffman bound first discovered by Rudolph [Ru1], with alternative proofs given by several authors. See [Fer] for a more detailed history of the subject.

Recall the definition of the Kauffman polynomial $F_K(a,x)$ of an oriented link K; we use the normalizations of [FT], which are the same as the original ones from [Kau2] except with a replaced by a^{-1}. First consider an unoriented link diagram T. The *unoriented* Kauffman polynomial (or L-polynomial) $L_T(a,x)$ is defined recursively via the following skein relations:

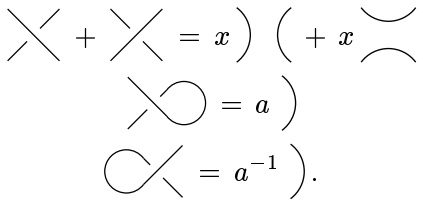

Now, given an oriented link K, let T be an oriented link diagram representing K, and let $w(T)$ denote the writhe of T, or the signed number of crossings in T, with signs determined by Figure 6-1. Then we define the Kauffman polynomial by $F_K(a,x) = a^{w(T)}L_T(a,x)$. Although L_T is only an invariant under regular isotopy (i.e., isotopy fixing the writhe), F_K is an invariant under smooth isotopy.

For a polynomial $P(a,x)$, let $v(P)$ denote the minimum degree of a in $P(a,x)$.

Theorem 6.1.1 (Kauffman bound). *If K is an (oriented) Legendrian link in standard contact $\mathbb{R}^3$, then $\overline{tb}(K) \leq v(F_K) - 1$.*

The Kauffman bound is not sharp in general; see, e.g., [Fer] or [EH]. Sharpness has been established, however, for some small classes of knots, including positive knots [Tan] and most torus knots [Eps, EH]. Etnyre and Honda have also exhibited in [EH] the first known family of knots for which the Kauffman inequality fails to be sharp.

In this chapter, we will investigate sharpness for two somewhat larger classes of links, 2-bridge (rational) links and three-stranded pretzel links. We will demonstrate that the Kauffman bound is sharp for all 2-bridge links and most pretzel links, and will exhibit classes of pretzel links for which we believe the Kauffman bound fails to be sharp. (Part of the calculation for pretzel links has already been performed in [FT]; see Remark 6.1.5.)

Remark 6.1.2. For two-bridge links and three-stranded pretzel links, the other bounds on tb (genus, slice genus, HOMFLY) fail to be sharp in general.

Before stating our main results, we recall the definitions of 2-bridge and pretzel links. A 2-bridge link is any nontrivial link which admits a diagram with four vertical tangencies (two on the left, two on the right). A (three-stranded) pretzel link is a link of the form $P(p_1,p_2,p_3)$ depicted in Figure 6-2. It is easy to see that the smooth isotopy class of the $P(p_1,p_2,p_3)$ is unchanged under permutations of the p_i.

We need one more piece of notation. For an oriented link K, define $\widetilde{tb}(K) = v(F_K) - 1 - \overline{tb}(K)$; then $\widetilde{tb}(K) \geq 0$, with equality if and only if the Kauffman bound is sharp for K.

Theorem 6.1.3. *If K is an oriented 2-bridge link, then $\widetilde{tb}(K) = 0$.*

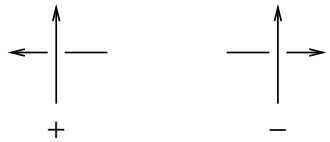

Figure 6-1: Calculating the writhe of an oriented link diagram. The writhe is the signed number of crossings of the link diagram, counted with the signs above.

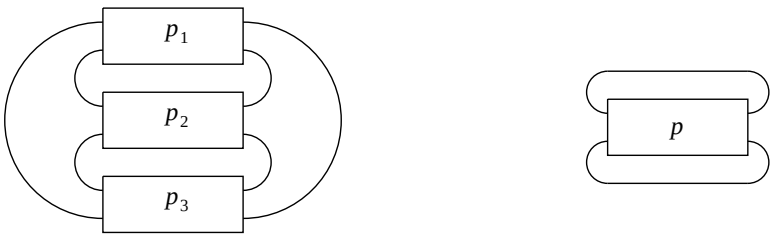

Figure 6-2: The pretzel link $P(p_1, p_2, p_3)$ and the torus link $T(p)$. Each box contains the specified number of half-twists, with the same conventions as in Figure 6-3.

Theorem 6.1.4. *Suppose $p_1, p_2, p_3 > 0$. Then $\widetilde{tb} = 0$ for $P(p_1, p_2, p_3)$, $P(-p_1, p_2, p_3)$, and $P(-p_1, -p_2, -p_3)$, and for $P(-p_1, -p_2, p_3)$ when $p_1 \geq p_2 \neq p_3 + 1$. For the remaining case, we have*

$$0 \leq \widetilde{tb}(P(-p_1, -p_3 - 1, p_3)) \leq \begin{cases} 2 & \text{if } p_1 \geq p_3 + 4, \\ 3 & \text{if } p_1 = p_3 + 3, \\ 1 & \text{if } p_1 = p_3 + 1 \text{ or } p_1 = p_3 + 2. \end{cases}$$

Remark 6.1.5. Theorem 6.1.4 is only partially original. Kanda [Kan2] calculated $\overline{tb}$ for $P(2n+1, 2n+1, 2n+1)$, $n \geq 1$, using Giroux's theory of convex surfaces. Fuchs and Tabachnikov [FT] subsequently calculated $\overline{tb}$ for $P(p_1, p_2, p_3)$ and $P(-p_1, -p_2, -p_3)$, using the Kauffman bound and the HOMFLY bound, respectively.

We will prove Theorem 6.1.3 in Section 6.2 and Theorem 6.1.4 in Section 6.3. Section 6.4 discusses consequences and possible ramifications of these results, and formulates ties with previous chapters.

6.2 Proof for 2-bridge links

In this section, we prove Theorem 6.1.3. Let K be a 2-bridge link; we first need to find a suitable Legendrian embedding of K. Say that a link diagram is in *rational form* if it is in the form $T(a_1, \ldots, a_n)$ illustrated by Figure 6-3 for some $a_1, \ldots, a_n$. Clearly any rational-form diagram corresponds to a 2-bridge link; by the classification of 2-bridge links ([Sch], or see [Mur] for a very accessible exposition), any 2-bridge link has a rational-form diagram.

To each $T(a_1, \ldots, a_n)$, we may associate a rational number, the continued fraction

$$[a_1, \ldots, a_n] = a_1 + \frac{1}{-a_2 + \dfrac{1}{a_3 + \dfrac{1}{-a_4 + \cdots + \dfrac{1}{(-1)^{n-1} a_n}}}}.$$

Note that our convention is the opposite of the convention in [Lic], and differs by alternating signs from the standard convention from, e.g., [Mur]. The classification of 2-bridge links further states that if $1/[a_1, \ldots, a_n] - 1/[b_1, \ldots, b_n] \in \mathbb{Z}$, then $T(a_1, \ldots, a_n)$ and $T(b_1, \ldots, b_n)$ are ambient isotopic. (The criterion stating precisely when two such links are isotopic is only slightly more complicated, but will not concern us here.)

Now define $T(a_1, \ldots, a_n)$ to be in *Legendrian rational form* if $a_i \geq 2$ for all i. Although $T(a_1, \ldots, a_n)$ corresponds to a Legendrian link whenever $a_i \geq 1$ for all i, it is crucial to the proof of Lemma 6.2.2 that $a_i \geq 2$ for $2 \leq i \leq n-1$. Indeed, if one of these a_i is 1, then it

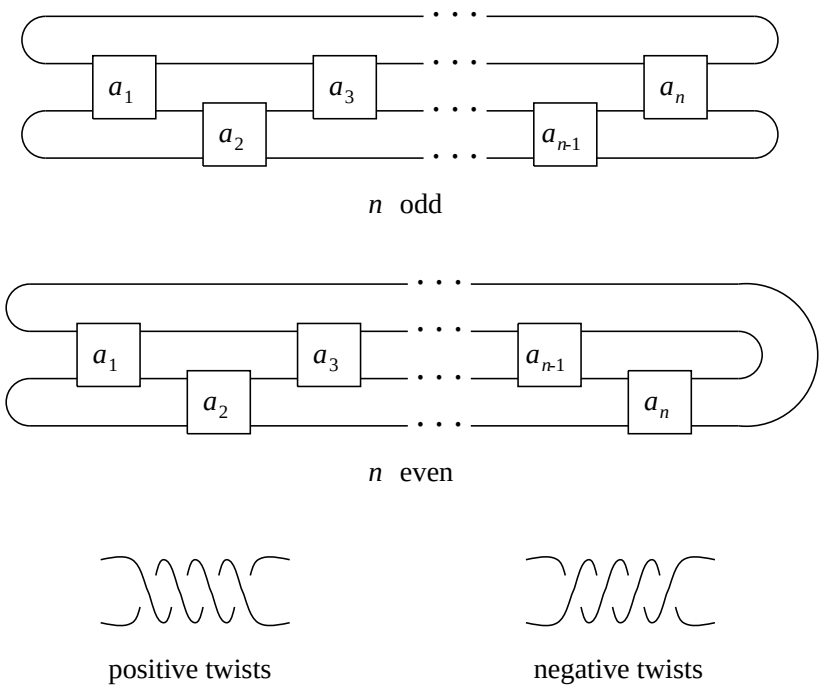

Figure 6-3: The rational-form diagram $T(a_1, \ldots, a_n)$. Each box contains the specified number of half-twists; positive and negative twists are shown.

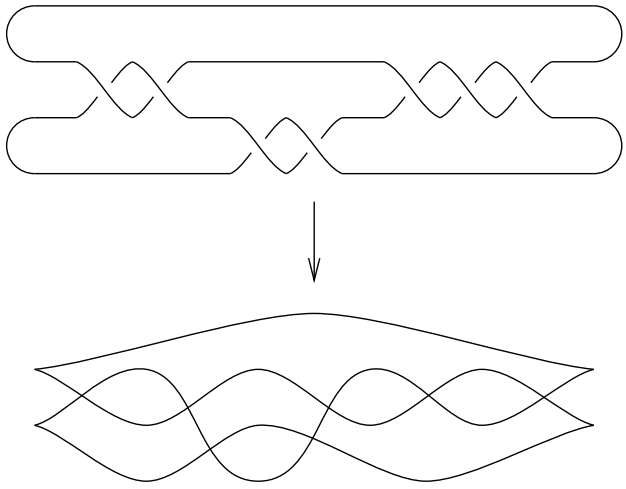

Figure 6-4: The correspondence between a diagram in Legendrian rational form (in this case, $T(2, 2, 3)$, or 5_2) and the front of a Legendrian link of the same ambient type.

is straightforward to see, by drawing the front, that the resulting Legendrian link does not maximize Thurston-Bennequin number.

Any link diagram in Legendrian rational form is easily converted into the front of a Legendrian link by replacing the four vertical tangencies by cusps; see Figure 6-4. Since the crossings in a front are resolved locally so that the strand with more negative slope always lies over the strand with more positive slope, a link diagram in Legendrian rational form is ambient isotopic to the corresponding front. (This observation explains our choice of convention for positive versus negative twists.)

Lemma 6.2.1. *Any 2-bridge link can be expressed as a diagram in Legendrian rational form.*

Proof. Let K be a 2-bridge link; let $T(a_1, \ldots, a_n)$ be a rational-form diagram for K, and write $[a_1, \ldots, a_n] = p/q$ for $p, q \in \mathbb{Z}$. The classification of 2-bridge links implies that K is isotopic to any rational-form diagram associated to the fraction $r = p/(q - \lfloor \frac{q}{p} \rfloor p) > 1$. (If q/p is an integer, then it is easy to see that K is the trivial knot, which is not 2-bridge.)

Define a sequence $x_1, x_2, \ldots$ of rational numbers by $x_1 = r$, $x_{i+1} = 1/(\lceil x_i \rceil - x_i)$. This sequence terminates at, say, x_m, where x_m is an integer. Write $b_i = \lceil x_i \rceil$. It is easy to see that $b_i \geq 2$ for all i, and that $r = [b_1, \ldots, b_m]$. Then K is isotopic to $T(b_1, \ldots, b_m)$, which is in Legendrian rational form. □

Consider a link diagram $T = T(a_1, \ldots, a_n)$ in Legendrian rational form, and let K be the (Legendrian link given by the) front obtained from T. We claim that the Thurston-Bennequin number of K agrees precisely with the Kauffman bound. Recall that the Kauffman polynomial $F_T(a, x)$ of T is $a^{w(T)}$ times the *unoriented* Kauffman polynomial (or L-polynomial) $L_T(a, x)$, where $w(T)$ is the writhe of the diagram T. (Here we use Kauffman's original notation [Kau1], except with a replaced by $1/a$.)

We will need a matrix formula for $L_T(a, x)$ due to [Lic]. Write

$$M = \begin{pmatrix} x & -1 & x \\ 1 & 0 & 0 \\ 0 & 0 & 1/a \end{pmatrix}, \quad S = \begin{pmatrix} 0 & 1 & 0 \\ 0 & 0 & 1 \\ 1/a & 0 & 0 \end{pmatrix}, \quad v = \begin{pmatrix} 1 \\ 0 \\ 0 \end{pmatrix}, \quad w = \begin{pmatrix} a \\ a^2 \\ \frac{a^2+1}{x} - a \end{pmatrix};$$

then

$$L_{T(a_1,\ldots,a_n)}(a, x) = \tfrac{1}{a} v^t M^{-a_1-1} S M^{-a_2-1} S \cdots M^{-a_n-1} S w,$$

where t denotes transpose.

Lemma 6.2.2. *If $a_1, a_n \geq 1$ and $a_i \geq 2$ for $2 \leq i \leq n-1$, then $v(L_{T(a_1,\ldots,a_n)}(a, x)) = -1$.*

Proof. None of M^{-1}, S, and w contains negative powers of a; thus the lemma will follow if we can show that $f(x) \neq 0$, where

$$f(x) = (v^t M^{-a_1-1} S M^{-a_2-1} S \cdots M^{-a_n-1} S w)|_{a=0}.$$

Define the auxiliary matrices

$$A = M^{-1}|_{a=0} = \begin{pmatrix} 0 & 1 & 0 \\ -1 & x & 0 \\ 0 & 0 & 0 \end{pmatrix}, \quad B = (M^{-2} S M^{-1})|_{a=0} = \begin{pmatrix} 1 & 0 & 0 \\ x & 0 & 0 \\ 0 & 0 & 0 \end{pmatrix}, \quad u = \begin{pmatrix} 0 \\ 1 \\ 0 \end{pmatrix}.$$

Then $(ASw)|_{a=0} = \frac{1}{x}Au$ and $B = Auv^t$, and so

$$\begin{aligned} f(x) &= v^t A^{a_1-1} B A^{a_2-2} B A^{a_3-2} B \cdots A^{a_{n-1}-2} B A^{a_n-1} (ASw)|_{a=0} \\ &= \tfrac{1}{x}(v^t A^{a_1} u)(v^t A^{a_2-1} u)(v^t A^{a_3-1} u) \cdots (v^t A^{a_{n-1}-1} u)(v^t A^{a_n} u). \end{aligned}$$

But if we define a sequence of functions $f_k(x) = v^t A^k u$, then an easy induction yields the recursion $f_{k+2}(x) = x f_{k+1}(x) - f_k(x)$ with $f_1(x) = 1$ and $f_2(x) = x$. In particular, for all $k \geq 1$, $f_k(x)$ has degree $k-1$ and is thus nonzero. From the given conditions on a_i, it follows that $f(x) \neq 0$, as desired. □

Proof of Theorem 6.1.3. Let T be a Legendrian rational form for a 2-bridge link K. The crossings of T are counted, with the same signs, by both the writhe of T and the Thurston-Bennequin number of the Legendrian link K' obtained from T; $tb(K')$, however, also subtracts half the number of cusps. Hence

$$\begin{aligned} tb(K') &= w(T) - 2 \\ &= v(F_T(a,x)) - v(L_T(a,x)) - 2 \\ &= v(F_T(a,x)) - 1 \end{aligned}$$

by Lemma 6.2.2. Since K' is ambient isotopic to K, we conclude that $\overline{tb}(K)$ is at least $v(F_T) - 1$; by the Kauffman bound, equality must hold. □

6.3 Proof for pretzel links

Theorem 6.1.4 follows from the following result.

Lemma 6.3.1. *Suppose $p_1, p_2, p_3 > 0$. Then*

$$\begin{aligned} v(P(p_1,p_2,p_3)) &= -2, \\ v(P(-p_1,p_2,p_3)) &= -p_1, \\ v(P(-p_1,-p_2,-p_3)) &= 2 - p_1 - p_2 - p_3, \end{aligned}$$

and, for $p_1 \geq p_2$,

$$v(P(-p_1,-p_2,p_3)) = \begin{cases} 2 - p_1 - p_2 + p_3 & \text{if } p_2 \geq p_3 + 2, \\ -p_1 & \text{if } p_2 \leq p_3, \\ 2 - p_1 & \text{if } p_1 - 3 \geq p_2 = p_3 + 1, \\ 3 - p_1 & \text{if } p_1 - 2 = p_2 = p_3 + 1, \\ 1 - p_1 & \text{if } p_1 - 1 = p_2 = p_3 + 1 \text{ or } p_1 = p_2 = p_3 + 1. \end{cases}$$

Before we prove Lemma 6.3.1, we deduce Theorem 6.1.4 from it.

Proof of Theorem 6.1.4. Fronts for Legendrian forms of the various pretzel knots are given in Figures 6-5 and 6-6. For the given form of $P(p_1,p_2,p_3)$, we have $tb = w(P(p_1,p_2,p_3)) - 3$, because the cusps contribute -3 and each crossing gives the same contribution to tb and to

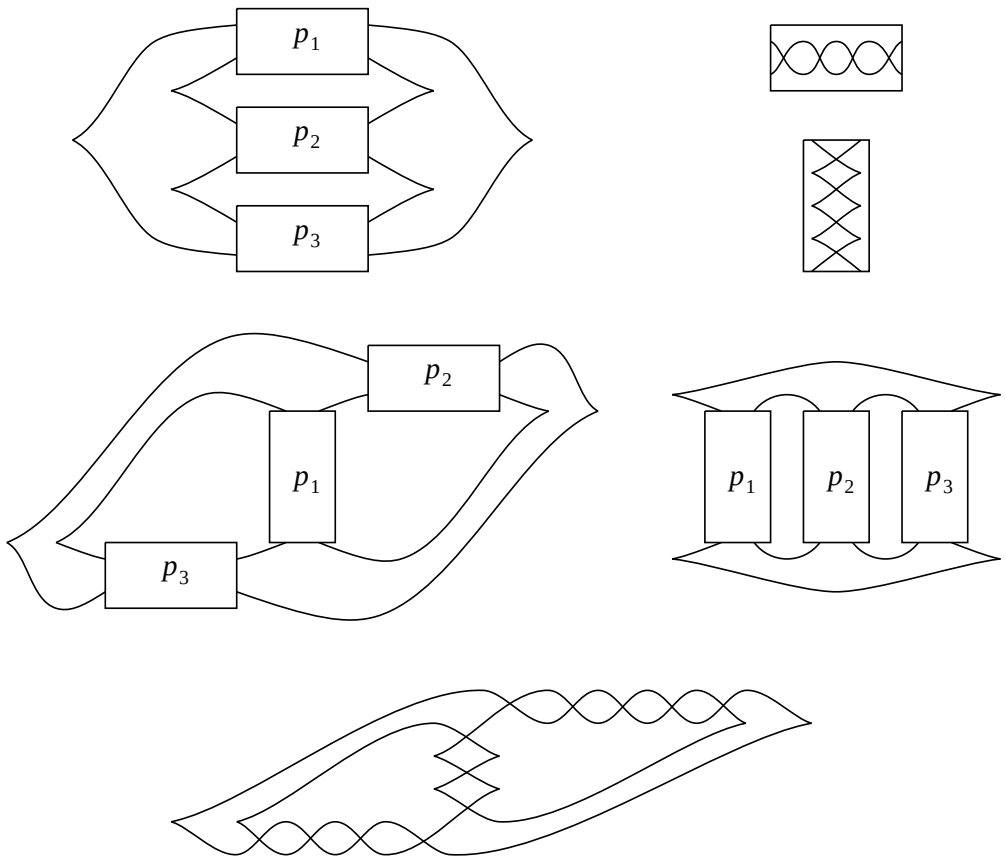

Figure 6-5: Fronts for $P(p_1, p_2, p_3)$, $P(-p_1, p_2, p_3)$, and $P(-p_1, -p_2, -p_3)$. Horizontal and vertical boxes represent the sample boxes depicted, with the label denoting the number of crossings. As an example, the front for $P(-3, 5, 4)$ is given at bottom.

the writhe w of the link diagram for $P(p_1, p_2, p_3)$ shown in Figure 6-2. By Lemma 6.3.1,

$$\begin{aligned} tb - v(F_{P(p_1,p_2,p_3)}) + 1 &= tb - v(L_{P(p_1,p_2,p_3)}) - w(P(p_1, p_2, p_3)) + 1 \\ &= -2 - v(P(p_1, p_2, p_3)) \\ &= 0, \end{aligned}$$

and the Kauffman bound is sharp. Similar calculations show that the Kauffman bound is sharp for the given Legendrian forms of $P(-p_1, p_2, p_3)$, for which $tb = w(P(-p_1, p_2, p_3)) - p_1 - 1$, and $P(-p_1, -p_2, -p_3)$, for which $tb = w(P(-p_1, -p_2, -p_3)) - p_1 - p_2 - p_3 + 1$.

For the Legendrian forms of $P(-p_1, -p_2, p_3)$ given in Figure 6-6, with $p_1 \geq p_2$, a routine calculation yields

$$tb = \begin{cases} w(P(-p_1, -p_2, p_3)) - p_1 - p_2 + p_3 + 1 & \text{if } p_2 \geq p_3 + 2, \\ w(P(-p_1, -p_2, p_3)) - p_1 - 1 & \text{if } p_2 \leq p_3 + 1. \end{cases}$$

Although Figure 6-6 only shows Legendrian forms for $p_2 \geq 2$, a similar calculation holds when $p_2 = 1$. We now use Lemma 6.3.1, as before, to conclude that the Kauffman bound is sharp for $p_2 \neq p_3 + 1$, and to deduce the bounds on $\widetilde{tb}$ in the statement of the proposition for $p_2 = p_3 + 1$. □

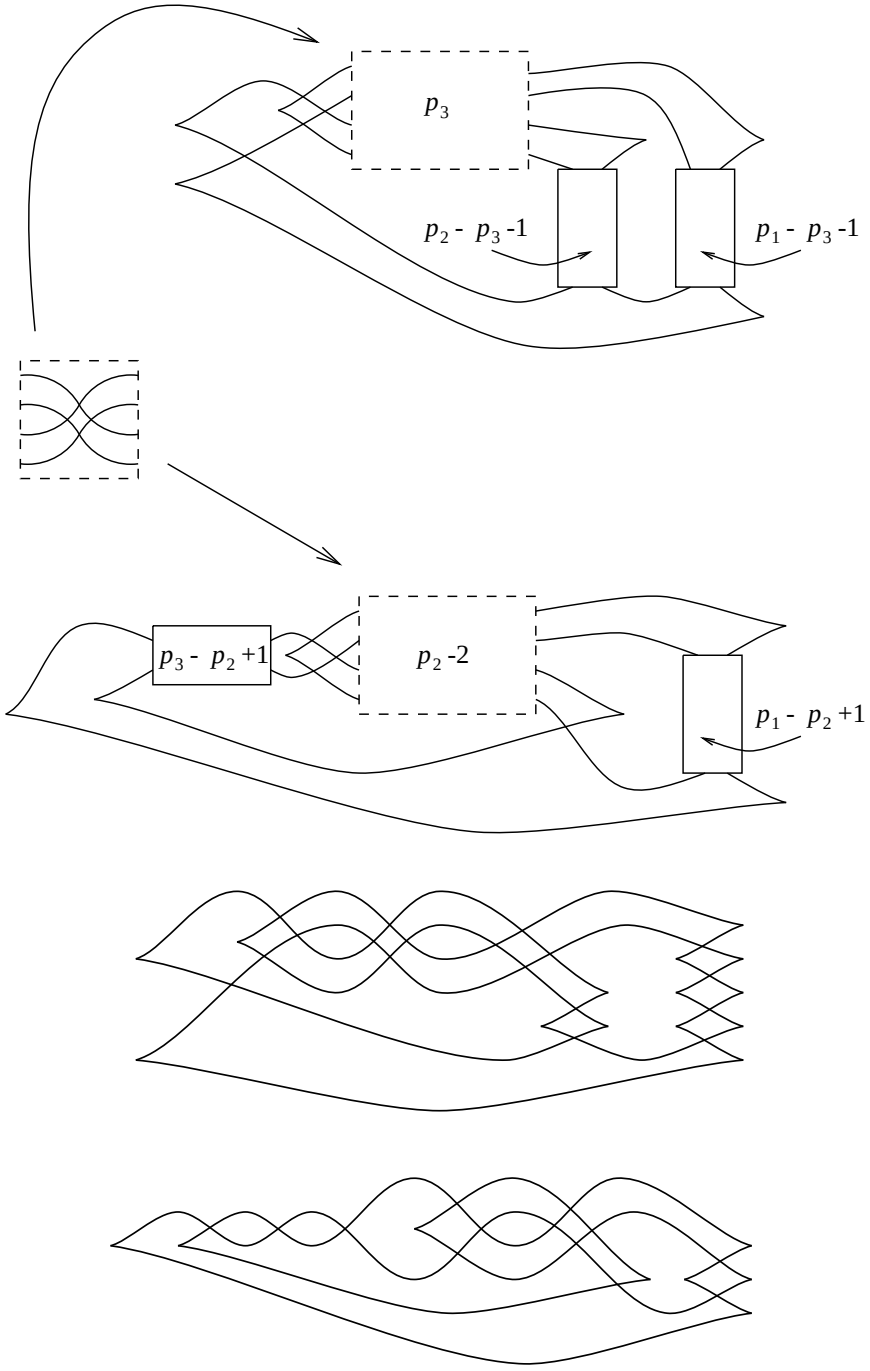

Figure 6-6: Fronts for $P(-p_1, -p_2, p_3)$, where $p_1 \geq p_2 \geq 2$. The top front is for $p_2 \geq p_3 + 2$; the second is for $p_2 \leq p_3 + 1$. Horizontal and vertical boxes are as in Figure 6-5; dashed boxes with a number inside indicate that number of concatenations of the small figure in the dashed box. As examples, the fronts for $P(-7, -5, 2)$ and $P(-4, -3, 5)$ are given at bottom.

The rest of this section is devoted to the proof of Lemma 6.3.1. Let $T(p)$ denote the torus link shown in Figure 6-2; by abuse of notation, we will write $T(p)$ also for the unoriented Kauffman polynomial of the knot diagram portrayed in Figure 6-2. We may compute $T(p)$ inductively from the following lemma, which follows directly from the Kauffman skein relations, applied to one of the crossings of $T(p)$.

Lemma 6.3.2. $T(p) + T(p-2) = x\,T(p-1) + xa^{p-1}$.

Lemma 6.3.2 allows us to calculate the part of the polynomial $T(p)$ with lowest degree in a, by induction from the well-known (or easily calculated) values for $T(0)$ and $T(1)$. For a polynomial $P(a,x)$, let $\lambda(P)$ be the sum of the terms in P with lowest degree in a, so that $\lambda(P)$ is the product of $a^{v(P)}$ and a polynomial in x.

Lemma 6.3.3. *We have*

$$\lambda(T(p)) = \begin{cases} (x^{p-1} + o(x^{p-1}))a^{-1} & \text{if } p \geq 1, \\ x^{-1}a^{-1} & \text{if } p = 0, \\ a & \text{if } p = -1, \\ (x - x^{-1})a^{-1} & \text{if } p = -2, \\ xa^{p+1} & \text{if } p \leq -3. \end{cases}$$

Here $o(\cdot)$, as usual, represents terms of lower order.

The key to the proof of Lemma 6.3.1 is the following result, which follows from an application of the Kauffman skein relation to one of the p_1 crossings of the link $P(p_1,p_2,p_3)$ when $p_1 > 0$, or to one of the $|p_1 - 2|$ crossings of the link $P(p_1-2,p_2,p_3)$ when $p_1 \leq 0$.

Lemma 6.3.4. $P(p_1,p_2,p_3) + P(p_1-2,p_2,p_3) = xP(p_1-1,p_2,p_3) + xa^{p_1-1}T(p_2+p_3)$.

Now suppose, as in the statement of Lemma 6.3.1, that $p_1,p_2,p_3 > 0$. The calculations of $v(P(p_1,p_2,p_3))$, $v(P(-p_1,p_2,p_3))$, $v(P(-p_1,-p_2,p_3))$, and $v(P(-p_1,-p_2,-p_3))$ are by induction, with varying degrees of difficulty, using Lemma 6.3.4.

For $P(p_1,p_2,p_3)$, Lemma 6.3.1 now follows from the following result.

Lemma 6.3.5. *For $p_1,p_2,p_3 \geq 0$, we have*

$$\lambda(P(p_1,p_2,p_3)) = \left(x^{p_1+p_2+p_3-2} + o(x^{p_1+p_2+p_3-2})\right) a^{-2}.$$

Proof. We prove this by induction on $p_1+p_2+p_3$. The cases $(p_1,p_2,p_3) = (0,0,0)$, $(0,0,1)$, $(0,1,1)$, and $(1,1,1)$ are all easily checked. Otherwise, assume without loss of generality that $p_1 \geq p_2 \geq p_3$; then $p_1 \geq 2$. By Lemma 6.3.3, $v(T(p_2+p_3)) = -1$, and by the induction assumption, $\lambda(P(p_1-1,p_2,p_3)) = \left(x^{p_1+p_2+p_3-3} + o(x^{p_1+p_2+p_3-3})\right) a^{-2}$ and $\lambda(P(p_1-2,p_2,p_3)) = \left(x^{p_1+p_2+p_3-4} + o(x^{p_1+p_2+p_3-4})\right) a^{-2}$. The result now follows from Lemma 6.3.4. □

The proofs of Lemma 6.3.1 for $P(-p_1,p_2,p_3)$ and $P(-p_1,-p_2,-p_3)$ are easy inductions along the lines of the proof of Lemma 6.3.5, and will be omitted.

Now consider $P(-p_1,-p_2,p_3)$. The following lemma, which completes the proof of Lemma 6.3.1, can be established by induction on $p_1+p_2+p_3$, as before. The precise computations, which are quite involved but straightforward given the statement of the lemma, are omitted here.

Lemma 6.3.6. *We have*

$$v(P(-p_1,-p_2,p_3)) = \begin{cases} 2-p_1-p_2+p_3 & \text{if } p_2 \geq p_3+2, \\ -p_1 & \text{if } p_2 \leq p_3, \\ 2-p_1 & \text{if } p_1-3 \geq p_2 = p_3+1, \end{cases}$$

and, furthermore,

$$\begin{aligned}
P(-(p_3+3),-(p_3+1),p_3) &= (-x^4+2x^2)a^{-p_3}+\cdots && p_3 \geq 3 \\
P(-(p_3+2),-(p_3+1),p_3) &= -a^{-p_3-1}+(-x^3+x)a^{-p_3}+\cdots && p_3 \geq 3 \\
P(-(p_3+1),-(p_3+1),p_3) &= -x^2a^{-p_3}+\cdots && p_3 \geq 3 \\
P(-p_3,-p_3,p_3) &= 2a^{-p_3}+\cdots && p_3 \geq 3 \\
P(-(p_3+1),-p_3,p_3) &= a^{-p_3-1}+0\cdot a^{-p_3}+\cdots && p_3 \geq 1 \\
P(-p_3,-(p_3-1),p_3) &= xa^{-p_3}+\cdots && p_3 \geq 2 \\
P(-(p_3+1),-(p_3-1),p_3) &= xa^{-p_3-1}+x^2a^{-p_3}+\cdots && p_3 \geq 2 \\
P(-p_3,-(p_3-2),p_3) &= (x^2-1)a^{-p_3}+\cdots && p_3 \geq 3,
\end{aligned}$$

where ellipses denote terms of higher degree in a.

6.4 Discussion

In this section, we discuss some intriguing connections between the maximal Thurston-Bennequin story and the Chekanov-Eliashberg story from previous chapters.

We first note that the Chekanov-Eliashberg DGA and the characteristic algebra are effective tools for determining when a given Legendrian link maximizes Thurston-Bennequin number. Recall that the DGA (and hence the characteristic algebra) of any stabilized link is trivial; see Remark 2.2.10. We believe that a converse statement may also hold.

Conjecture 6.4.1. *If a Legendrian link K has trivial characteristic algebra, then it is Legendrian isotopic to a stabilization.*

Even if this conjecture is not true, triviality of the characteristic algebra is often a good indication, in practice, that tb is not maximal.

Here is a related proposal.

Conjecture 6.4.2. *Any Legendrian link which is not Legendrian isotopic to a stabilization maximizes Thurston-Bennequin number.*

This conjecture would be difficult to prove from the DGA standpoint. If true, however, it would combine with the DGA picture to facilitate computations of maximal tb when the Kauffman bound fails. Any Legendrian link whose characteristic algebra did not vanish would then automatically maximize tb. (This is our basis for asserting probable maximal Thurston-Bennequin numbers below for certain links.)

There appear to be mysterious connections between nonsharpness of the Kauffman inequality and the Chekanov-Eliashberg algebra. D. Fuchs [Fu] has proposed the following statement, which he calls an "irresponsible conjecture."

Conjecture 6.4.3 ([Fu]). *The Kauffman bound is sharp for a Legendrian knot K if and only if the Chekanov-Eliashberg DGA for K admits an (ungraded) augmentation.*

(For the definition of augmentation, see Section 3.2.) The conjecture was originally stated for graded augmentations, but is false in this case. We would like to propose a related conjecture, for which we have some (but not overwhelming) empirical evidence.

Conjecture 6.4.4. *The Kauffman bound is sharp for a Legendrian knot K if and only if the abelianized characteristic algebra of K is not trivial.*

Certainly, if the abelianized characteristic algebra of K is trivial, then the DGA for K admits no augmentation. Recall that we conjectured in Section 3.2 that the abelianized characteristic algebra of K, when K maximizes tb, depends only on the smooth isotopy class of K.

For the remainder of this section, we survey what is known about sharpness of the Kauffman bound for particular links. We begin with prime knots with small numbers of crossings, for which we can apply our 2-bridge result.

The class of 2-bridge links includes many prime knots with a small number of crossings. More precisely, all prime knots with seven or fewer crossings are 2-bridge, as are all prime knots with eight or nine crossings except the following: 8_5, 8_{10}, 8_{15}–8_{21}, 9_{16}, 9_{22}, 9_{24}, 9_{25}, 9_{28}, 9_{29}, 9_{30}, and 9_{32}–9_{49}. Examples drawn by hand by N. Yufa [Yu] and the author show that the Kauffman bound is sharp for all of the above eight-crossing knots except for 8_{19} (more precisely, the mirror image of the version drawn in [Rol]). Since 8_{19} is the $(4,-3)$ torus knot, a result of [EH] yields $\overline{tb} = -12$ in this case, while the Kauffman bound gives $\overline{tb} \leq -11$. These calculations and Theorem 6.1.3 yield the following result.

Proposition 6.4.5. *The Kauffman bound is sharp for all prime knots with eight or fewer crossings, except the $(4,-3)$ torus knot 8_{19}, for which $\widetilde{tb} = 1$.*

Further drawings show that the Kauffman bound is sharp for all of the nine-crossing prime knots which are not 2-bridge, except possibly for 9_{42} (more precisely, the mirror of the one in [Rol]). For this last knot, we believe that $\widetilde{tb} = 2$. In Appendix B, we include a table of $\overline{tb}$ for prime knots with nine or fewer crossings.

We next consider other knots. The only known family of knots for which the Kauffman bound is not sharp are the $(p,-q)$ torus knots with $p > q > 0$ and q odd [EH]; for these knots, we have $\widetilde{tb} = p - q$. Our results with pretzel links suggest more families for which Kauffman may not be sharp.

Recall from Theorem 6.1.4 that $\widetilde{tb}(P(-p_1, -p_3 - 1, p_3))$ is not necessarily zero when $p_1 \geq p_3 + 1$, while Kauffman is sharp for all other three-stranded pretzel links. Among these exceptional pretzel links, the only cases for which $\widetilde{tb}$ is known are the two pretzel knots which are also torus knots: $P(-3,-3,2)$ is the $(4,-3)$ torus knot, while $P(-5,-3,2)$ is the $(5,-3)$ torus knot. From [EH], we conclude that $\widetilde{tb}(P(-3,-3,2)) = 1$ and $\widetilde{tb}(P(-5,-3,2)) = 2$.

Calculations with the characteristic algebra lead us to believe that $\widetilde{tb}(P(-p,-p,p-1)) = 1$ in general. This would give the second known class of links for which Kauffman is not sharp. For the other exceptional cases, we do not currently have guesses for what $\widetilde{tb}$ ought to be; the characteristic algebra, however, suggests that the Legendrian links shown in Figure 6-6 do not maximize tb in these cases.

Appendix A

Front projection proofs

In this appendix, we provide proofs for the major results about the Chekanov-Eliashberg DGA over $\mathbb{Z}[t, t^{-1}]$ described in Section 2.4, in the front-projection setup. Although these results have already been established in [ENS] for the Lagrangian projection, it is sometimes useful to have proofs for the front projection available for reference.

A.1 Proof of Proposition 2.4.1

Please refer to Section 2.2 for terminology and notation. This proof is quite similar to the corresponding proof (of Lemma 4.7) in [ENS].

Consider an admissible map f in the front projection of a Legendrian knot K, having initial vertex at a_i and corner vertices at $a_{j_1}, \dots, a_{j_\ell}$. Since this contributes a term $\pm t^{-n(f)} a_{j_1} \cdots a_{j_\ell}$ to ∂a_i, we wish to prove that

$$\deg a_i = \sum_{k=1}^{\ell} \deg a_{j_k} - 2n(f)r(K) + 1.$$

For any oriented path γ in the diagram of K, write $c(\gamma)$ for the number of cusps traversed upwards along γ, minus the number of cusps traversed downwards. Let $\tilde{\gamma}$ be the closed curve which is the union of the (counterclockwise oriented) boundary of the image of f and the capping paths γ_i, $-\gamma_{j_1}, \dots, -\gamma_{j_\ell}$. Then the winding number of $\tilde{\gamma}$ along K is $n(f)$ by definition, and so $c(\tilde{\gamma}) = -2n(f)r(K)$.

On the other hand, we also have

$$c(\tilde{\gamma}) = c(f(\partial D^2)) + c(\gamma_i) - \sum_{k=1}^{\ell} c(\gamma_{j_k}).$$

Since some of the paths begin and end at right cusps, we need a convention for when right cusps are included in these paths. For convenience, we impose the following conventions:

- capping paths for right cusps oriented upwards include the cusp (traversed upwards);
- capping paths for right cusps oriented downwards exclude the cusp at both of their endpoints;
- $f(\partial D^2)$ does not include its initial vertex if this vertex is a right cusp;

- $f(\partial D^2)$ includes a corner-vertex right cusp once, traversed upwards, if it enters and leaves the cusp from above; once, traversed downwards, if it enters and leaves from below; and once, traversed upwards, if it enters from above and leaves from below (i.e., the cusp is counted twice as a corner vertex).

It is straightforward to check that these conventions form a consistent way to include and exclude right cusps. From the definitions, it is obvious that $c(\gamma_i) = \deg a_i$ and $c(\gamma_{j_k}) = \deg a_{j_k}$, and a simple diagram chase shows that $c(f(\partial D^2)) = -1$. The result follows. □

A.2 Proof of Proposition 2.4.2

Fix i; we wish to prove that $\partial^2 a_i = 0$. The idea is to show that every monomial in $\partial^2 a_i$ occurs twice, with opposite signs and the same powers of t. A monomial in $\partial^2 a_i$ is given pictorially by two admissible maps, one, f_1, with initial vertex at a_i, and the other, f_2, with initial vertex at some corner vertex a_j of f_1. (If a_j is a right cusp, then we account for the extra 1 term in ∂a_j by artificially allowing f_2 to be possibly the constant map at the point a_k, corresponding to the monomial 1.)

The maps f_1 and f_2 share a common boundary beginning at a_j and ending at some other vertex a_k; moreover, it is easy to see that this common boundary is smooth and travels only from right to left (starting at a_j and ending at a_k), and that a_k is a node. We can glue the two maps along their common boundary to get another map f_3 from D^2 to the plane, which no longer has a corner vertex at a_j, and which would be admissible, with initial vertex at a_i, except for the singularity at a_k; the image of f_3 occupies three of the four regions around a_k (but not the region on the "left").

Fix f_3. The common boundary C between a_j and a_k can then be viewed as the smooth image under f_3 of a smooth curve in D^2 starting at (the preimage of) a_k and ending either on the boundary of D^2 or at (the preimage of) a cusp, such that C always lies in the knot projection Y. There are two possible ways to draw C, depending on which curve we choose to leave a_k through; each splits the image of f_3 into two regions (one possibly empty), and each of which contributes the same monomial, up to sign, to $\partial^2 a_i$. (One of these two regions is empty when a_j is a right cusp and f_2 is the constant map at a_j.) We need to check that the two choices for C give two different signs, and the same power of t, to the monomials they contribute to $\partial^2 a_i$. See Figure A-1 for a concrete illustration.

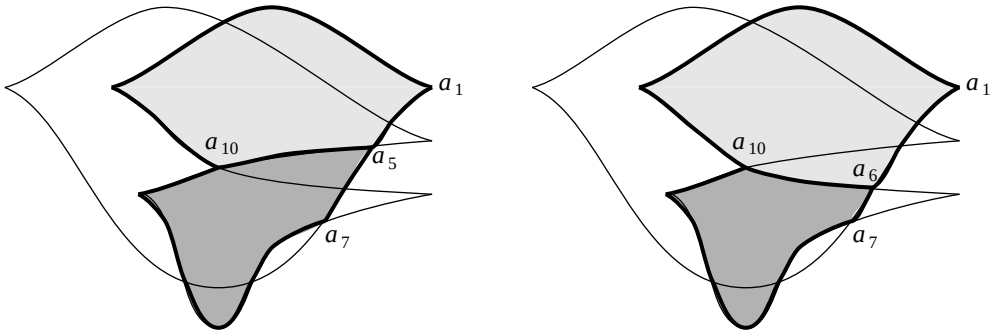

Figure A-1: Two contributions to $\partial^2 a_1$ for the front from Figure 2-6 which glue together to form the same map, and which each contribute the monomial $\pm a_{10} a_7$ to $\partial^2 a_1$. The left diagram corresponds to the terms $a_{10} a_5$ in ∂a_1 and a_7 in ∂a_5; the right, a_6 in ∂a_1 and $-a_{10} a_7$ in ∂a_6.

We first verify the powers of t. As described in Section 2.2, $n(f_i)$, for $i = 1, 2$, is the winding numbers around K of the oriented closed curve consisting of the union of $f_i(\partial D^2)$ and the capping paths of the vertices of f_i. The power of t associated to the monomial in $\partial^2 a_i$ given by f_1 and f_2 is $n(f_1) + n(f_2)$. It is easy to see, however, that the sum of the closed curves associated to f_1 and f_2 depends only on f_3, and so $n(f_1) + n(f_2)$ is the same for both of the decompositions of f_3.

The rest of this section is devoted to verifying the signs. We will need some more notation. Define the sign of f_3 analogously to our definition of the sign of an admissible map: $\operatorname{sgn} f_3$ is the product of $(-\operatorname{sgn} a_\ell)$ over all downward corner vertices a_ℓ. Given two vertices v, w on the boundary of f_3, let $\overline{vw}$ denote the section of the boundary of f_3 between them (counterclockwise from v to w), and then let $\operatorname{sgn} \overline{vw}$ be the product of the signs of all (not necessarily downward) corner vertices in the interior of the section. For convenience, let σ be the sign of the contribution of f_1 and f_2 to $\partial^2 a_i$. Then we claim that

$$\sigma = \pm(\operatorname{sgn} \overline{a_i a_k})(\operatorname{sgn} a_k)(\operatorname{sgn} f_3),$$

where the $\pm$ sign is $+$ if C follows the curve of higher slope from a_k, and $-$ if it follows the curve of lower slope. The desired result will then follow.

From the definition of ∂, σ is $(\operatorname{sgn} f_1)(\operatorname{sgn} f_2)$ times the product of the signs of the corner vertices in f_1 which occur before a_j. On the other hand, there is nearly a one-to-one correspondence between downward corner vertices in f_3 and the aggregate of downward corner vertices in f_1 and f_2, so that $(\operatorname{sgn} f_1)(\operatorname{sgn} f_2)$ is nearly $(\operatorname{sgn} f_3)$.

We now have several cases, illustrated in Figure A-2, depending on whether the endpoint a_j of C is a vertex on the boundary of f_3 before a_k, a vertex on the boundary after a_k, or a right cusp in the interior of f_3. (This last case occurs when f_2 is the trivial constant map at the right cusp a_j.) Write $\tau = (\operatorname{sgn} \overline{a_i a_k})(\operatorname{sgn} a_k)(\operatorname{sgn} f_3)$; then we want to establish $\sigma = \pm\tau$ for the appropriate sign.

In Case 1, every downward corner vertex in f_1 or f_2 appears as a downward corner vertex in f_3, except for a_j, which only appears in f_1; hence $(\operatorname{sgn} f_1)(\operatorname{sgn} f_2) = (-\operatorname{sgn} a_j)(\operatorname{sgn} f_3)$. From Proposition 2.4.1 applied to f_2, we know that $\operatorname{sgn} a_j = -(\operatorname{sgn} \overline{a_j a_k})(\operatorname{sgn} a_k)$. Hence

$$\sigma = (\operatorname{sgn} \overline{a_i a_j})(\operatorname{sgn} f_1)(\operatorname{sgn} f_2) = (\operatorname{sgn} \overline{a_i a_j})(-\operatorname{sgn} \overline{a_j a_k})(\operatorname{sgn} f_3) = \tau.$$

We deal with the other cases similarly, by counting the downward corner vertices in f_1 or f_2 but not in f_3:

$$\sigma = (\operatorname{sgn} \overline{a_i a_j})(\operatorname{sgn} f_1)(\operatorname{sgn} f_2) = (\operatorname{sgn} \overline{a_i a_j})(\operatorname{sgn} a_j)(\operatorname{sgn} a_k)(\operatorname{sgn} f_3) = -\tau \qquad \text{(case 2)}$$

$$\sigma = (\operatorname{sgn} \overline{a_i a_k})(\operatorname{sgn} a_k)(\operatorname{sgn} f_1)(\operatorname{sgn} f_2) = \tau \qquad \text{(case 3)}$$

$$\sigma = (\operatorname{sgn} \overline{a_i a_k})(\operatorname{sgn} f_1)(\operatorname{sgn} f_2) = -\tau \qquad \text{(case 4)}$$

$$\sigma = (\operatorname{sgn} \overline{a_i a_k})(\operatorname{sgn} a_k)(\operatorname{sgn} f_1) = \tau \qquad \text{(case 5)}$$

$$\sigma = (\operatorname{sgn} \overline{a_i a_k})(\operatorname{sgn} f_1) = -\tau \qquad \text{(case 6). } \square$$

A.3 Proof of Theorem 2.4.3

To show that the differential algebra of a front is invariant (up to stable isomorphism) under Legendrian isotopy, it suffices to show that it is invariant under each of the Legendrian Reidemeister moves shown in Figure 1-1. The methods used in this proof closely follow those used in [Ch, section 10].

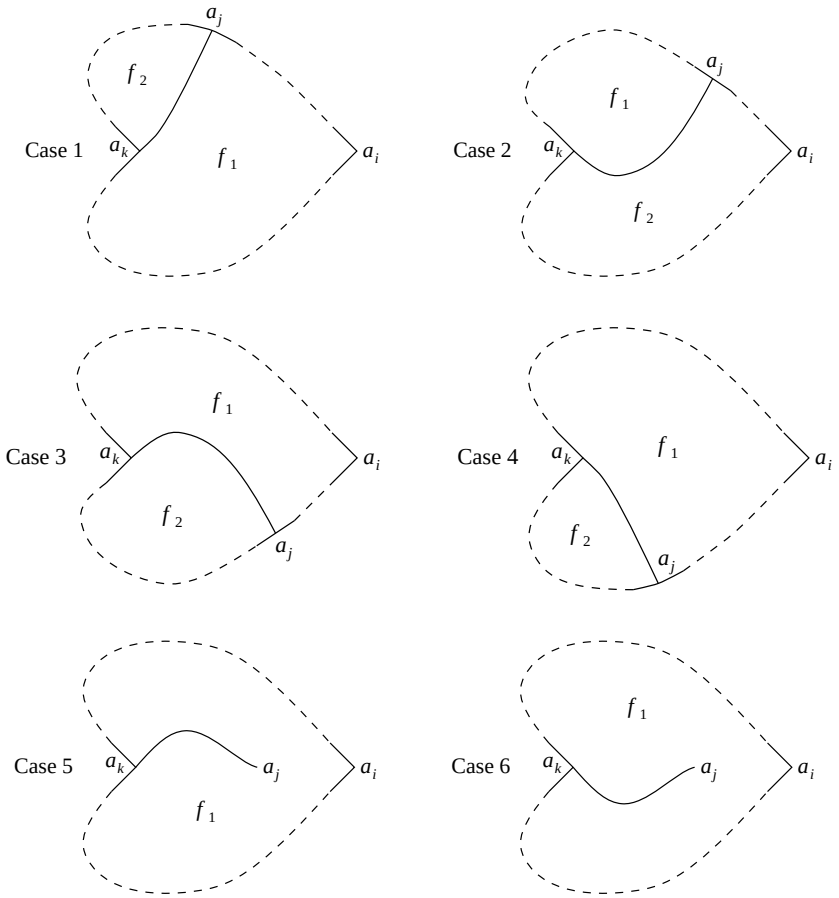

Figure A-2: Gluing two admissible maps f_1 and f_2 together. The dashed curve represents the boundary of the combination map f_3. In Cases 5 and 6, f_2 is the trivial constant map at the right cusp a_j.

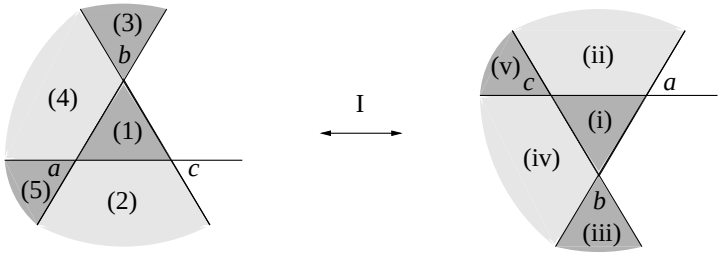

Figure A-3: The vertices affected by move I, with several relevant regions labelled.

We first deal with move I, which is shown in Figure A-3. The three vertices affected by the move are labelled by a, b, c in each diagram, and all other vertices $a_1, \ldots, a_{n-3}$ are unaffected by the move. We have also shaded in ten relevant regions. Denote the front projection on the left by K, and the one on the right by K'; let ∂ and ∂' be the differentials on the algebra $A = \mathbb{Z}[t, t^{-1}]\langle a, b, c, a_1, \ldots, a_{n-3}\rangle$ corresponding to K and K', respectively. We claim that $\partial' = g\partial g^{-1}$, where g sends b to $b + ca$ and leaves the other generators of A fixed.

It is immediate by inspection of Figure A-3 that $\partial a = \partial' a$ and $\partial c = \partial' c$. We can assume that a, b, and c are arbitrarily close to each other, so that no term in any of $\partial a, \partial' a, \partial c$, or $\partial' c$ involves b: any admissible map with a negative corner vertex at b must have a corner vertex to the right of a, b, c. Thus $\partial' a = g\partial g^{-1}(a)$ and $\partial' c = g\partial g^{-1} b$.

Now consider another vertex a_i besides a, b, c. Any admissible map in K or K' with initial vertex at a_i has a unique analogous map in the other front, unless part of its boundary looks like (2) or (ii). An admissible map M in K which locally looks like (2) has a companion admissible map $\tilde{M}$ in K which has (1) glued onto (2) (so that corner vertices a and c are replaced by b); this companion map corresponds to an admissible map M' in K' which locally looks like (iii), and the combined contribution of M and $\tilde{M}$ to ∂a_i is precisely the contribution of M' to $\partial' a_i$, except with b replaced by $b - ca$. (In fact, $(-\operatorname{sgn} b)b$ is replaced by $(-\operatorname{sgn} b)b + (-\operatorname{sgn} a)(-\operatorname{sgn} c)ca$, but it is easy to show that $\operatorname{sgn} b = (\operatorname{sgn} a)(\operatorname{sgn} c)$; just adapt the proof of Proposition 2.4.1.)

Similarly, an admissible map M' in K' which locally looks like (ii) has a companion admissible map $\tilde{M'}$ in K', which corresponds to an admissible map M in K, and the combined contribution of M' and $\tilde{M'}$ to $\partial' a_i$ is precisely the contribution of M to ∂a_i, except with b replaced by $b + ca$. All other admissible maps (ones whose monomials contain neither b nor ca) in K or K' can be matched up one-to-one. Summing up the contributions of all admissible maps with initial vertex at a_i, we conclude that $\partial' a_i = g\partial a_i = g\partial g^{-1} a_i$.

Note that we do not need to worry about powers of t here or elsewhere for move I. The capping paths for K and K' limit to each other as we approach the triple-point singularity, as do the boundaries of the images of corresponding admissible maps in K and K'. Thus the winding numbers giving the powers of t must be the same for corresponding terms in K and K'.

It remains to show that $\partial' b = g\partial g^{-1} b$. Admissible maps in K with initial vertex at b fall into two categories: (A) those which look like (4) near b (i.e., have a corner vertex at a), and (B) those which look like the union of (4) and (5) near b (i.e., do not have a as a corner vertex). Similarly, admissible maps in K' with initial vertex at b are either (A$'$) those which look like (iv) near b, or (B$'$) those which look like the union of (iv) and (v) near b. Write the contribution of (A) maps and (B) maps to ∂b as $\partial_1 b$ and $\partial_2 b$, respectively, and similarly for (A$'$) and (B$'$).

There is a one-to-one correspondence between (B) maps and (B$'$) maps, and so $\partial_2 b = \partial_2' b$. There is also a one-to-one correspondence between (A) maps and admissible maps with initial vertex at c (simply glue region (1) to region (4), which gets rid of the corner vertex at a); hence $\partial_1 b = (\partial c)a$. Similarly, $\partial_1' b = (-\operatorname{sgn} c)c\,\partial' a = -(\operatorname{sgn} c)c\,\partial a$. We conclude that

$$\partial' b = \partial_1' b + \partial_2' b = -(\operatorname{sgn} c)c\,\partial a + \partial_2(b) = \partial(b - ac) = g\partial g^{-1} b.$$

This completes the proof for move I. Moves II, III, and IV can be addressed at the same time, with varying degrees of difficulty.

Each of these moves begins with a front projection and adds two vertices to it: either

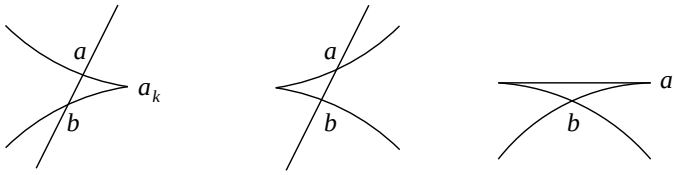

II III IV

Figure A-4: The new vertices a and b created by moves II, III, and IV.

two nodes (in the case of II and III), or a node and a right cusp (in the case of IV). We will prove invariance for the moves as drawn in Figure 1-1; the proofs for the mirror images of these moves in the z axis, while not identical, are entirely similar.

Denote the original front projection by K, and the new one (with two more vertices) by K'. Write the vertices of K (in order from highest to lowest x coordinate) as $a_1, \ldots, a_n$; these are also the vertices of K', along with the two new vertices a and b (where a is to the right of b). If we arrange the vertices of K' in order from right to left, we may assume that a and b are adjacent, so that the vertices occur in the order $a_1, \ldots, a_k, a, b, a_{k+1}, \ldots, a_n$ for some k. (For II, a_k is thus the right cusp next to a and b.) See Figure A-4.

For brevity, we will refer to $\mathbb{Z}[t, t^{-1}]\langle a_1, \ldots, a_n\rangle$ as A, and to $\mathbb{Z}[t, t^{-1}]\langle a_1, \ldots, a_n, a, b\rangle$ as A'. Let the differentials on A, A' arising from K, K' be ∂, ∂', respectively. To show that (A, ∂) and (A', ∂') are stably isomorphic, we first need to stabilize A: let $S(A)$ be the stabilization $\mathbb{Z}[t, t^{-1}]\langle a_1, \ldots, a_n, e_1, e_2\rangle$ of A, where the degrees of e_1 and e_2 will be determined later, with the differential (also denoted ∂) inherited from A and also satisfying $\partial e_1 = e_2, \partial e_2 = 0$. Let $\tilde{A}$ be the submodule of $S(A)$ over $\mathbb{Z}[t, t^{-1}]$ generated by monomials containing either e_1 or e_2, so that $S(A)$ has the submodule decomposition $S(A) = A \oplus \tilde{A}$. Finally, if a is a right cusp in K or K', write $\eta(a) = 1$ if a is oriented upwards and $\eta(a) = t^{-1}$ if a is oriented downwards, so that ∂a or $\partial' a$ contains $\eta(a)$ as a term.

We first define an isomorphism ϕ between $S(A)$ and A'. Send a_i to a_i, and map e_1 and e_2 as follows:

$$\phi : e_1,\, e_2 \mapsto \begin{cases} a - \eta(a_k)^{-1} a_k b, & -b + v + \eta(a_k)^{-1} a_k w & \text{for move II} \\ a, & b & \text{for move III} \\ a, & b + \eta(a) & \text{for move IV.} \end{cases}$$

For move II, define $w = \partial' b$; we still need to define v. There is a one-to-one correspondence between admissible maps on K' with initial vertex a and a corner vertex at b, and admissible maps with initial vertex a_k, by deleting/appending the "curved triangle" with vertices a, b, a_k. Hence the contribution to $\partial' a$ of maps with a corner vertex at b is, up to powers of t, $(\partial' a_k - 1)b = (\partial a_k - 1)b$.

To calculate the appropriate powers of t, let γ_a, γ_b, γ_{a_k} denote the capping paths associated to a, b, a_k. Independent of the orientations of various sections of K, $\gamma_a - \gamma_b$ is the closed curve winding around the curved triangle once counterclockwise. A bit of thought then shows that the desired contribution to $\partial' a$ is $(\eta(a_k)^{-1}\partial a_k - 1)b$.

We now define v be the contribution to $\partial' a$ of maps *without* a corner vertex at b, i.e., $v = \partial' a - (\eta(a_k)^{-1}\partial a_k - 1)b$.

Returning to the definition of ϕ, we note that, for each move, $\phi(e_1)$ and $\phi(e_2)$ are of pure degree in $\mathbb{Z}$, and $\deg \phi(e_1) = \deg \phi(e_2) + 1$. For example, for move II, the fact that $\gamma_a - \gamma_b$ is the curved triangle counterclockwise shows that $\deg a = \deg b + 1$, and so

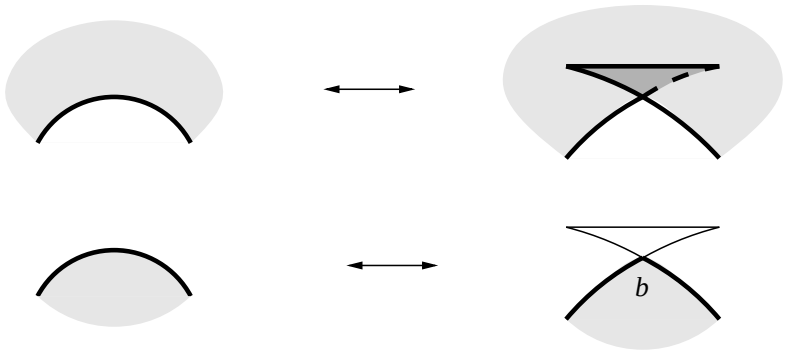

Figure A-5: Locally deforming admissible maps in K to admissible maps in K' in move IV. The bottom diagram requires the addition of corner vertex b.

$\deg v = \deg b = \deg(\eta(a_k)^{-1} a_k w)$. Thus ϕ gives a graded differential isomorphism between $S(A)$ and A'.

Under ϕ, ∂' pulls back to a differential on $S(A)$, which we also write as ∂'. It then suffices to exhibit an automorphism on $S(A)$ sending ∂ to ∂'. Note that we have defined ϕ so that $\partial' e_1 = e_2, \partial' e_2 = 0$: for move II, this follows from the definitions of v, w above, while for moves III and IV, this follows from the fact that $\partial' a = b$ and $\partial' a = \eta(a) + b$, respectively.

We now have the following key result (cf. Lemma 10.2 in [Ch, Lemma 10.2]).

Lemma A.3.1. *For all i, $\partial a_i - \partial' a_i$ is in $\tilde{A} \subset S(A)$.*

Proof. We prove the lemma separately for each move. We view ϕ as giving relations between e_1, e_2, a, and b, and will henceforth identify A' with $S(A)$ and suppress ϕ.

For move III, simply observe that every admissible map in K' not using $a = e_1$ or $b = e_2$ as a corner vertex gives a corresponding admissible map in K, and vice versa.

For move IV, any admissible map in K whose initial vertex is one of the a_i can be locally deformed to an admissible map in K' by using the correspondence in Figure A-5 wherever necessary. Conversely, it is straightforward to see that any admissible map in K' not containing a as a corner vertex arises from an admissible map in K in this way. (Any admissible map in K' containing a as a corner vertex contributes a monomial to $\partial' a_i$ which is in $\tilde{A}$.) The admissible maps in the upper diagram in Figure A-5 contribute the same amount to ∂a_i and $\partial' a_i$. The contributions of the maps in the lower diagram differ by the introduction of $(-\operatorname{sgn} b)\eta(a)^{-1} b = -\eta(a)^{-1} b = 1 - \eta(a)^{-1} e_2$ into the monomials in K'; thus each term in $\partial a_i - \partial' a_i$ contains e_2.

We now consider move II. Fix a vertex a_i; the terms in $\partial a_i - \partial' a_i$ arise from the admissible maps which locally look like one of the figures in Figure A-6. (These are precisely the maps in K or K' which have no analogue in the other front.) The maps in K' depicted in the top row can be paired up by appending/deleting the curved triangle; the contribution to $\partial a_i - \partial' a_i$ of each of these pairs is a multiple of $a - \eta(a_k)^{-1} a_k b = e_1$, since the monomial for the right-hand map is identical to that for the left-hand map, except with $(-\operatorname{sgn} b)\eta(a_k)^{-1} a_k b = (\operatorname{sgn} a)\eta(a_k)^{-1} a_k b$ instead of $(-\operatorname{sgn} a)\, a$. Similarly, we can dispose of the maps in K' depicted in the second row of Figure A-6.

The third row of Figure A-6 is more complicated. Any map in K corresponding to the middle or right figure (in the third row) breaks up into two maps in K' if we imagine dragging the right cusp a_k past the crossing line; see Figure A-7. One is precisely a map

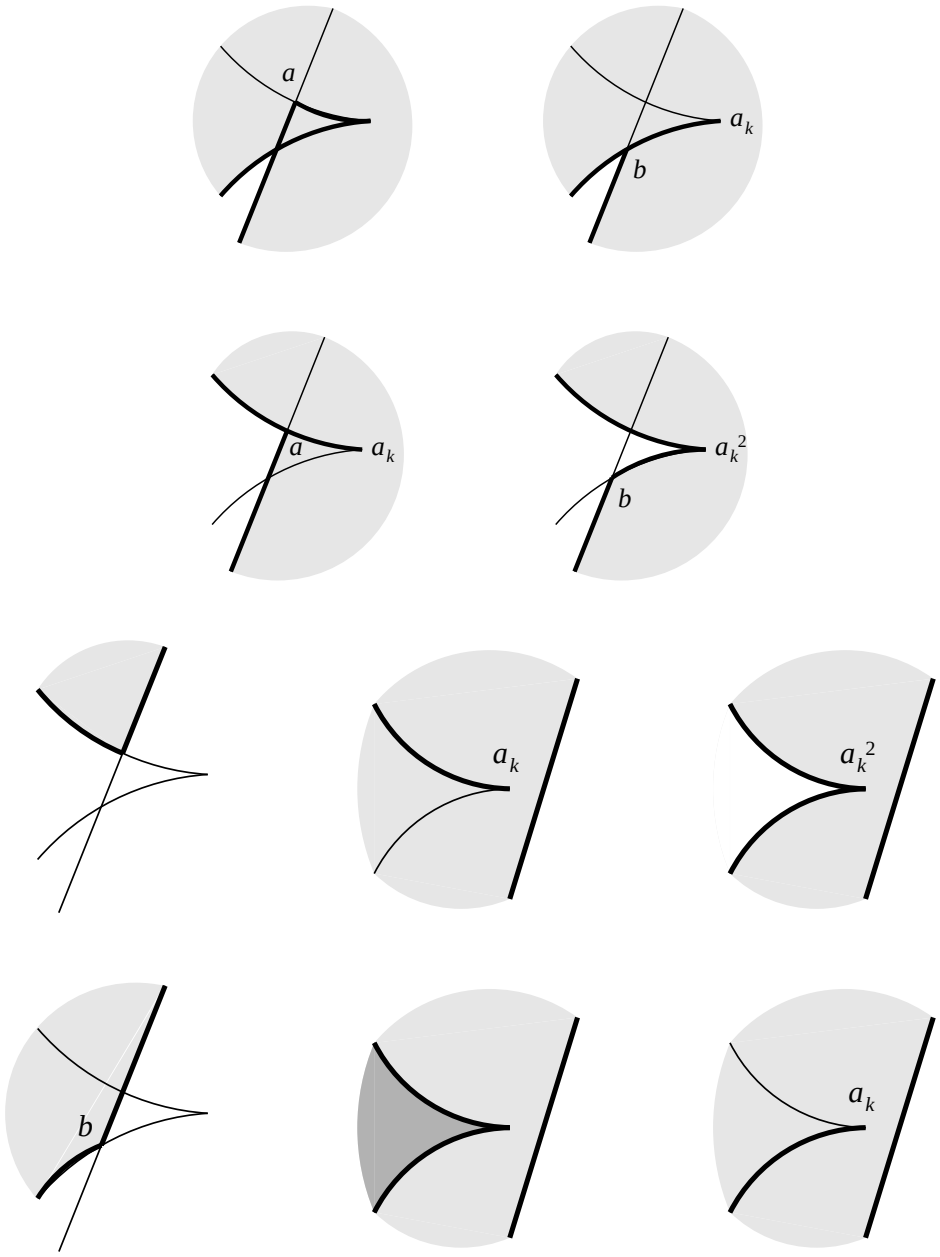

Figure A-6: The maps in K and K' contributing to $\partial a_i - \partial' a_i$ in move II. As usual, heavy lines indicate the boundary of the map, and heavy shading indicates overlapping. Negative corner vertices are marked, with multiplicity.

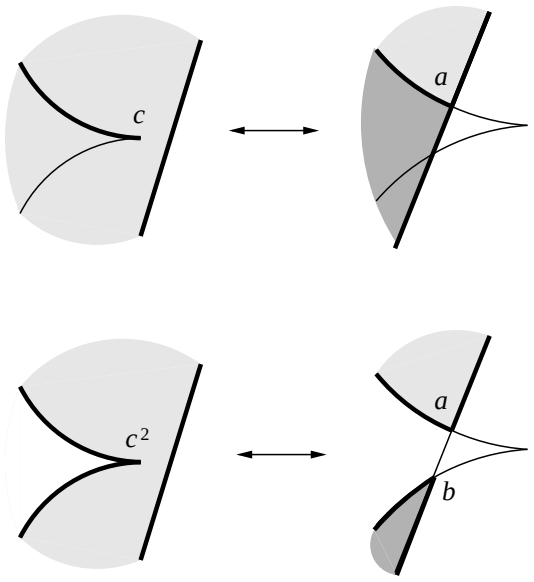

Figure A-7: Splitting a map in K into two maps (shaded differently) in K', for move II.

like the left figure (of the third row); the other corresponds to an entry in v (for the middle figure) or w (for the right figure). Conversely, we can assemble any two such maps in K' to give such a map in K. Thus a map like the left figure gives the same contribution to $\partial a_i - \partial' a_i$ as the corresponding maps like the middle or right figures, except with a replaced by $-\eta(a_k)^{-1}a_k v - \eta(a_k)^{-2}a_k^2 w$. But $a - \eta(a_k)^{-1}a_k v - \eta(a_k)^{-2}a_k^2 w = e_1 - \eta(a_k)^{-1}a_k e_2$, so the contribution of the third row *in toto* is in $\tilde{A}$. An identical argument works for the fourth row of Figure A-6; here we use the fact that $b - v - \eta(a_k)^{-1}a_k w = -e_2$. □

Define a *terraced differential* with respect to the ordering $a_1, \ldots, a_k, e_1, e_2, a_{k+1}, \ldots, a_n$ to be a differential such that ∂ maps a variable to an expression only involving variables following this variable in the list; by our observation that the rightmost point in an admissible map must be the initial vertex, we conclude that both ∂ and ∂' are terraced. Theorem 2.4.3 then follows from Lemma A.3.1 and the following lemma (cf. [Ch, p. 26]).

Lemma A.3.2. *If ∂ and ∂' are terraced differentials with respect to $a_1, \ldots, a_k$, e_1, e_2, $a_{k+1}, \ldots, a_n$, such that $\partial e_1 = \partial' e_1 = b$, $\partial e_2 = \partial' e_2 = 0$, $\partial a_i = \partial' a_i$ for $i \geq k+1$, and $\partial a_i - \partial' a_i \in \tilde{A}$ for all i, then ∂ and ∂' are tamely isomorphic.*

Proof. For each $i \leq k+1$, define $A_{[i]} \subset S(A)$ to be the algebra generated by $a_i, \ldots, a_k, e_1, e_2$, $a_{k+1}, \ldots, a_n$, and note that $\partial = \partial'$ on $A_{[k+1]}$. We construct a series of automorphisms g_i of A', for $i = 1, \ldots, k$, so that if we inductively define $\partial_{[k+1]} = \partial, \partial_{[i]} = g_i \partial_{[i+1]} g_i^{-1}$, then $\partial_{[i]} = \partial'$ on $A_{[i]}$. The automorphism g_i will send a_i to $a_i + q_i$ (where $q_i \in \tilde{A} \cap A_{[i+1]}$ is to be determined), and will leave the other generators of A' fixed.

Suppose by induction that we have determined $q_{i+1}, \ldots, q_k$ so that $\partial_{[i+1]}$ agrees with ∂' on $A_{[i+1]}$; we want to define $q_i \in \tilde{A} \cap A_{[i+1]}$ so that $\partial_{[i]} = g_i \partial_{[i+1]} g_i^{-1}$ agrees with ∂' on $A_{[i]}$. Note that $\partial_{[i+1]}$ maps $A_{[i+1]}$ to itself (because of the terraced differential condition), and so $\partial_{[i]}$ will certainly agree with ∂' on $A_{[i+1]}$; thus we simply need to find q_i such that $\partial_{[i]} a_i = \partial' a_i$.

Now $\partial_{[i+1]} a_i \in A_{[i+1]}$ by the terraced condition again, and $\partial_{[i+1]} q_i = \partial' q_i$ by the induction

hypothesis (and the fact that $q_i \in A_{[i+1]}$); thus

$$\partial_{[i]} a_i = g_i \partial_{[i+1]} g_i^{-1} a_i = g_i \partial_{[i+1]} (a_i - q_i) = \partial_{[i+1]} a_i - \partial' q_i.$$

If we write $r_i = \partial_{[i+1]} a_i - \partial' a_i$, then it suffices to define q_i so that $\partial' q_i = r_i$.

Since $q_{j+1}, \ldots, q_k \in \tilde{A}$ by induction assumption, and $\partial a_i - \partial' a_i \in \tilde{A}$ by hypothesis, we see that $r_i \in \tilde{A}$. In addition, since $\partial_{[i+1]} a_i \in A_{[i+1]}$, and ∂ and ∂' are differentials, we have $\partial' r_i = \partial' \partial_{[i+1]} a_i - \partial'^2 a_i = \partial_{[i+1]}^2 a_i - \partial'^2 a_i = 0$.

Now define the linear map $h : S(A) \to S(A)$ as follows: if $w \in A$, then $h(w) = 0$; if $y \in A$ and $z \in S(A)$, then $h(ye_1z) = 0$ and $h(ye_2z) = (\operatorname{sgn} y) ye_1z$. We claim that $h\partial' + \partial' h$ is the vector space projection from $S(A) = A \oplus \tilde{A}$ to $\tilde{A}$. Indeed, $h\partial' + \partial' h$ vanishes on A; also, if $y \in A$, then $(h\partial' + \partial' h)(ye_1z) = (\operatorname{sgn} y) h(ye_2z) = ye_1z$, and

$$(h\partial' + \partial' h)(ye_2z) = h\left((\partial' y)e_2z + (\operatorname{sgn} ye_2) ye_2(\partial' z)\right) + (\operatorname{sgn} y)\partial'(ye_1z) = ye_2z.$$

If we define $q_i = h(r_i)$, then it now follows that

$$\partial' q_i = \partial' h(r_i) = h\partial' r_i + r_i = r_i.$$

Also, $r_i \in A_{[i+1]}$, and so $q_i \in \tilde{A} \cap A_{[i+1]}$. This completes the induction. $\square$

Appendix B

Maximal Thurston-Bennequin number for small knots

The table on the next page gives the maximal Thurston-Bennequin number for all prime knots with nine or fewer crossings. Note that this table improves on the corresponding one from [Tan], which only considers one knot out of each mirror pair, and does not achieve sharpness in a number of cases. By Theorem 6.1.3, we can calculate $\overline{tb}(K)$ from the Kauffman polynomial when K is 2-bridge; the computations when K is not 2-bridge follow from figures drawn by N. Yufa [Yu] and the author.

We distinguish between knots and their (topological) mirrors by using the diagrams in [Rol]: the knots K are the ones drawn in [Rol], with mirrors $\tilde{K}$. The boldfaced numbers indicate the knots for which the Kauffman bound is not sharp (for 8_{19}), or probably not sharp (for 9_{42}). As mentioned in Section 6.4, we believe that $\overline{tb} = -5$ for the mirror 9_{42} knot; the best known bound, however, is the Kauffman bound $\overline{tb} \leq -3$.

K	$\overline{tb}(K)$	$\overline{tb}(\tilde{K})$	K	$\overline{tb}(K)$	$\overline{tb}(\tilde{K})$	K	$\overline{tb}(K)$	$\overline{tb}(\tilde{K})$	K	$\overline{tb}(K)$	$\overline{tb}(\tilde{K})$
0_1	-1	‡	8_8	-4	-6	9_8	-8	-3	$9_{29}{}^{\dagger}$	-8	-3
3_1	-6	1	8_9	-5	‡	9_9	-16	5	$9_{30}{}^{\dagger}$	-6	-5
4_1	-3	‡	$8_{10}{}^{\dagger}$	-2	-8	9_{10}	3	-14	9_{31}	-9	-2
5_1	-10	3	8_{11}	-9	-1	9_{11}	1	-12	$9_{32}{}^{\dagger}$	-2	-9
5_2	-8	1	8_{12}	-5	‡	9_{12}	-10	-1	$9_{33}{}^{\dagger}$	-6	-5
6_1	-5	-3	8_{13}	-4	-6	9_{13}	3	-14	$9_{34}{}^{\dagger}$	-6	-5
6_2	-7	-1	8_{14}	-9	-1	9_{14}	-4	-7	$9_{35}{}^{\dagger}$	-12	1
6_3	-4	‡	$8_{15}{}^{\dagger}$	-13	3	9_{15}	-10	-1	$9_{36}{}^{\dagger}$	1	-12
7_1	-14	5	$8_{16}{}^{\dagger}$	-8	-2	$9_{16}{}^{\dagger}$	5	-16	$9_{37}{}^{\dagger}$	-6	-5
7_2	-10	1	$8_{17}{}^{\dagger}$	-5	‡	9_{17}	-8	-3	$9_{38}{}^{\dagger}$	-14	3
7_3	3	-12	$8_{18}{}^{\dagger}$	-5	‡	9_{18}	-14	3	$9_{39}{}^{\dagger}$	-1	-10
7_4	1	-10	$8_{19}{}^{\dagger}$	5	$\mathbf{-12}$	9_{19}	-6	-5	$9_{40}{}^{\dagger}$	-9	-2
7_5	-12	3	$8_{20}{}^{\dagger}$	-6	-2	9_{20}	-12	1	$9_{41}{}^{\dagger}$	-7	-4
7_6	-8	-1	$8_{21}{}^{\dagger}$	-9	1	9_{21}	-1	-10	$9_{42}{}^{\dagger}$	-3	$\mathbf{-5}(?)$
7_7	-4	-5	9_1	-18	7	$9_{22}{}^{\dagger}$	-3	-8	$9_{43}{}^{\dagger}$	1	-10
8_1	-7	-3	9_2	-12	1	9_{23}	-14	3	$9_{44}{}^{\dagger}$	-6	-3
8_2	-11	1	9_3	5	-16	$9_{24}{}^{\dagger}$	-6	-5	$9_{45}{}^{\dagger}$	-10	1
8_3	-5	‡	9_4	-14	3	$9_{25}{}^{\dagger}$	-10	-1	$9_{46}{}^{\dagger}$	-7	-1
8_4	-7	-3	9_5	1	-12	9_{26}	-2	-9	$9_{47}{}^{\dagger}$	-2	-7
$8_5{}^{\dagger}$	1	-11	9_6	-16	5	9_{27}	-6	-5	$9_{48}{}^{\dagger}$	-1	-8
8_6	-9	-1	9_7	-14	3	$9_{28}{}^{\dagger}$	-9	-2	$9_{49}{}^{\dagger}$	3	-12
8_7	-2	-8									

Table B.1: Maximal Thurston-Bennequin numbers for prime knots with nine or fewer crossings. A dagger next to a knot indicates that it is not two-bridge; a double dagger indicates that the knot is amphicheiral (identical to its unoriented mirror).

Bibliography

[Ar] V. I. Arnol'd, The first steps in symplectic topology, *Uspekhi Mat. Nauk* **41** (1986), 3–18 (Russian); *Russian Math. Surveys* **41** (1986), 1–21 (English translation).

[B] D. Bennequin, Entrelacements et équations de Pfaff, *Astérisque* **107–108** (1983), 87–161.

[Ch] Yu. V. Chekanov, Differential algebra of Legendrian links, preprint, 1999.

[CP] Yu. V. Chekanov and P. E. Pushkar, Arnold's four cusp conjecture and invariants of Legendrian knots, preprint. A summary of the results from both this paper and [Ch], titled *New invariants of Legendrian knots*, is available on the web at `http://www.mathematik.uni-bielefeld.de/~rehmann/ECM/cdrom/3ecm/mmsym.html`.

[E1] Ya. Eliashberg, A theorem on the structure of wave fronts and its application in symplectic topology, *Funct. Anal. Appl.* **21** (1987), 227–232.

[E2] Ya. Eliashberg, Contact 3-manifolds twenty years since J. Martinet's work, *Ann. Inst. Fourier* **42** (1992), 165–192.

[E3] Ya. Eliashberg, Legendrian and transversal knot in tight contact 3-manifolds, in *Topological methods in modern mathematics (Stony Brook, NY, 1991)* (Publish or Perish, Houston, 1993).

[E4] Ya. Eliashberg, Invariants in contact topology, *Doc. Math. J. DMV Extra Volume ICM 1998* (electronic), 327-338.

[EF] Ya. Eliashberg and M. Fraser, Classification of topologically trivial Legendrian knots, in *Geometry, topology, and dynamics (Montreal, PQ, 1995)*, CRM Proc. Lecture Notes, 15 (Amer. Math. Soc., Providence, 1998).

[EGH] Ya. Eliashberg, A. Givental, and H. Hofer, Introduction to symplectic field theory, preprint available on arXiv as math.SG/0010059.

[Eps] J. Epstein, On the invariants and isotopies of Legendrian and transverse knots, Ph.D. thesis, U.C. Davis, 1997.

[EFM] J. Epstein, D. Fuchs, and M. Meyer, Chekanov-Eliashberg invariants and transverse approximations of Legendrian knots, *Pacific J. Math.*, to appear.

[EH] J. Etnyre and K. Honda, Knots and contact geometry, preprint available on arXiv as math.GT/0006112.

[ENS] J. Etnyre, L. Ng, and J. Sabloff, Coherent orientations and invariants of Legendrian knots, submitted, preprint available on arXiv as math.SG/0101145.

[Fer] E. Ferrand, On Legendrian knots and polynomial invariants, preprint available on arXiv as math.GT/0002250.

[Fu] D. Fuchs, Chekanov-Eliashberg invariants of Legendrian knots: existence of augmentations, preprint.

[FT] D. Fuchs and S. Tabachnikov, Invariants of Legendrian and transverse knots in the standard contact space, *Topology* **36** (1997), 1025–1054.

[Gr] J. Gray, Some global properties of contact structures, *Ann. of Math. (2)* **69** (1959), 421–450.

[Kan1] Y. Kanda, The classification of tight contact structures on the 3-torus, *Comm. Anal. Geom.* **5** (1997), 413–438.

[Kan2] Y. Kanda, On the Thurston-Bennequin invariant of Legendrian knots and non exactness of Bennequin's inequality, *Invent. Math.* **133** (1998), 227–242.

[Kau1] L. Kauffman, *On Knots* (Princeton University Press, Princeton, 1987).

[Kau2] L. Kauffman, An invariant of regular isotopy, *Trans. Amer. Math. Soc.* **318** (1990), 417–471.

[Kir] R. Kirby, Problems in low-dimensional topology, in *Geometric Topology*, AMS/IP Stud. Adv. Math. 2.2 (AMS, Providence, 1997).

[KM] P. Kronheimer and T. Mrowka, Monopoles and contact structures, *Invent. Math.* **130** (1997), 209–255.

[Lic] W. B. R. Lickorish, Linear skein theory and link polynomials, *Topology Appl.* **27** (1987), 265–274.

[LM] P. Lisca and G. Matić, Tight contact structures and Seiberg-Witten invariants, *Invent. Math.* **129** (1997), 509–525.

[Mi] K. Michatchev, Relative homotopy splitting of differential algebra of Legendrian link, preprint, 2001.

[Mur] K. Murasugi, *Knot Theory and Its Applications* (Birkhäuser, Boston, 1996).

[Ng1] L. Ng, Legendrian mirrors and Legendrian isotopy, preprint available on arXiv as math.GT/0008210.

[Ng2] L. Ng, Maximal Thurston-Bennequin number of two-bridge links, preprint available on arXiv as math.GT/0008242.

[Ng3] L. Ng, Computable Legendrian invariants, preprint available on arXiv as math.GT/0011265.

[NT] L. Ng and L. Traynor, in preparation. Please note that any references to this paper are preliminary.

[Rol] D. Rolfsen, *Knots and Links* (Publish or Perish, Houston, 1990).

[Ru1] L. Rudolph, A congruence between link polynomials, *Math. Proc. Camb. Phil. Soc.* **107** (1990), 319–327.

[Ru2] L. Rudolph, Quasipositivity as an obstruction to sliceness, *Bull. Amer. Math. Soc. (N.S.)* **29** (1993), 51–59.

[Ru3] L. Rudolph, An obstruction to sliceness via contact geometry and "classical" gauge theory, *Invent. Math.* **119** (1995), 155–163.

[Sch] H. Schubert, Knoten mit zwei Brücken, *Math. Zeit.* **65** (1956), 133–170.

[Swi] J. Swiatkowski, On the isotopy of Legendrian knots, *Ann. Global Anal. Geom.* **10** (1992), 195–207.

[Tan] T. Tanaka, Maximal Bennequin numbers and Kauffman polynomials of positive links, *Proc. Amer. Math. Soc.* **127** (1999), 3427–3432.

[Tr] L. Traynor, Generating function homology for legendrian links, preprint.

[Yu] N. Yufa, Calculating the Thurston-Bennequin invariant of Legendrian knots, senior thesis, MIT, 2001.